On the Dynamics and Control of Space Manipulators

by

EVANGELOS G. PAPADOPOULOS

Diploma in Mechanical Engineering, National Technical University of Athens (1981)
MSME, Massachusetts Institute of Technology (1983)

Submitted to the
Department of Mechanical Engineering
in Partial Fulfillment of the Requirements
for the Degree of

DOCTOR OF PHILOSOPHY

at the
MASSACHUSETTS INSTITUTE OF TECHNOLOGY
October 1990

Signature of Author _____
Department of Mechanical Engineering
October 31, 1990

Certified by _____
Steven Dubowsky, Thesis Supervisor
Professor of Mechanical Engineering

Accepted by _____
Ain A. Sonin
Chairman, Departmental Graduate Committee

On the Dynamics and Control of Space Manipulators

by

Evangelos G. Papadopoulos

Submitted to the Department of Mechanical Engineering on October 31st 1990, in partial fulfillment of the requirements for the degree of *Doctor of Philosophy*.

Abstract

Dynamic coupling between a manipulator and its spacecraft can introduce control problems not found in fixed-base manipulators. This thesis takes a fundamental approach to the dynamic modeling and control of manipulators mounted on spacecraft. An efficient and compact modeling methodology based on barycenters and Lagrangian dynamics is developed. This methodology provides closure equations, differential kinematics and equations of motion for space systems.

The nature of a *free-floating* system, one in which the spacecraft is uncontrolled and free to move in reaction to manipulator motions, is analyzed. The existence of *Dynamic Singularities*, which are functions of the mass and inertia properties of the system, is shown. *All* control algorithms that use an inverse Jacobian will fail computationally at a dynamic singularity, while *all* those that use a transposed Jacobian will result in large errors. The reachable workspace is composed of *Path Dependent Workspaces*, which contain all points that may lead to dynamically singular configurations, and of *Path Independent Workspaces*, which contain all "trouble-free" points. Free-floating manipulators are controllable in joint space but in general, uncontrollable in cartesian space. It is shown that nearly any motion control algorithm which can be implemented on a terrestrial robotic manipulator also can be applied successfully to a free-floating space manipulator if certain mild conditions are met.

The control of *free-flying* manipulator systems, ones in which the spacecraft reaction jets are turned on, is studied also. *Coordinated Control* of both a system's spacecraft and of its manipulator is achieved by augmenting system outputs to include the spacecraft's coordinates.

Finally the problem of controlling a failed joint of a space manipulator is addressed. It is shown that *Failure Recovery Control* is possible when dynamic coupling exists between the failed joint and some working joint, and when the system inertia matrix is invariant with respect to the failed joint angle.

Thesis Committee: Dr. Steven Dubowsky, Chairman
Professor of Mechanical Engineering

Dr. Haruhiko Asada
Professor of Mechanical Engineering

Dr. Mark H. Raibert
Professor of Computer Science and Engineering and Motor Control

To Evie

Acknowledgments

I wish to express my gratitude to my advisor, Prof. Steven Dubowsky, for his invaluable insights, support and guidance over the course of this research, and for providing the unique environment and resources that made my years at MIT an enriching experience. I would also like to thank Profs. Harry Asada and Marc Raibert for their encouragement and constructive comments as members of my committee.

I would like to take this opportunity to express my thanks to a host of individuals who contributed greatly to my education and character. These include my professors at Athens College, my advisor at NTU, Prof. Nicholas Krikelis, and my past advisors at MIT, Profs. David Hardt, Michael Athans and Lena Valavani. Thank you all.

The support and love of my parents, George and Vassiliki, and my brother Constantine has been as always, invaluable. They were the ones who helped me keep a balanced perspective during those academically intense years. I am most grateful to them.

I also wish to thank Norbert Hootsmans, Miguel Torres, Joe Deck, Charles Oppenheimer, Uwe Mueller, Akhil Madhani, and the other members of our research group for many stimulating conversations, for sitting through my "dry runs" and for making my life at MIT very enjoyable.

Finally, but more importantly, my deepest gratitude and love goes to my wife, Evie, for her loving affection and for taking care of all the necessary diversions in life. Without her encouragement to continue toward a Ph.D. after my Navy service, this thesis would not have existed. If she were not an already excellent graphic designer, her patience in listening to everything from physics to space robots would have earned her at least an engineering degree!

The support of this work was provided by NASA's Langley Research Center, Automation Branch, under Grant NAG-1-801, and is greatly appreciated.

Table of Contents

List of Figures

List of Tables

List of Abbreviations

BC	Barycenter
CM	Center of Mass
DOF	Degrees of Freedom
EVA	Extra Vehicular Activity
FTS	Flight Telerobotic Servicer
MIMO	Multi Input Multi Output
PD	Proportional-Derivative
PDW	Path Dependent Workspace
PID	Proportional-Integral-Derivative
PIW	Path Independent Workspace
VM	Virtual Manipulator

List of Symbols

In this thesis, both *physical (Gibbsian) vectors/dyadics* and *column vectors/matrices* are used. Physical vectors are denoted by underlined, bold and lower case characters, with the exception of $\underline{\mathbf{R}}$ and its variants. Dyadics are denoted by underlined, bold and upper case characters. Greek characters are not bold, with the exception of ω, ρ, and τ, (when it appears without a subscript), which are always bold. Bold lower case symbols represent column vectors, bold upper case matrices. Right superscripts must be interpreted as "with respect to," left as "expressed in frame." A missing left superscript implies a column vector expressed in the inertial frame.

$\mathbf{0}$	Zero matrix
$\mathbf{0}_i$	A matrix obtained from 0 after removal of its ith column
$\mathbf{1}$	Unit matrix
$\underline{\mathbf{1}}$	Unit dyadic
$\mathbf{1}_i$	A matrix obtained from 1 after removal of its i^{th} column
$\mathbf{A}$	"A" matrix in linear control systems
${}^{i-1}\mathbf{A}_i$	Transformation matrix, transforms column vectors given in frame i to column vectors in frame i-1
$\mathbf{a}$	Rotation axis direction, also parameter vector
$\mathbf{B}$	"B" control matrix in linear control systems
$\mathbf{C}$	"C" output matrix in linear control systems
$\mathbf{C}$	Nonlinear Coriolis and centrifugal terms for a fixed-based system
$\mathbf{C}^*$	Nonlinear Coriolis and centrifugal terms for a free-floating system
$\mathbf{C}^+$	Nonlinear Coriolis and centrifugal terms for a free-flying system
c_{12}	$\cos(q_1+q_2)$
$\underline{\mathbf{c}}_i$	Vector from body k's CM to its barycenter
$\underline{\mathbf{c}}_i^*$	Vector from body k's barycenter to its CM
$\underline{\mathbf{D}}_{ij}$	Mixed inertia dyadic corresponding to bodies i and j
$\underline{\hat{\mathbf{d}}}_{ij}$	Term depending on cross products of barycentric vectors

$\mathbf{D}_{ij}$	Inertia matrix corresponding to $\underline{\mathbf{D}}_{ij}$
${}^0\mathbf{D}$	Total system inertia about the system CM
${}^0\mathbf{D}_{ij}$	Inertia matrix corresponding to $\underline{\mathbf{D}}_{ij}$ but expressed in the spacecraft frame (body 0)
${}^0d_{ij}$	Inertia scalar quantities for planar systems
${}^0\mathbf{D}_j$	Sum of ${}^0\mathbf{D}_{ij}$ over all i
${}^0\mathbf{D}_q$	Sum of ${}^0\mathbf{D}_{ij}{}^0\mathbf{F}_j$ over all i
${}^0\mathbf{D}_{qq}$	Sum of ${}^0\mathbf{F}_i^T\,{}^0\mathbf{D}_{ij}{}^0\mathbf{F}_j$ over all i and j
$\mathbf{e}$	Error in feedback control
$\mathbf{e}$	Euler parameter
${}^0\mathbf{F}_k$	Projection matrix, describing the effect of $\dot{\mathbf{q}}$ to ω_k^0
$\underline{\mathbf{f}}_{ext}$	External forces acting on the system
$\underline{\mathbf{f}}_{k,m}$	External force acting at point m of body k
$\mathbf{G}^*$	Vector due to initial momentum
$\mathbf{H}$	Inertia matrix of a fixed-based manipulator system
$\mathbf{H}^*$	Inertia matrix of free-floating manipulator system
$\mathbf{H}^+$	Inertia matrix of free-flying manipulator system
$\underline{\mathbf{h}}$	Angular momentum about the inertial origin O
$\underline{\mathbf{h}}_{cm}$	Angular momentum about the system CM
$\mathbf{h}_{cm}$	Total angular momentum about the system CM
$\mathbf{h}_{cm,0}$	Total angular momentum about the system CM, at time 0
h_{ij}	Entries of the inertia matrix of a fixed-base manipulator
$\underline{\mathbf{I}}_k$	Inertia dyadic of body k with respect to its CM
${}^k\mathbf{I}_k$	Inertia of body k, expressed in frame k, a diagonal matrix
${}^i\mathbf{v}_{ik}$	Barycentric vector of body i, expressed in frame i
$\mathbf{J}$	Jacobian matrix of a fixed-base manipulator
$\mathbf{J}^*$	Jacobian matrix of a free-floating manipulator system
$\mathbf{J}^+$	Jacobian matrix of free-flying system
$\mathbf{J}^+_{k,m}$	Jacobian matrix of free-flying system, corresponding to m^{th} point on body k
$\mathbf{J}_z$	Transformation Jacobian from $\dot{\mathbf{z}}_0$ to $\dot{\mathbf{z}}_1$
${}^0\mathbf{J}^*$	Free-floating system Jacobian relating joint velocities to end-effector velocities seen in the spacecraft frame
${}^0\mathbf{J}_{11}$	Jacobian submatrices, also ${}^0\mathbf{J}_{12}$, ${}^0\mathbf{J}_{22}$
${}^0\mathbf{J}_{11k,m}$	Jacobian submatrix corresponding to m^{th} point on body k. Also, ${}^0\mathbf{J}_{12k,m}$, ${}^0\mathbf{J}_{22k,m}$

$\mathbf{K}_d$	Control gain multiplying velocities
$\mathbf{K}_p$	Control gain multiplying positions
$\underline{\mathbf{l}}_i$	Vector from body k's CM to its "left" joint
$\underline{\mathbf{l}}_i^*$	Vector from body k's barycenter to its left joint
M	Total mass of the system
m_k	Mass of body k
N	Number of degrees of freedom
n	Euler parameter
$\underline{\mathbf{n}}_{ext}$	External torques
$\underline{\mathbf{n}}_{tot}$	Sum of external torques and torques due to external forces
$\mathbf{p}_0$	Linear momentum at time 0
$\underline{\mathbf{p}}$	Linear momentum about the inertial origin O
$\mathbf{Q}$	Generalized forces vector
$\mathbf{q}$	Joint angles vector
$\dot{\mathbf{q}}$	Column vector of joint velocities
$\mathbf{Q}_c$	Control forces
$\mathbf{Q}_d$	Disturbances
q_i	Relative (gimbal) angle corresponding to the i^{th} joint
$\mathbf{Q}_{s,i}$	The i^{th} singular hypersurface in the joint space
R	Distance of the end-effector from system CM
R	Routhian function
$\dot{\mathbf{r}}_E$	End-effector linear velocity expressed in the inertial frame
$\dot{\mathbf{r}}_{E,k}$	Linear velocity of the end-effector due to motion of joint k
$\dot{\underline{\mathbf{r}}}_{cm}$	Linear velocity of the system CM
$\dot{\underline{\mathbf{r}}}_{cm,0}$	Linear velocity of the system CM at time 0
$\dot{\underline{\mathbf{r}}}_E$	Linear velocity of the end-effector
$\dot{\underline{\mathbf{R}}}_k$	Linear velocity of body k's CM
$\dot{\underline{\rho}}_k$	Linear velocity of body k's CM with respect to the system's CM
$\dot{\underline{\mathbf{R}}}_{k,m}$	Linear velocity of point m in body k
$\underline{\mathbf{r}}_{cm}$	Vector from inertial origin O to the system CM
$\underline{\mathbf{r}}_{cm,0}$	Position of the system CM at time 0
$\underline{\mathbf{r}}_E$	Vector from inertial origin O to the end-effector
$\underline{\mathbf{r}}_i$	Vector from body k's CM to its "right" joint
$\underline{\mathbf{r}}_i^*$	Vector from body k's barycenter to its "right" joint
$\underline{\mathbf{R}}_k$	Vector from the inertial origin O to to kth body's CM

$\underline{R}_{k,m}$	Vector from the inertial origin to point of interest m on the k^{th} body
$\underline{r}_{k,m}$	Vector from k body's CM to point of interest m on the same body
r_E	End-effector position with respect to an inertial frame
R_{min}, R_{max}	Reachable workspace boundaries
$R_{min,i}$, $R_{max,i}$	Workspace boundaries corresponding to $Q_{s,i}$
R^n	Cartesian n-dimensional space
S	Sum
s_1	$\sin(q_1)$
T	Kinetic energy
t	Time
T_0	Transformation matrix, transforms column vectors given in frame 0 to column vectors in inertial frame
T_i	Transformation matrix, transforms column vectors given in frame i (i=0,...,N) to column vectors in inertial frame
${}^0T_i$	Transformation matrix, transforms column vectors given in frame i to column vectors in frame 0
u	Control input
u^*	Constant control input
${}^k u_k$	Column vector, corresponding to the k^{th} joint axis expressed in the k^{th} frame
V	Potential energy
$\underline{v}_{ik}$	Barycentric vector
$\underline{v}_{ik,m}$	$= \underline{v}_{ik} + \delta_{im}\, \underline{r}_{k,m}$
$\underline{v}_{iN,E}$	$= \underline{v}_{iN} + \delta_{iN}\, \underline{r}_N$
x	End-effector position and orientation in the inertial frame
$\dot{x}$	End-effector linear and angular velocity in the inertial frame
$\dot{x}_{k,m}$	Inertial linear and angular velocity of point m on body k
x_{des}	Desired position and orientation x in the inertial frame
Y	Matrix multiplying parameter vector a
z_0	Vector of coordinates used in equations of motion
z_1	Vector of coordinates to be controlled, output coordinates

Greek symbols

$\alpha, \beta, \gamma, \varepsilon, \zeta, \eta$	Lengths of barycentric vectors, shorthand notation
δ_{im}	Kronecker delta, (0 always unless i=m, then 1)
δW	Virtual work
μ_i	Mass distribution
θ	Rotation around axis a. spacecraft attitude in planar systems
θ	Spacecraft attitude, corresponding to a three-parameter description
θ_i	Absolute angle of link i in planar systems
$\underline{\rho}_k$	Vector from the system CM to kth body's CM
τ	Torque vector
τ_i	Torque input due tot he i^{th} actuator
$\underline{\omega}_i^{i-1}$	Angular velocity of body i with respect to body i-1
ω_0	Spacecraft angular velocity, expressed in the inertial frame
${}^0\omega_0$	Spacecraft angular velocity, expressed in its reference frame
$\underline{\omega}_E$	Angular velocity of the end-effector
$\underline{\omega}_k$	Angular velocity of body k (k=0,...,N)
ω_E	End-effector angular velocity, expressed in the inertial frame
ω_j^0	Angular velocity of body i with respect to body 0, expressed in the inertial frame

Other symbols

$()^{\#}$	Denotes a space system with a failed actuator
$()^*$	Denotes a free-floating system
$()^+$	Denotes a free-flying system
$\dot{(\bullet)}$	Denotes a time derivative of (•), (velocity)
$\ddot{(\bullet)}$	Denotes a double time derivative of (•), (acceleration)
$(\bullet)^\times$	Denotes a skew symmetric matrix obtained from vector (•)
$[\bullet,\bullet]$	Denotes operation between the two arguments
$[\bullet]_{k,m}$	Denotes the k,m^{th} element of matrix •
$()_E$	Denotes the end-effector
$()_S$ or $()_0$	Denotes a spacecraft, also denoted by 0
$()^T$	Denotes transposition
$\|\|(\bullet)\|\|$	Denotes the norm (length) of a vector (•)

1 Introduction

1.1 MOTIVATION

During the coming decades, a major thrust in the scientific exploration, military and commercial use of space will be seen. In order to meet these challenges, the capability to perform a number of construction, inspection and repair tasks in space will be required. However, Extra Vehicular Activity (EVA) by astronauts in the space environment is dangerous. In order to minimize the hazards to astronauts, much training, extensive life support systems and safety procedures are required, but these are very costly. These dangers and costs can be minimized by the use of robotic space manipulator systems.

Space manipulators are often seen as astronaut "assistants" or astronaut surrogates capable of performing EVA. Ideally, space manipulators will be mobile, versatile, dexterous and autonomous. Current designs of space manipulators under construction are the Flight Telerobotic Servicer (FTS) [23] and the EVA Retriever [12]. The FTS, see Figure 1.1, will be mounted on mobile platforms or on the Space Shuttle arm and will be mainly used for assembly operations while the EVA Retriever, see Figure 1.2, will be an autonomous free-flying system used in retrieval, inspection and contingency operations.

The use of manipulator systems in space introduces many new planning and control challenges. An earth-based manipulator can have a fixed base and its tasks can be planned relative to its base. A number of control laws have been developed to enable manipulators accomplish their tasks. In contrast to fixed-base manipulators, space manipulator systems have no fixed base. Manipulator motions will produce dynamic forces resulting in motions of the spacecraft which carries the manipulator.

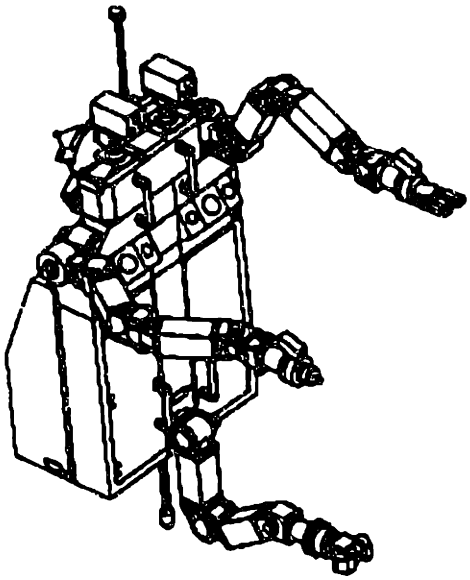

Figure 1.1. The FTS space robotic system.

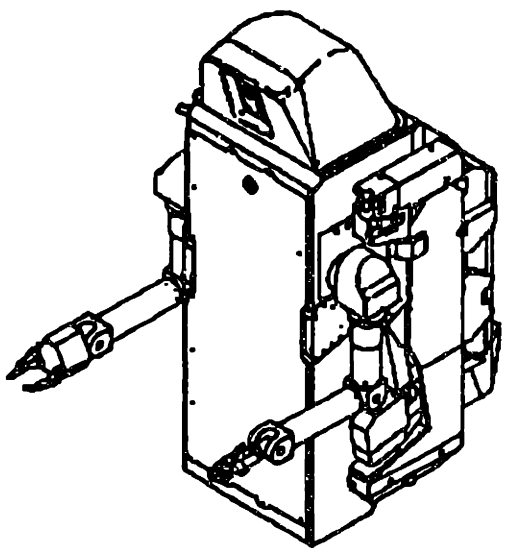

Figure 1.2. The EVA Retriever space robotic system.

The dynamic behavior of space robotic systems is not well-understood and cannot be adequately described by dynamic equations derived assuming a fixed base. Symbolic or

numerical computer programs may be employed in modeling space manipulators, but in general these are not well suited in revealing a system's dynamic structure. In addition, in space it is not possible to use directly control algorithms developed for fixed-base manipulators. Control algorithms for such systems are currently proposed on an ad-hoc basis. Some of these depend on a particular dynamic formulation, while others are based on a mainly kinematic description of the system. Further, it is not clear what sensory information is required and why, and what is the nature and remedies to control problems encountered. Hence, some of the open questions that need to be resolved are:

- What is the kinematic and dynamic nature of spacecraft-borne robotic systems?
- What is the nature of control problems for these systems? What are the differences, similarities and limitations of the characteristics of space systems as opposed to fixed-based systems? Is it possible to use in space algorithms developed for terrestrial systems and if yes, under what conditions? What sensory information is needed in space and why? What is the behavior of space manipulator control systems in the presence of disturbances or unknown system parameters?
- Is it possible to design a system for improved robustness against actuator failures?

Clearly, in order to deploy robotic systems in space, a better understanding of the fundamental nature of the dynamics and control of such systems is required. This is the major theme of this thesis.

1.2 LITERATURE REVIEW

1.2.1 Background

Early assessments agree that robotic systems must be used in space, for four main reasons [2,8,19,66]: (a) Crew time and availability will be scarce. Robotic systems may increase

crew productivity by a factor of two to three. (b) Complex life-support systems, required by EVA, are costly to send into orbit. (c) The space environment is hazardous to people, due to radiations, meteorites, etc. (d) Over a period of 10-20 years, the estimated total costs of robotic systems in space are predicted to be much lower than the costs of employing humans for the same mission objectives.

Various studies have identified space operations which are candidate to be performed by robotic systems [2,11,12,19,23,52]. These include: (a) Scheduled servicing of satellites and spacecraft, including refueling tasks. (b) Inspection of remote sites or verification of structures etc. (c) Retrieval of tumbling tools or astronauts. (d) Assembly or welding of space structures. (e) Contingency operations.

Many researchers have been active in investigating several aspects of space robotic manipulation. These include man-machine and teleoperation aspects, selection of system architecture, applications of artificial intelligence, mechanical design of manipulators, development of sensors, and finally, dynamics and control issues, the theme of this thesis.

In order to control a space robotic system, two basic functions are required. The first and hierarchically higher function is realized by a human or by a computer, according to the selected mode: *teleoperated*, *supervised* or *independent* control mode [66,67]. This level deals mainly with the generation of commands to the second and hierarchically lower level, which is a feedback control system. However, in order to ever realize high level control functions, low-level feedback control algorithms, responsible for executing the given commands, are needed.

In this thesis, two types of space manipulator systems will be considered: *free-flying* and *free-floating*. Both systems include a spacecraft or platform on which one or more robotic manipulators are mounted. In the case of a free-flying system, a spacecraft's control system is active and hence, the entire spacecraft/manipulator system is capable of being transferred and oriented arbitrarily in space. In the case of a free-floating system, a spacecraft's control system is turned off and therefore, the spacecraft is free to translate or

rotate in reaction to forces and torque generated by its manipulator. However, the system center of mass cannot experience a net translation in space.

1.2.2 Multibody Systems and Space Manipulator Dynamics

Dynamics of multibody systems have been studied by many researchers in both the aerospace and robotics communities, resulting in many different formulations [30,39,5]. A short review of the main approaches to multibody dynamics in the aerospace literature is given by Hughes [30]. For a more comprehensive review, see Jerkovsky [31]. Hughes distinguishes two basic formulations. The first is based on Newton-Euler methods and was pioneered by Hooker and Margulies [29], Hooker [27], and Roberson and Wittenburg [53]. General characteristics of these methods are the use of a tree topology to describe open chains of multibody systems, the choice of the system center of mass to represent the translational Degrees-of-Freedom (DOF) and the introduction of the so-called barycenters and augmented bodies which simplify the repeated and systematic occurrence of certain weighted linear combinations. In some cases, this formulation results in simple translational equations of motion that can be decoupled from the rotational equations.

The second basic formulation in deriving the equations of motion is to choose one body of the system as a home body and a point on it to represent the translational DOF of the system. The equations that result are coupled but simpler to interpret. This method was called the direct-path method by Ho [24], see also Frisch [20], and Hooker [28].

The robotics community has been mainly interested in fixed-based manipulator dynamics, with primary focus on Newton-Euler [42] and Lagrangian formulations [26] and recently on Kane's method [32]. These methods result in fundamentally the same equations of motion, one being preferred over the other depending on how efficient a method is in terms of required algebraic operations and computer memory.

Equations of motion for space manipulators can be written using multibody dynamic formulations. The Virtual Manipulator (VM) technique, proposed by Vafa, can be used to

simplify the dynamics of space robotic systems [17,62-65]. The VM is an idealized kinematic chain that corresponds to the real manipulator and describes the motion of its end-effector. The VM's base is at the system CM, called Virtual Ground. In the case of a free-floating system, the VM decouples the translational DOF and hence, it simplifies the equations of motion. In Masutani et al., closure equations were written about a spacecraft's center of mass, and conservation equations were used to reduce a system's equations of motion [44]. Due to the involved complexity, researchers have sometimes derived equations of motion for specific systems, usually employing general purpose programs like MACSYMA [3,58]. However, in such a case, a system's kinematic and dynamic structure may not be clear.

1.2.3 Control of Space Manipulators

Motion control implies that the manipulator moves its end-effector to specified locations in the inertial or spacecraft frames, without significant force interactions between its end-effector and its environment, with the exception of those with its payload. However, a manipulator's payload may be considered as part of its last link.

A number of control techniques for space manipulator systems have been proposed. These schemes can be classified in three categories. In the first category, studied by Dubowsky et al., spacecraft position and attitude are controlled by reaction jets which compensate for any manipulator dynamic forces exerted on the spacecraft [18]. In this case, control laws for earth-bound manipulators can be used, but the utility of such systems may be limited because manipulator motions may either saturate the reaction jet system or consume relatively large amounts of attitude control fuel, limiting its useful life. In order to extend a system's life, Dubowsky and Torres proposed some heuristic path planning methods which can reduce the use of control fuel [16]. In the same context, Umetani and Yoshida correlated spacecraft disturbances induced by manipulator motions to manipulator manipulability ellipsoids. However, their results were mostly qualitative [61].

In the second category, a spacecraft's attitude is controlled, while its translation is not. Longman et al. proposed a control scheme that estimates the required torques to keep a spacecraft's orientation fixed and uses reaction wheels to provide[1] these to the spacecraft [41]. In general, manipulator control of controlled-attitude space systems is somewhat more involved than that where both position and attitude are controlled, although the VM technique can be used in modeling, path planning and workspace analysis of such systems [63,64].

In order to conserve fuel or electrical power, or to avoid sudden motions of the manipulator end-effector due to firing of jet actuators, the third category of control approaches has been proposed [3,40,44,60,63]. In these systems, called here free-floating, a spacecraft is permitted to move freely (rotate and translate) in response to its manipulator motions. The analysis of these systems, too, can be simplified using the VM approach [62-65] while related work, tailored to a specific system, is discussed in [40]. Alexander and Cannon proposed a control scheme based on the resolved acceleration algorithm, and used it to control succesfully an experimental two-DOF free-floating system [3,43]. Their controller relied on end-point position feedback provided by a vision camera mounted on the spacecraft. Umetani and Yoshida derived a Generalized Jacobian for a free-floating system and proposed a control algorithm based on the resolved rate algorithm [60,69]. Their experimental two DOF system used end-point measurements provided by an inertially fixed video camera. Masutani et al. proposed a transposed Jacobian controller using a Jacobian derived for a fixed-based system [44]. This controller includes end-point feedback and drives the manipulator end-effector to a desired location provided that the spacecraft mass and inertia are large; otherwise, stability problems are encountered.

With the intention to minimize use of reaction fuel and maintain a large workspace, Spofford and Akin proposed a blending of the first and third methods and assumed a free-

[1] A spacecraft's orientation also can be fixed by using reaction jets (thrusters), but this method has the same drawbacks as discussed above [18].

flying system switching between free-flying and free-floating control modes [58]. This work focused mainly on algorithm switching as well as on man-machine considerations. Nakamura and Mukherjee explored the "non-holonomic nature"[2] of path-planning for free-floating space manipulators and tried, to employ Lyapunov functions for path generation [45]. Finally, Vafa proposed a planning scheme that takes advantage of the redundant nature of free-floating systems in order to simultaneously control a system's manipulator and its spacecraft's attitude [63].

Concluding this review, it must be pointed out that past works on the control of space manipulator systems have generally proposed particular algorithms and showed their validity on a case by case basis. Control algorithms which do not take into account the kinematic or dynamic nature of a system have been found to have problems [44].

1.3 CONTRIBUTIONS OF THIS THESIS

This thesis is founded on the idea that a fundamental knowledge of the kinematic and dynamic nature of a space manipulator system is a prerequisite in designing effective control algorithms. Therefore, initial emphasis is placed in the development of a coherent modeling methodology capable of revealing the structure of free-flying and free-floating space systems.

Important characteristics of the modeling methodology developed in this thesis are: (a) The position of a system's CM, its spacecraft's attitude and the relative joint angles between two adjacent bodies are selected to be the system's independent coordinates. Relative joint angles are preferred because these coordinates can be measured and controlled readily. (b) The equations of motion are derived with respect to the system CM,

[2]The word is in quotation marks, because strictly speaking, a free-floating system is a holonomic system exhibiting nonholonomic characteristics due to the non-integrability of the angular momentum. For further details, please refer to section 3.2.2.

whose coordinates, represent the translation of the system. The motivation for doing so is that in the absence of external forces and torques, the equations of motion decouple automatically, resulting in a reduced dynamic system. Such an approach suggests the adoption of barycentric vectors that are essential in describing both the kinematics and the dynamics of space systems. (c) A Lagrangian approach is used to obtain a system's equations of motion. With this approach, constraint forces are automatically eliminated and the structure of the equations of motion becomes more clear. This is a departure point from derivations like [29,53], where a Newton-Euler approach was adopted. Further, in the case of a free-floating system, this approach easily yields a reduced positive definite symmetric inertia matrix which describes all the necessary dynamic structure. (d) Very compact expressions for the angular momentum and its time derivative are derived and used to obtain kinematic and dynamic equations.

The modeling methodology used in this thesis is well suited for free-floating systems and can be used to describe free-flying systems, although in this case, other approaches can be used equally well. In the negative side, it should be pointed out that the barycentric vectors and the new position of the system CM must be re-calculated when a payload is picked up. This is because a payload becomes part of the last link, and therefore changes its mass properties. However, this new CM position must be re-calculated anyway, because a free-floating system's reachable workspace is a sphere with its center at the system's CM and with a radius which depends on the mass properties of the manipulator system *and* the payload. Also, no comparisons with respect to computer efficiency for time domain simulations were attempted; the focus was placed on the analysis of structure.

The developed methodology is first applied to the analysis of the kinematic and dynamic structure of free-floating systems. A free-floating system's Jacobian is formed in a systematic way and based on it, a system's *Dynamic Singularities* were found. At a dynamic singularity the manipulator is unable to move its end-effector in some inertial direction; thus dynamic singularities must be considered in the design, planning, and control

of free-floating space manipulator systems. The existence and location of dynamic singularities cannot be predicted solely from the manipulator kinematic structure because they are also functions of the system dynamic properties, namely the mass and inertia of the system, unlike the singularities for fixed-based manipulators. Workspaces of free-floating systems are defined according to the reachability properties of the points that belong to them. A system's reachable workspace is divided to *Path Independent Workspaces*, which contain points reachable with any path, and to *Path Dependent Workspaces*, which contain points reachable with some paths only.

Then the dynamics of an N+6 DOF free-floating system with an N DOF manipulator are shown to be governed by just N second order equations. The state and output controllability of a free-floating system is investigated and it is shown that such a system is always state controllable but it may not be output controllable in the Path Dependent Workspace. This lack of controllability is due to the existence of dynamic singularities and cannot be altered, because it is a *physical* limitation of the system. Based on a detailed comparison of the kinematics and dynamics of fixed-based and free-floating systems, it is shown that nearly *any* algorithm which can be applied to conventional fixed-based manipulators can be directly applied to free-floating manipulators, with a few weak additional conditions. These are the avoidance of dynamic singularities and the estimation of a spacecraft's attitude. It is further shown that internal feedback is enough for control purposes if a system's mass and inertia properties are sufficiently well known. If this is not the case, end-point feedback or attitude measurements may be needed.

The basic idea that system structure must be used to design effective controllers is carried further in the control of free-flying manipulator systems. The inherent redundancy in free-flying systems is used to control in addition a spacecraft's position and attitude. A control law that achieves such a task and is called *Coordinated Control*, is designed and demonstrated. Using the basic kinematic and dynamic description of free-flying manipulators, other control laws can be applied equally well.

In this thesis, another important type of control for space manipulators called *Failure Recovery Control* is considered. A failure recovery controller uses the working actuators of a system to control a joint angle whose actuator has failed. Once a desired set-point for such an angle is reached, the corresponding joint can be locked using the joint's brakes, and the system may continue operating with somehow reduced capabilities. It is shown that in order for such a controller to be effective, two basic conditions must be observed. These are the existence of dynamic coupling in the system and the invariance of the system's inertia matrix with respect to the failed joint's angle.

1.4 ORGANIZATION OF THIS THESIS

This thesis is organized into six chapters and six appendices. In Chapter 2 the modeling methodology used throughout this thesis is developed. This methodology includes development of closure equations, differential kinematics, momentum equations and equations of motions for free-flying systems subject to force interactions. When a system is planar, these equations simplify considerably and are given in a closed form.

Chapter 3 uses the methodology developed in Chapter 2 to analyze the fundamental kinematic and dynamic nature of a free-floating system. Integrals of motion are used to derive a system's Jacobian and the nature of the Dynamic Singularities is investigated. A system's workspaces are defined according to the associated reachability properties and some guidelines that may help in maximizing the less troublesome Path Independent Workspace are given. The effect of nonzero initial momentum in the system is also considered.

Chapter 4 focuses on motion control of free-floating and free-flying space systems. The various control modes of such systems are categorized and emphasis is placed in selecting the appropriate description with respect to a system's task. Based on this description, a free-floating system's state/output controllability is determined and based on

the fact that the kinematic and dynamic nature of a free-floating system is essentially the same to that of a fixed-based system, control algorithms are proposed. The required sensory measurements are analyzed with respect to whether system parameters are adequately known. The effect of disturbances is examined. Along the same lines, the "plant" structure of a free-flying system is analyzed and Coordinated Control that allows simultaneous control of both the spacecraft and its manipulator is designed.

Chapter 5 introduces the idea of Failure Recovery Control and examines some engineering systems for which independent control of more outputs than available control actuators is possible. This analysis is further developed in the case of a space manipulator with failed actuators and the necessary conditions for failure recovery control are identified. Finally, Chapter 6 concludes this thesis and suggests some directions for future research.

2 Modeling of Free-Flying Manipulator Systems

2.1 INTRODUCTION

In this chapter, the fundamental kinematic and dynamic relationships are formulated for the spatial free-flying manipulator system depicted in Figure 2.1. This system consists of a spacecraft and of a manipulator mounted on it. The spacecraft and its manipulator are assumed rigid, an assumption which is reasonable for systems like the FTS and EVA Retriever. Most proposed systems assume revolute[1] manipulator joints, hence this assumption will be made in this thesis also. Space manipulators systems will be equipped with two or more manipulators, cameras, antennas and thus will be extremely complicated dynamic systems. In this thesis the focus will be on a system consisting of a spacecraft and one manipulator. As it will be explained later in this thesis, this formulation can be extended to include more than one manipulators or other moving bodies.

Some of the formulation's basic characteristics are: (a) The system CM is chosen to represent the translation of the system. (b) Spacecraft attitude and relative angle joints (gimbal angles) are chosen to describe the system's orientation and configuration. These variables were chosen to be the independent coordinates of the system, because then the equations of motion assume a compact and very useful form. (c) The notion of *barycenters* is used to simplify resulting kinematic and dynamic equations. (d) Momentum and Lagrangian methods are employed in deriving equations of motion. (e) A dyadic vectorial

---

[1]Revolute joints are proposed mainly for three reasons: (a) they can be driven by small direct drive electric motors that use renewable energy (electric energy from solar panels), (b) they maximize workspace to manipulator weight ratio and (c) manipulators with revolute joints can designed to be anthropomorphic facilitating their teleoperation by humans.

form is used for presenting the results in a compact way and avoiding unnecessary derivations involving transformations. All equations are converted to a scalar (matrix) form when it is absolutely required; this reduces the effort of writing equations substantially.

The approach taken in this thesis has the advantage that the resulting kinematic and dynamic equations are general, compact and explicit[2]. Also, other approaches result in forms in which the integrals of motion (the conservation of momentum equations), do not decouple when no external forces or torques act on the system. In contrast to this, the formulation presented in this chapter results in equations of motion that *decouple* and hence, the integrals of motion are readily available.

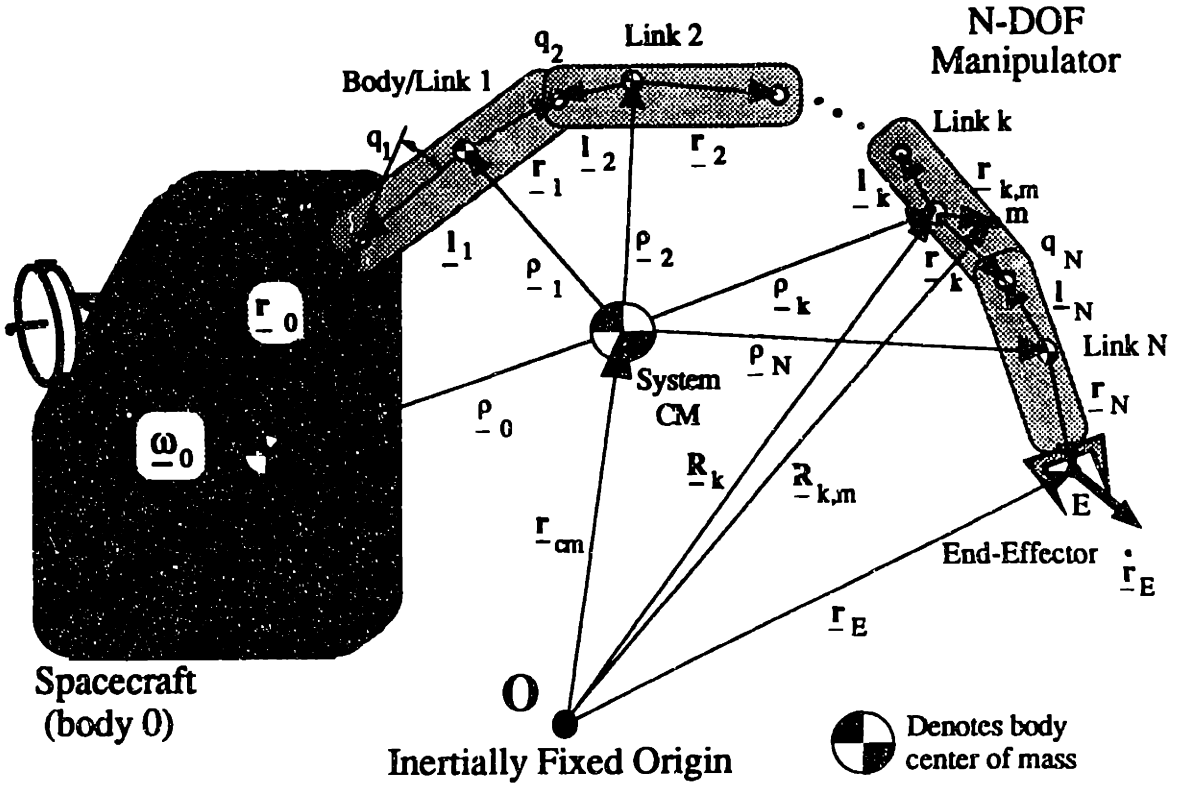

Figure 2.1. A spatial (nonplanar) free-flying manipulator system.

[2]For example, this author found that to derive analytically the dynamic equations of a planar two-DOF manipulator on a three-DOF spacecraft, required fifteen pages of derivations when a Newton-Euler approach was used, but only four pages when the formulation in this thesis was used.

In Section 2.2 the kinematic relationships are written in vectorial form. First, the position of an arbitrary system point is given as a function of the position of the system CM and of its barycentric vectors. Expressions for the linear velocity of an arbitrary point and of the angular velocity of any link are derived as functions of the linear velocity of the system CM, of the angular velocity of the spacecraft, and of the relative angular velocities. These vectorial formulas are converted to scalar equations required to form Jacobians that relate the controlled velocities (system CM linear velocity, spacecraft angular velocity and manipulator joint velocities) to the linear and angular velocity of any point of the system. In Section 2.3 vectorial momentum equations and their derivatives are derived. Then, these are converted to scalar equations. In Section 2.4 the general equations of motion are derived using a Lagrangian approach. Section 2.5 deals with the simplification of these equations for planar systems. Two examples are used to illustrate the formulation developed in this chapter. Finally, Section 2.6 outlines ways in which these methods can be applied to similar systems, and Section 2.7 closes this chapter.

2.2 KINEMATIC MODELING

The objective here is to obtain analytical expressions for the position and velocity of an arbitrarily located point of a space manipulator system, as the one shown in Figure 2.1. To this end, position vectors are expressed as vectorial sums of a minimum number of body-fixed vectors, called barycentric vectors. These barycentric vectors are calculated once and are used to find all the important kinematic and dynamic quantities of the system. Hence, they play an important role in the kinematic and dynamic analysis of space systems. Linear velocities are obtained by differentiating position vectors. Due to the specific decomposition of the position vectors, expressions for velocities are particularly compact, efficient and elegant. The orientation of the different links is described with the help of

transformation matrices and the angular velocities are written as functions of the controlled angular velocities. More features of the modeling methodology developed in this thesis will be apparent in later sections.

The body 0 in Figure 2.1 represents the spacecraft and the bodies k (k=1,...,N) represent the N manipulator links. The manipulator is in an open-chain configuration so that a system with an N degree-of-freedom (DOF) manipulator will have in total N+6 DOF, the additional 6 DOF corresponding to the spacecraft position and attitude.

2.2.1 Position of arbitrary system points

From Figure 2.1, it can be seen that the vector from the inertially fixed origin O to an arbitrary point m on body k, $\underline{\mathbf{R}}_{k,m}$ is given by:

$$\underline{\mathbf{R}}_{k,m} = \underline{\mathbf{R}}_k + \underline{\mathbf{r}}_{k,m} \qquad k = 0,\ldots,N \qquad (2\text{-}1)$$

where $\underline{\mathbf{R}}_k$ is the vector from the inertially fixed origin O to k body's CM, and $\underline{\mathbf{r}}_{k,m}$ is a body-fixed vector from k body's CM to the point of interest m. As shown in Figure 2.1 $\underline{\mathbf{R}}_k$ can be further decomposed to:

$$\underline{\mathbf{R}}_k = \underline{\mathbf{r}}_{cm} + \underline{\rho}_k \qquad k = 0,\ldots,N \qquad (2\text{-}2)$$

where $\underline{\mathbf{r}}_{cm}$ and $\underline{\rho}_k$ are defined in Figure 2.1. The CM locations of the individual links and the spacecraft with respect to the system CM are defined uniquely by some system configuration and thus it is possible to express $\underline{\rho}_k$ vectors as sums of weighted, body-fixed vectors $\underline{\mathbf{l}}_i$, and $\underline{\mathbf{r}}_i$ (i=0,...,N), defined in Figure 2.1. Indeed, from Figure 2.1 we have the following N equations in N+1 unknowns:

$$\underline{\rho}_k - \underline{\rho}_{k-1} = \underline{\mathbf{r}}_{k-1} - \underline{\mathbf{l}}_k \qquad k = 1,\ldots,N \qquad (2\text{-}3)$$

Since the $\underline{\rho}_k$ vectors are defined with respect to the system CM, it holds that:

$$\sum_{k=0}^{N} m_k \underline{\rho}_k = 0 \tag{2-4}$$

where m_k is the mass of body k. As shown in Appendix C, equations (2-3) and (2-4) can be solved to yield $\underline{\rho}_k$ as a function of $\underline{r}_k$ and $\underline{l}_k$. The result is:

$$\underline{\rho}_k = \sum_{i=1}^{k} (\underline{r}_{i-1} - \underline{l}_i)\,\mu_i \; - \sum_{i=k+1}^{N} (\underline{r}_{i-1} - \underline{l}_i)\,(1-\mu_i) \qquad k = 0,\ldots,N \tag{2-5}$$

where μ_i represents the mass distribution defined by:

$$\mu_i \equiv \begin{cases} 0 & i = 0 \\ \sum_{j=0}^{i-1} \frac{m_j}{M} & i = 1,\ldots,N \\ 1 & i = N+1 \end{cases} \tag{2-6}$$

M is the total system mass. As shown in Appendix C, Equation (2-5) can be written as the sum of mass-weighted vectors, each fixed in one of the N+1 bodies of the system. Although the resulting expression is quite complex, it can be simplified by using the notion of a body's barycenter (BC) defined in [29,72]. The barycenter of the i^{th} body can be found by adding a point mass equal to $M\mu_i$ to joint i, and a point mass equal to $M(1-\mu_{i+1})$ to joint i+1, forming an *augmented body* . The barycenter is then the center of mass of the augmented body as shown in Figure 2.2. The barycenter location for the i^{th} body with respect to its CM is defined by the body fixed vector $\underline{c}_i$ shown in Figure 2.2 and given by:

$$\underline{c}_i = \underline{l}_i\,\mu_i + \underline{r}_i\,(1-\mu_{i+1}) \qquad i = 0,\ldots,N \tag{2-7}$$

Figure 2.2 also shows a set of body-fixed vectors, called in this thesis *barycentric vectors*, which are defined by:

$$\underline{c}_i^{*} = -\,\underline{c}_i \tag{2-8a}$$

$$\underline{r}_i^* = \underline{r}_i - \underline{c}_i \tag{2-8b}$$

$$\underline{l}_i^* = \underline{l}_i - \underline{c}_i \tag{2-8c}$$

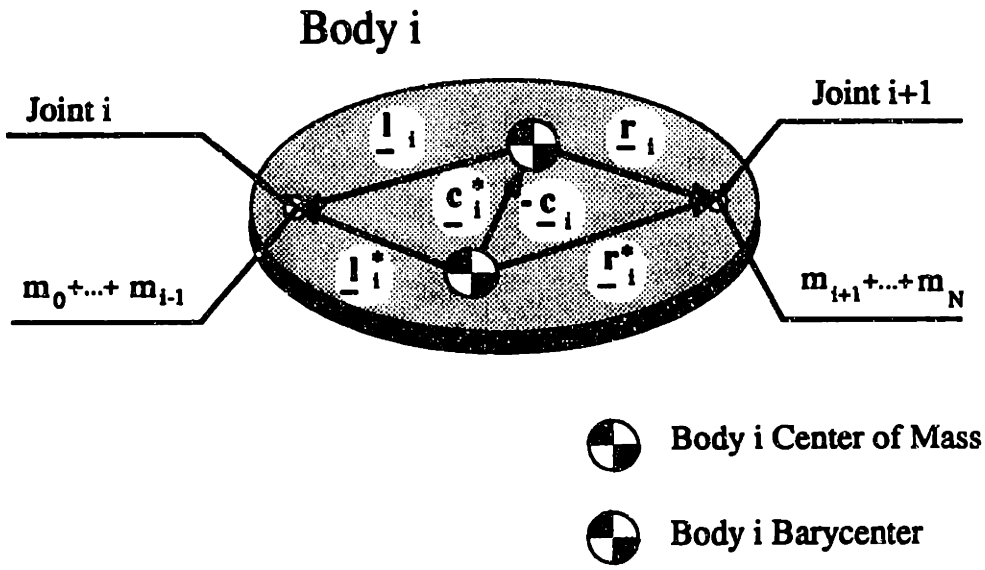

Figure 2.2. Barycenter and barycentric vectors

Using these definitions, Equation (2-5) can be written in a compact and general form as:

$$\underline{\rho}_k = \sum_{i=0}^{N} \underline{v}_{ik} \qquad k = 0,\ldots,N \tag{2-9}$$

where the barycentric vectors $\underline{v}_{ik}$ are given by the following expression, see Appendix C:

$$\underline{v}_{ik} \equiv \begin{cases} \underline{r}_i^* & i<k \\ \underline{c}_i^* & i=k \\ \underline{l}_i^* & i>k \end{cases} \tag{2-10}$$

Equation (2-9) plays a central role in the subsequent analysis, because it decomposes $\underline{\rho}_k$ to a set of N+1 independent body-fixed vectors and provides an easy way for its construction:

$\underline{\rho}_k$ is the sum of all the $\underline{l}_i^*$ before body k, the $\underline{c}_k^*$ of body k and all the $\underline{r}_i^*$ after body k[3]. Figure 2.3 shows the construction of $\underline{\rho}_k$ for k=3 and N=4. Further, Equation (2-9) reveals an interesting characteristic of space manipulators, namely that the position of the center of mass of link k in inertial space depends on the position of *all* links, including the ones *after* link k as well as on the position of the base. This is to be contrasted with the case of fixed-base manipulators where the position of a link depends on the positions of the *previous* links only.

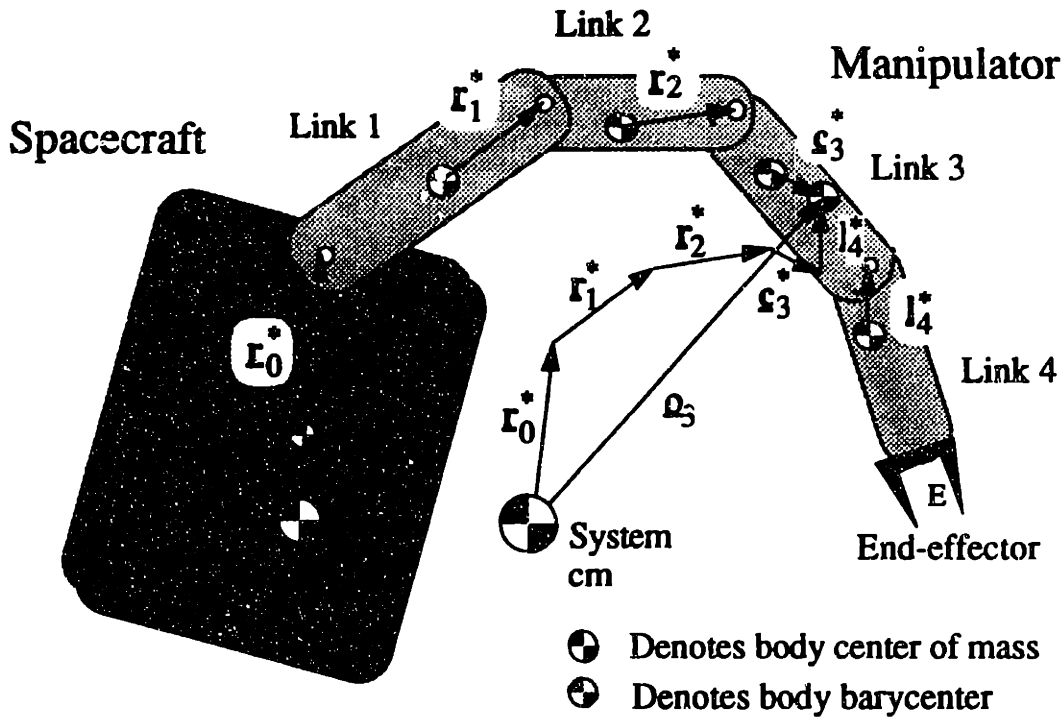

Figure 2.3. Construction of $\underline{\rho}_k$ for k=3 and N=4.

The expression for $\underline{\rho}_k$ can be substituted in Equations (2-1) and (2-2) to yield $\underline{\mathbf{R}}_k$ and $\underline{\mathbf{R}}_{k,m}$ as a vectorial sums of the vector pointing to the system CM and of a set of barycentric

[3]Equation (2-9) has similarities to the Virtual Manipulator (VM) constructed to the CM of body k. However, each VM link is equal to a sum of various body-fixed vectors, and therefore, it may result in unnecessary algebraic operations, especially when derivatives of $\underline{\rho}_k$ must be written.

vectors:

$$\begin{aligned} \underline{\mathbf{R}}_{k,m} &= \underline{\mathbf{r}}_{cm} + \underline{\rho}_k + \underline{\mathbf{r}}_{k,m} \\ &= \underline{\mathbf{r}}_{cm} + \sum_{i=0}^{N} \underline{\mathbf{v}}_{ik} + \underline{\mathbf{r}}_{k,m} \\ &= \underline{\mathbf{r}}_{cm} + \sum_{i=0}^{N} \underline{\mathbf{v}}_{ik,m} \end{aligned} \qquad (2\text{-}11)$$

where $\underline{\mathbf{v}}_{ik,m}$ just absorbs $\underline{\mathbf{r}}_{k,m}$, according to the formula:

$$\underline{\mathbf{v}}_{ik,m} = \underline{\mathbf{v}}_{ik} + \delta_{im}\, \underline{\mathbf{r}}_{k,m} \qquad i, k = 0,\ldots,N \qquad (2\text{-}12)$$

δ_{im} is a Kronecker delta. The end-effector position vector, $\underline{\mathbf{r}}_E$, can be written by applying Equations (2-11) and (2-12), noting that $\underline{\mathbf{r}}_{N,E} = \underline{\mathbf{r}}_N$:

$$\underline{\mathbf{r}}_E = \underline{\mathbf{r}}_{cm} + \sum_{i=0}^{N} \underline{\mathbf{v}}_{iN,E} \qquad (2\text{-}13)$$

This completes the closure analysis for a space system. Obviously, no vectorial equations can be written about the orientation of the bodies in the chain, because rotations are not vectors. These orientations can be described by transformation matrices, see Section 2.2.3. In the next section, expressions for the linear and angular velocities are written.

2.2.2 Linear/angular velocities of arbitrary points/bodies.

In order to write expressions for the linear velocities of arbitrary system points, derivatives of $\underline{\rho}_k$ must be obtained first. Since $\underline{\mathbf{v}}_{ik}$ is a body-fixed vector in body i, its time derivative is written using Equation (2-9) as:

$$\dot{\underline{\rho}}_k = \sum_{i=0}^{N} \underline{\omega}_i \times \underline{\mathbf{v}}_{ik} \qquad k = 0,\ldots,N \qquad (2\text{-}14)$$

Similarly, differentiating Equations (2-11) and (2-13) yields the following expression for the velocity of a point m in body k, $\dot{\underline{R}}_{k,m}$, and of the end-effector, $\dot{\underline{r}}_E$:

$$\dot{\underline{R}}_{k,m} = \dot{\underline{r}}_{cm} + \sum_{i=0}^{N} \underline{\omega}_i \times \underline{v}_{ik,m} \tag{2-15}$$

$$\dot{\underline{r}}_E = \dot{\underline{r}}_{cm} + \sum_{i=0}^{N} \underline{\omega}_i \times \underline{v}_{iN,E} \tag{2-16}$$

Expressions (2-15) and (2-16) can be written as functions of relative angular velocities which correspond to the controlled manipulator joint rates: the angular velocity $\underline{\omega}_k$ of the k^{th} body is written as a sum of relative angular velocities of body i with respect to body i-1, called $\underline{\omega}_i^{i-1}$, as:

$$\underline{\omega}_k = \underline{\omega}_0 + \sum_{i=1}^{k} \underline{\omega}_i^{i-1} \qquad j = 1,\ldots,N \tag{2-17}$$

where $\underline{\omega}_0$ is the spacecraft angular velocity. The end-effector angular velocity is obviously the angular velocity of the last link in the system and is given by:

$$\underline{\omega}_E = \underline{\omega}_0 + \sum_{i=1}^{N} \underline{\omega}_i^{i-1} \tag{2-18}$$

Equations (2-14), through (2-18) relate the linear and angular velocities of an arbitrary point and of the end-effector in inertial coordinates $\dot{\underline{R}}_{k,m}$, $\dot{\underline{r}}_E$ and $\underline{\omega}_k$, $\underline{\omega}_E$, to the controlled relative angular velocities $\underline{\omega}_i^{i-1}$, to the spacecraft angular velocity, $\underline{\omega}_0$, and to the system CM linear velocity $\dot{\underline{r}}_{cm}$.

2.2.3 Free-flying system differential kinematics - Jacobians

The vectorial description of the kinematics is very powerful and independent of specific frames of reference. However, for simulation and control design reasons, it is effective to

write the kinematic equations in matrix form, including the construction of Jacobians. The Jacobians derived in this section relate the input (independent) velocities of the system, namely the system CM linear velocity, the spacecraft angular velocity and the manipulator joint rates, to the output (dependent) velocities, namely the linear and angular velocities corresponding to any point of the system. To this end, Equations (2-15) to (2-18) must be expressed in matrix form. A reference frame with axes parallel to each body's principal axes is attached to each center of mass. The body inertia matrix expressed in this frame is diagonal. As noted in the List of Symbols Section, bold lower case symbols represent column vectors, bold upper case matrices. Right superscripts must be interpreted as "with respect to," left as "expressed in frame." A missing left superscript implies a column vector expressed in the inertial frame.

The 3×1 column vectors ${}^{i}\mathbf{v}_{ik}$ expressed in frame i are represented by a set of three constant numbers. These are transformed in the inertial frame as follows:

$$\mathbf{v}_{ik} = \mathbf{T}_i \, {}^{i}\mathbf{v}_{ik} = \mathbf{T}_0 \, {}^{0}\mathbf{v}_{ik} \tag{2-19a}$$

$${}^{0}\mathbf{v}_{ik} = {}^{0}\mathbf{T}_i \, {}^{i}\mathbf{v}_{ik} \tag{2-19b}$$

where $\mathbf{T}_i$ is a 3×3 transformation matrix that describes the orientation of the i^{th} frame with respect to the inertial frame. This matrix can be written as:

$$\mathbf{T}_i(\mathbf{e}, \mathbf{n}, q_1, \ldots, q_i) = \mathbf{T}_0(\mathbf{e}, \mathbf{n}) \, {}^{0}\mathbf{T}_i(q_1, \ldots, q_i) \tag{2-20a}$$

$${}^{0}\mathbf{T}_i(q_1, \ldots, q_i) = {}^{0}\mathbf{A}_1(q_1) \ldots {}^{i-1}\mathbf{A}_i(q_i) \tag{2-20b}$$

Note that ${}^{i-1}\mathbf{A}_i(q_i)$ transforms a column vector expressed in frame i to a column vector in frame i-1 and is a function of the relative joint angle of the two frames, q_i. The 3×3 transformation matrix $\mathbf{T}_0$ can be computed using the Euler parameters e and n [30]:

$$\mathbf{T}_0(\mathbf{e}, \mathbf{n}) = (\mathbf{n}^2 - \mathbf{e}^T\mathbf{e}) \, \mathbf{1} + 2 \, \mathbf{e} \, \mathbf{e}^T + 2 \, \mathbf{n} \, \mathbf{e}^{\times} \tag{2-21a}$$

$$e(\mathbf{a}, \theta) = \mathbf{a} \sin(\theta/2) \tag{2-21b}$$

$$n(\mathbf{a}, \theta) = \cos(\theta/2) \tag{2-21c}$$

where **a** is the unit vector of the instant axis about which the spacecraft is rotated for an angle θ, the ^{T} superscript denotes transposition, and the $^\times$ superscript denotes a skew-symmetric matrix that is formed from a vector **e** according to Equation (B-3). Note that $\mathbf{T}_0$ follows the definition used in robotics and not the one used in dynamics, where the matrix $\mathbf{T}_0^T$ is usually used. **1** is the 3×3 identity matrix. Other vectors transform in a similar way. For example, the position of the end-effector is written according to Equations (2-13) and (2-19) as:

$$\mathbf{r}_E = \mathbf{r}_{cm} + \mathbf{T}_0 \sum_{i=0}^{N} {}^0\mathbf{T}_i \, {}^i\mathbf{v}_{iN,E} \tag{2-22}$$

The scalar form of Equation (2-17) can now be written as:

$$\omega_k = \omega_0 + \omega_k^0 = \omega_0 + \mathbf{T}_0 \sum_{i=1}^{k} {}^0\mathbf{T}_i \, {}^i\mathbf{u}_i \, \dot{q}_i \tag{2-23a}$$

$$= \omega_0 + \mathbf{T}_0 \, {}^0\mathbf{F}_k \, \dot{\mathbf{q}} \qquad k = 1,\ldots,N \tag{2-23b}$$

where $^i\mathbf{u}_i$ is the unit column vector in frame i parallel to the revolute axis through joint i, and $^0\mathbf{F}_k$ is a 3×N matrix given by:

$${}^0\mathbf{F}_k \equiv [{}^0\mathbf{T}_1 \, {}^1\mathbf{u}_1, {}^0\mathbf{T}_2 \, {}^2\mathbf{u}_2, \ldots, {}^0\mathbf{T}_k \, {}^k\mathbf{u}_k, \mathbf{0}] \qquad k = 1,\ldots,N \tag{2-24}$$

where **0** is a 3×(N-k) zero element matrix, and:

$$\mathbf{q} = [q_1, q_2, \ldots, q_k, \ldots, q_N]^T \tag{2-25}$$

Using Equations (2-19) through (2-25), Equations (2-15) and (2-17) yield scalar expressions for the linear and angular velocities of an arbitrary point m on body k:

$$\dot{R}_{k,m} = \dot{r}_{cm} + T_0 \{ {}^0J_{11k,m}\, {}^0\omega_0 + {}^0J_{12k,m}\, \dot{q} \} \tag{2-26}$$

$$\omega_k = T_0 \{ {}^0\omega_0 + {}^0J_{22k,m}\, \dot{q} \} \tag{2-27}$$

where:

$${}^0J_{11k,m} \equiv -\sum_{i=0}^{N} [{}^0T_i\, {}^iv_{ik,m}]^{\times} \tag{2-28a}$$

$${}^0J_{12k,m} \equiv -\sum_{i=1}^{N} [{}^0T_i\, {}^iv_{ik,m}]^{\times}\, {}^0F_i \tag{2-28b}$$

$${}^0J_{22k,m} \equiv {}^0F_k \tag{2-28c}$$

Equations (2-26) and (2-27) reflect the fact that the motion of point m of body k is the sum of two partial velocities. The first is due to the motion of the joints, the second to the motion of the spacecraft with the joint angles fixed. ${}^0J_{11k,m}$ is a skew-symmetric 3×3 matrix whose elements correspond to the vector from the system CM to point m, expressed in the spacecraft frame. This can be understood by recalling that Jacobians are matrices that correspond to cross products of a position vectors with an angular velocities (products like $-r^{\times}\omega$). ${}^0J_{12k,m}$ and ${}^0J_{22k,m}$ are 3×N matrices describing the effect of joint motions on the motion of point m. All matrices in Equations (2-28) depend on the system configuration q, only. Expressions (2-26) and (2-27) can be combined in one single matrix equation as follows:

$$\dot{x}_{k,m} = \begin{bmatrix} \dot{R}_{k,m} \\ \omega_k \end{bmatrix} = J^{+}_{k,m} \begin{bmatrix} {}^0\dot{r}_{cm} \\ {}^0\omega_0 \\ \dot{q} \end{bmatrix} \tag{2-29}$$

where:

$$J^{+}_{k,m}(e,n,q) = \mathrm{diag}(T_0,T_0)\, {}^0J^{+}_{k,m}(q) \tag{2-30a}$$

$$ {}^0\mathbf{J}^+_{k,m}(\mathbf{q}) = \begin{bmatrix} \mathbf{1} & {}^0\mathbf{J}_{11k,m} & {}^0\mathbf{J}_{12k,m} \\ \mathbf{0} & \mathbf{1} & {}^0\mathbf{J}_{22k,m} \end{bmatrix} \tag{2-30b} $$

where $\mathbf{1}$ is the unity 3×3 matrix and $\mathbf{0}$, the zero 3×3 matrix[4]. ${}^0\mathbf{J}^+_{k,m}$ is a function of the barycentric vectors of the system, which are functions of the masses and geometry of all the system bodies, including the spacecraft, and of the configuration $\mathbf{q}$. $\mathbf{J}^+_{k,m}$ is a Jacobian matrix that relates the controlled variables to the linear and angular motion of a point m in body k. Its size is 6×(N+6), so even when N=6, it is a non-square matrix. This is due to the redundant nature of a free-flying space manipulator system: a point in space can be reached by either moving the end-effector or by moving the whole system. The dependence of $\mathbf{J}^+_{k,m}$ on the spacecraft attitude is expressed through the matrix $\mathbf{T}_0$, see Equation (2-30a). Note that these Jacobians are what Khatib calls *basic Jacobians*, that is Jacobians independent of the particular set used to describe end-effector orientation [33]. Kinematic equations relating attitude variables to angular velocities also must be used.

Similar equations can be written for the end-effector, by noting that body k in this case is body N and that point m is the end-effector point E. The subscripts N and E are dropped for simplicity and the resulting expressions are repeated here for future reference:

$$ \dot{\mathbf{r}}_E = \dot{\mathbf{r}}_{cm} + \mathbf{T}_0 \{ {}^0\mathbf{J}_{11}\, {}^0\boldsymbol{\omega}_0 + {}^0\mathbf{J}_{12}\, \dot{\mathbf{q}} \} \tag{2-31} $$

---

[4]This definition of the Jacobian does not follow the usual transformation rules. The appropriate definition would be:

$$ \mathbf{J}^+_{k,m}(e,n,q) = \mathrm{diag}(\mathbf{T}_0,\mathbf{T}_0)\, {}^0\mathbf{J}^+_{k,m}(q)\, \mathrm{diag}(\mathbf{T}_0,\mathbf{T}_0,\mathbf{1})^T $$

Such a $\mathbf{J}^+_{k,m}$ would map controlled velocities in the inertial frame to inertial velocities of point m in body k:

$$ \dot{\mathbf{x}}_{k,m} = \mathbf{J}^+_{k,m} \begin{bmatrix} \dot{\mathbf{r}}_{cm} \\ \boldsymbol{\omega}_0 \\ \dot{\mathbf{q}} \end{bmatrix} $$

However, in this thesis we assume that the controlled variables are defined in the spacecraft frame, hence we are interested in a map from spacecraft-measured velocities to inertial velocities.

$$\omega_E = T_0 \{ {}^0\omega_0 + {}^0J_{22}\,\dot{q} \} \tag{2-32}$$

where:

$${}^0J_{11} \equiv -\sum_{i=0}^{N} [{}^0T_i\, {}^iv_{iN,E}]^\times \tag{2-33a}$$

$${}^0J_{12} \equiv -\sum_{i=1}^{N} [{}^0T_i\, {}^iv_{iN,E}]^\times\, {}^0F_i \tag{2-33b}$$

$${}^0J_{22} \equiv {}^0F_N \tag{2-33c}$$

${}^0J_{11}$ is a skew-symmetric 3×3 matrix whose elements correspond to the vector from the system *CM* to the end-effector, expressed in the spacecraft frame. ${}^0J_{12}$ is a 3×N matrix whose N columns are the components of vectors starting at the manipulator joints and ending at the end-effector. Along with ${}^0J_{22}$, they correspond to the Jacobian of the end-effector Virtual Manipulator [65], with the first link fixed. (This is also equivalent to the Jacobian of a fixed attitude spacecraft). Again all matrices in Equations (2-33) depend on the system configuration **q**, only.

$$\dot{x} = \begin{bmatrix} \dot{r}_E \\ \omega_E \end{bmatrix} = J^+ \begin{bmatrix} {}^0\dot{r}_{cm} \\ {}^0\omega_0 \\ \dot{q} \end{bmatrix} \tag{2-34}$$

$$J^+(e,n,q) = \mathrm{diag}(T_0,T_0)\, {}^0J^+(q) \tag{2-35a}$$

$${}^0J^+(q) = \begin{bmatrix} 1 & {}^0J_{11} & {}^0J_{12} \\ 0 & 1 & {}^0J_{22} \end{bmatrix} \tag{2-35b}$$

Note that the rank of J^+ is always six, because its first six columns always contain six independent column vectors. This reflects the fact that even when the manipulator does not move, its end-effector can reach any position or orientation by moving the spacecraft alone. Of course, the same remark applies equally well to $J^+_{k,m}$.

As the system moves, T_0 must be updated. The new e and n are computed according to Equation (2-36) given below, see also [30]:

$$\dot{e} = 1/2 \, [\, e^{\times} + n \, \mathbf{1} \,] \, {}^0\omega_0 \tag{2-36a}$$

$$\dot{n} = -1/2 \, e^T \, {}^0\omega_0 \tag{2-36b}$$

Equations (2-30) and (2-34) describe the differential kinematics of any point in the system, including the end-effector. They will be used again later on.

2.3 MOMENTUM EQUATIONS

In this section, the linear and angular momentum equations are formulated. These become important when no external forces or torques act on the system, see chapter 3. Also, some of the equations of motion can be derived by differentiating momentum equations, thus avoiding the additional complexity of using quasi-coordinates [30,70].

2.3.1 Linear momentum

For the system shown in Figure 2.1, the linear momentum vector $\underline{p}$ with respect to the origin O is simply given by:

$$\underline{p} = M \, \dot{\underline{r}}_{cm} = \sum_{k=0}^{N} m_k \, \dot{\underline{R}}_k \tag{2-37}$$

The time derivative of the linear momentum results in the translational equations of motion for the system CM:

$$\dot{\underline{p}} = M \, \dot{\underline{r}}_{cm} = \underline{f}_{ext} \tag{2-38}$$

where $\underline{f}_{ext}$ is the resultant of the external forces acting on the system. If by $\underline{f}_{k,m}$ we denote the external force acting on point m of body k, then $\underline{f}_{ext}$ is given by:

$$\underline{f}_{ext} = \sum_{k=0}^{N} \sum_{m} \underline{f}_{k,m} \tag{2-39}$$

In other words, $\underline{f}_{ext}$ is the sum of all forces acting on all bodies at all points.

2.3.2 Angular momentum

The system angular momentum with respect to the inertial origin is given by:

$$\underline{h} = \sum_{k=0}^{N} \{ \underline{I}_k \cdot \underline{\omega}_k + m_k \underline{R}_k \times \dot{\underline{R}}_k \} \tag{2-40}$$

where $\underline{I}_k$ is the inertia dyadic of body k with respect to its center of mass. Using Equations (2-2) and (2-4) it is easy to show that $\underline{h}$ can be written as:

$$\underline{h} = \underline{r}_{cm} \times \underline{p} + \underline{h}_{cm} \tag{2-41a}$$

where $\underline{h}_{cm}$ is the angular momentum of the system with respect to its CM and is given by:

$$\underline{h}_{cm} = \sum_{k=0}^{N} \{ \underline{I}_k \cdot \underline{\omega}_k + m_k \underline{\rho}_k \times \dot{\underline{\rho}}_k \} \tag{2-41b}$$

Using Equations (2-9) and (2-14), $\underline{h}_{cm}$ can be written as:

$$\underline{h}_{cm} = \sum_{k=0}^{N} \underline{I}_k \cdot \underline{\omega}_k + \sum_{j=0}^{N} \sum_{i=0}^{N} \sum_{k=0}^{N} m_k \underline{v}_{ik} \times \underline{\omega}_j \times \underline{v}_{jk} \tag{2-42}$$

As shown in Appendix D, Equation (2-42) can be simplified to yield a very compact expression for $\underline{h}_{cm}$:

$$\underline{h}_{cm} = \sum_{j=0}^{N} \sum_{i=0}^{N} \underline{D}_{ij} \cdot \underline{\omega}_j \tag{2-43}$$

where the $\underline{D}_{ij}$ are inertia dyadics given by:

$$\underline{\mathbf{D}}_{ij} \equiv \begin{cases} -M\left\{(\underline{\mathbf{l}}_j^* \cdot \underline{\mathbf{r}}_i^*)\,\underline{\mathbf{1}} - \underline{\mathbf{l}}_j^*\,\underline{\mathbf{r}}_i^*\right\} & i<j \\ \underline{\mathbf{I}}_i + \sum_{k=0}^{N} m_k\left\{(\underline{\mathbf{v}}_{ik} \cdot \underline{\mathbf{v}}_{ik})\,\underline{\mathbf{1}} - \underline{\mathbf{v}}_{ik}\,\underline{\mathbf{v}}_{ik}\right\} & i=j \\ -M\left\{(\underline{\mathbf{r}}_j^* \cdot \underline{\mathbf{l}}_i^*)\,\underline{\mathbf{1}} - \underline{\mathbf{r}}_j^*\,\underline{\mathbf{l}}_i^*\right\} & i>j \end{cases} \tag{2-44}$$

where $\underline{\mathbf{1}}$ is the unit dyadic. Note that the inertia dyadics $\underline{\mathbf{D}}_{ij}$ are functions of the barycentric vectors only; once these are found, all other quantities, including $\underline{\mathbf{D}}_{ij}$, are easily derived. The dyadic $\underline{\mathbf{D}}_{ii}$ can be expanded further, see Equation (D-12b).

Next, the angular momentum, given by Equations (2-41a) and (2-45) is differentiated with respect to time, see Appendix D. If $\underline{\mathbf{n}}_{ext}$ is the resultant external torque acting on the system, and $\underline{\mathbf{n}}_{tot}$ is the total torque which includes the effect of external forces, then:

$$\begin{aligned} \dot{\underline{\mathbf{h}}} = \underline{\mathbf{n}}_{tot} = \underline{\mathbf{r}}_{cm} \times \underline{\mathbf{f}}_{ext} + \sum_{j=0}^{N}\sum_{i=0}^{N} \underline{\mathbf{D}}_{ij} \cdot \dot{\underline{\omega}}_j \quad + \\ + \sum_{j=0}^{N}\sum_{i=0}^{N} \underline{\omega}_j \times \underline{\mathbf{D}}_{ji} \cdot \underline{\omega}_j \quad + \\ + \sum_{j=0}^{N}\sum_{i=0}^{N} \hat{\underline{\mathbf{d}}}_{ij}\, \|\dot{\underline{\omega}}_j\|^2 \end{aligned} \tag{2-45}$$

where:

$$\underline{\mathbf{n}}_{tot} = \underline{\mathbf{n}}_{ext} + \sum_{k=0}^{N}\sum_{m} \underline{\mathbf{R}}_{k,m} \times \underline{\mathbf{f}}_{k,m} \tag{2-46}$$

$$\underline{\mathbf{n}}_{ext} = \sum_{k=0}^{N}\sum_{m} \underline{\mathbf{n}}_{k,m} \tag{2-47}$$

and:

$$\hat{\underline{\mathbf{d}}}_{ij} \equiv \begin{cases} -M\,(\underline{\mathbf{l}}_j^* \times \underline{\mathbf{r}}_i^*) & i<j \\ \mathbf{0} & i=j \\ -M\,(\underline{\mathbf{r}}_j^* \times \underline{\mathbf{l}}_i^*) & i>j \end{cases} \tag{2-48}$$

Equation (2-45) is the equivalent of the Euler equations for a single rigid body. Its form is very compact and demonstrates once more the importance of the barycentric vectors, since all other quantities depend on them.

2.3.3 Scalar momentum equations

Developing the matrix form of the linear momentum equation is straightforward, see Equations (2-37) and (2-38). Using the transformation properties found in Appendix B (Section B.6), Equation (2-43) is written as:

$$\mathbf{h}_{cm} = \mathbf{T}_0 \left({}^0\mathbf{D}\, {}^0\boldsymbol{\omega}_0 + {}^0\mathbf{D}_q\, \dot{\mathbf{q}} \right) \tag{2-49}$$

where for simplicity the following defining equations were used:

$${}^0\mathbf{D}_j \equiv \sum_{i=0}^{N} {}^0\mathbf{D}_{ij} \qquad (j = 0,\ldots,N) \tag{2-50a}$$

$${}^0\mathbf{D} \equiv \sum_{j=0}^{N} {}^0\mathbf{D}_j \tag{2-50b}$$

$${}^0\mathbf{D}_q \equiv \sum_{j=1}^{N} {}^0\mathbf{D}_j\, {}^0\mathbf{F}_j \tag{2-50c}$$

$${}^0\mathbf{D}_{qq} \equiv \sum_{j=1}^{N} {}^0\mathbf{F}_i^T\, {}^0\mathbf{D}_j\, {}^0\mathbf{F}_j \tag{2-50d}$$

${}^0\mathbf{D}$ is the 3×3 inertia matrix of the entire system as seen from the system CM, expressed in the spacecraft frame, and as such it is a positive definite symmetric matrix. ${}^0\mathbf{D}_q$ is a 3×N matrix which corresponds to the inertia of the system's moving parts. ${}^0\mathbf{D}_{qq}$ is an N×N matrix which will be used in Equation (2-57). The mixed inertia matrices ${}^0\mathbf{D}_{ij}$ (i,j=0,…,N) correspond to the mixed inertia dyadics, and are derived from Equation (2-44) with the help of identities from Section B.6, Appendix B. For example, ${}^0\mathbf{D}_{ij}$ (i<j) is given by:

$$ {}^0\mathbf{D}_{ij}(q_1,\ldots,q_j) = -M\,({}^0\mathbf{r}_i^*)^{\times}({}^0\mathbf{l}_j^*)^{\times} \qquad i<j \qquad (2\text{-}51a) $$

$$ = -M\,{}^0\mathbf{T}_i\,({}^i\mathbf{r}_i^*)^{\times}\,{}^i\mathbf{A}_j\,({}^j\mathbf{l}_j^*)^{\times}\,{}^0\mathbf{T}_j^T \qquad i<j \qquad (2\text{-}51b) $$

Since ${}^i\mathbf{r}_i^*$, ${}^j\mathbf{l}_j^*$ are constants, ${}^0\mathbf{D}_{ij}$ is a function of $(q_1,\ldots,q_j)$ $(i<j)$, see also Equations (2-20). Similarly, ${}^0\mathbf{D}_{ii}$ is a function of $(q_1,\ldots,q_i)$. Then, all inertia matrices in Equations (2-50) are functions of the system configuration $\mathbf{q}$. Due to Equation (2-51), the following is true:

$$ {}^0\mathbf{D}_{ij}^T = {}^0\mathbf{D}_{ji} \qquad i, j = 0,\ldots,N \qquad (2\text{-}52) $$

Of interest is also the time derivative of the angular momentum with respect to system CM, $\mathbf{h}_{cm}$. This can be done by transforming Equation (2-45) in matrix form using Equations (2-23), (2-24). The external torque $\mathbf{n}_{tot}$ in Equation (2-46) is written as:

$$ \mathbf{n}_{tot} = \mathbf{n}_{ext} + \mathbf{r}_{cm}^{\times}\,\mathbf{f}_{ext} + \mathbf{T}_0 \sum_{k=0}^{N} \sum_{m} {}^0\mathbf{J}_{1\,1k,m}^T\,{}^0\mathbf{f}_{k,m} \qquad (2\text{-}53) $$

where $\mathbf{f}_{ext}$ is the resultant of all the forces applied on the system, see Equation (2-39). The second term in Equation (2-53) cancels the first term in Equation (2-45) and the result is:

$$ \dot{\mathbf{h}}_{cm} = \mathbf{T}_0\,\{{}^0\mathbf{D}\,{}^0\dot{\omega}_0 + {}^0\mathbf{D}_q\,\ddot{\mathbf{q}} + \mathbf{C}_1^+(\mathbf{q}, {}^0\omega_0, \dot{\mathbf{q}})\} $$

$$ = \mathbf{T}_0 \sum_{k=0}^{N} \sum_{m} \{{}^0\mathbf{n}_{ext} + {}^0\mathbf{J}_{1\,1k,m}^T\,{}^0\mathbf{f}_{k,m}\} \qquad (2\text{-}54) $$

$\mathbf{C}_1^+$ is a 3×1 vector containing the nonlinear terms in velocities; since this term is very complex, only the linear acceleration terms are provided explicitly.

2.4 EQUATIONS OF MOTION

In this section, the equations of motion are derived for rigid link free-flying manipulator

systems. The approach taken is based on Lagrange's equations, because constraint forces and torques are automatically eliminated. They also yield a minimum number of equations, equal to the number of generalized variables. Their drawback is that in the general case, it is quite involved to differentiate the Lagrangian of the system and obtain "closed form" equations. However, in this thesis we are primarily interested in the structure of the dynamics of space systems, and Lagrange's method serves ideally this purpose. In the case of a planar N DOF system, closed form equations of motion are obtained explicitly.

In order to form the Lagrangian of the system, we need an expression for the kinetic energy of the system. The potential energy due to gravity is zero and since the system is assumed to be rigid, the potential energy due to flexibility is also zero. The kinetic energy T, of a space manipulator system is:

$$T = \frac{1}{2} M \, \underline{\dot{r}}_{cm} \cdot \underline{\dot{r}}_{cm} + \frac{1}{2} \sum_{k=0}^{N} \{ \, \underline{\omega}_k \cdot \underline{\mathbf{I}}_k \cdot \underline{\omega}_k + m_k \, \underline{\dot{\rho}}_k \cdot \underline{\dot{\rho}}_k \, \} \tag{2-55}$$

where all terms have been defined previously. Using summation properties, and Equations (2-14), (A-8), and (D-8), it is relatively easy to show that the kinetic energy can be compactly written in the form:

$$T = \frac{1}{2} M \, \underline{\dot{r}}_{cm} \cdot \underline{\dot{r}}_{cm} + \frac{1}{2} \sum_{j=0}^{N} \sum_{i=0}^{N} \underline{\omega}_i \cdot \underline{\mathbf{D}}_{ij} \cdot \underline{\omega}_j \tag{2-56}$$

where the first part represents the translational energy of the system and the second part, the rotational energy, which is also the energy of the system with respect to its CM.

In order to use Lagrange's equations, we need the kinetic energy in matrix form. Using Equations (B-6), (2-23), and (2-50), the kinetic energy can be written as:

$$T = \frac{1}{2} M \, \dot{\mathbf{r}}_{cm}^T \dot{\mathbf{r}}_{cm} + \frac{1}{2} {}^0\omega_0^T \, {}^0\mathbf{D} \, {}^0\omega_0 + {}^0\omega_0^T \, {}^0\mathbf{D}_q \, \dot{\mathbf{q}} + \frac{1}{2} \dot{\mathbf{q}}^T \, {}^0\mathbf{D}_{qq} \, \dot{\mathbf{q}} \tag{2-57a}$$

It can be written also in the more usual form as:

$$T = \frac{1}{2} \left[{}^0\dot{\mathbf{r}}_{cm}^T, {}^0\boldsymbol{\omega}_0^T, \dot{\mathbf{q}}^T \right] \mathbf{H}^+(\mathbf{q}) \begin{bmatrix} {}^0\dot{\mathbf{r}}_{cm} \\ {}^0\boldsymbol{\omega}_0 \\ \dot{\mathbf{q}} \end{bmatrix} \tag{2-57b}$$

where $\mathbf{H}^+(\mathbf{q})$ is given by:

$$\mathbf{H}^+(\mathbf{q}) = \begin{bmatrix} \mathbf{M1} & \mathbf{0} & \mathbf{0} \\ \mathbf{0} & {}^0\mathbf{D}(\mathbf{q}) & {}^0\mathbf{D}_{\mathbf{q}}(\mathbf{q}) \\ \mathbf{0} & {}^0\mathbf{D}_{\mathbf{q}}(\mathbf{q})^T & {}^0\mathbf{D}_{\mathbf{qq}}(\mathbf{q}) \end{bmatrix} \tag{2-58}$$

where **1** is the unit matrix. The inertia matrix $\mathbf{H}^+(\mathbf{q})$ is obviously positive definite symmetric and its size is (N+6)×(N+6). It depends upon the mass and inertia properties of the system and is a function of the configuration **q** only. In other words, the spacecraft attitude is an *ignorable* variable. This fact will be used later.

The generalized forces required in the Lagrangian approach are found using the principle of virtual work. The virtual work that corresponds to the forces applied on the system is given by:

$$\begin{aligned} \delta W &= \boldsymbol{\tau}^T \delta \mathbf{q} + \sum_{k,m} \left[{}^0\mathbf{f}_{k,m}, {}^0\mathbf{n}_{k,m} \right]^T {}^0\delta \mathbf{x}_{k,m} \\ &= \mathbf{Q}_r^T {}^0\delta \mathbf{r}_{cm} + \mathbf{Q}_\theta^T \mathbf{a} \delta\theta + \mathbf{Q}_q^T \delta \mathbf{q} \end{aligned} \tag{2-59}$$

where $\boldsymbol{\tau}$ is an N×1 torque vector, **a** is an instantaneous axis of rotation, $\delta\theta$ the corresponding angle of rotation, see [30], $\mathbf{Q}_r$, $\mathbf{Q}_\theta$, $\mathbf{Q}_q$ are generalized forces corresponding to translation of the whole system, to rotation around the CM and to change in the configuration, and ${}^0\mathbf{f}_{k,m}$ and ${}^0\mathbf{n}_{k,m}$ is the force and torque acting on point m of body k, as measured (seen) from the spacecraft. The ${}^0\delta\mathbf{x}_{k,m}$ term is the virtual displacement of point m in body k and can be written with the help of Equation (2-29) as:

$$ {}^0\delta x_{k,m} = {}^0J^+_{k,m} \begin{bmatrix} {}^0\delta r_{cm} \\ a\delta\theta \\ \delta q \end{bmatrix} \tag{2-60} $$

where ${}^0J^+_{k,m}$ is a Jacobian given by Equation (2-30b). In this case the Jacobian represents the cross product $r^{\times}f$, that is it represents the lever of a force **f**. Equations (2-59) and (2-60) can be combined to yield the generalized forces:

$$ Q \equiv \begin{bmatrix} Q_r \\ Q_\theta \\ Q_q \end{bmatrix} = \begin{bmatrix} 0 \\ 0 \\ \tau \end{bmatrix} + \sum_{k=0}^{N} \sum_{m} \left\{ {}^0J^+_{k,m}(q) \right\}^T \begin{bmatrix} {}^0f_{k,m} \\ {}^0n_{k,m} \end{bmatrix} \tag{2-61a} $$

If some of the forces are defined or measured in the i^{th} frame, then ${}^0f_{k,m}$ can be replaced by ${}^0T_i\,{}^if_{k,m}$. The same observations hold for the applied torques. In particular, if a force is measured in the inertial frame, this procedure yields:

$$ Q \equiv \begin{bmatrix} Q_r \\ Q_\theta \\ Q_q \end{bmatrix} = \begin{bmatrix} 0 \\ 0 \\ \tau \end{bmatrix} + \sum_{k=0}^{N} \sum_{m} \left\{ J^+_{k,m}(e, n, q) \right\}^T \begin{bmatrix} f_{k,m} \\ n_{k,m} \end{bmatrix} \tag{2-61b} $$

Note that the generalized forces, **Q**, are in general a function of the spacecraft attitude (**e**, **n**) and of the system configuration **q**. This results in a coupled system. However, in some cases decoupling of the equations of motion can be achieved. One such case occurs when no external forces act on the system; this case will be examined thoroughly in Chapter 3.

Lagrange's equations will be used to write the system's equations of motion. However, as noted in [30], Lagrange's equations are not well suited for problems involving three-dimensional rigid body rotations[5]. *Quasi-coordinates* can be used, but the

---

[5]Note that after eliminating the matrix T_0, Equation (2-54) can be written as:

$$ {}^0D\,{}^0\dot{\omega}_0 + {}^0D_q\,\ddot{q} + C^+_1(q, {}^0\omega_0, \dot{q}) = Q_\theta $$

process is cumbersome [39]. It is much simpler to use momentum equations to derive that part of equations that corresponds to differentiation of T with respect to ${}^0\omega_0$. To this end, Equation (2-45) or (2-54) can be used. The result follows:

$$\mathbf{H}^+(\mathbf{q}) \begin{bmatrix} {}^0\ddot{\mathbf{r}}_{cm} \\ {}^0\dot{\boldsymbol{\omega}}_0 \\ \ddot{\mathbf{q}} \end{bmatrix} + \mathbf{C}^+(\mathbf{q}, {}^0\boldsymbol{\omega}_0, \dot{\mathbf{q}}) = \mathbf{Q} \tag{2-62}$$

where the inertia matrix $\mathbf{H}^+(\mathbf{q})$ is given by Equation (2-58) and the nonlinear terms in the equations of motion have the form:

$$\mathbf{C}^+(\mathbf{q}, {}^0\boldsymbol{\omega}_0, \dot{\mathbf{q}}) = \begin{bmatrix} \mathbf{0} \\ \mathbf{C}_1^+(\mathbf{q}, {}^0\boldsymbol{\omega}_0, \dot{\mathbf{q}}) \\ \mathbf{C}_2^+(\mathbf{q}, {}^0\boldsymbol{\omega}_0, \dot{\mathbf{q}}) \end{bmatrix} \tag{2-63}$$

Equation (2-62) represent N+6 equations and it describes in the most general way the motion of a free-flying manipulator system under the effect of external forces and torques and internal actuator torques. The first term in the left side of Equation (2-62) is an inertia matrix times an acceleration vector, while the second term contains all the centripetal and Coriolis terms. The first three equations are just Equations (2-38) written in the spacecraft frame. If all the external forces are defined in one frame, these three equations are totally decoupled from the rotational equations. For example, if the external forces are the ones due to the spacecraft actuators, then the translational equations are decoupled. If all external forces are zero, these three equations can be integrated twice. If integrated once,

---

This equation would also result from a *quasi-Lagrangian* formulation of the equations of motion, by noting that T is not a function of the spacecraft attitude, see also [30]:

$$\frac{d}{dt}\left\{\frac{\partial T}{\partial {}^0\boldsymbol{\omega}_0}\right\} - 0 = {}^0\mathbf{D}\,{}^0\dot{\boldsymbol{\omega}}_0 + {}^0\mathbf{D}_q\,\ddot{\mathbf{q}} + \mathbf{C}_1^+(\mathbf{q}, {}^0\boldsymbol{\omega}_0, \dot{\mathbf{q}}) = \mathbf{Q}_\theta$$

Lagrange's equations corresponding to the q's are straightforward.

they result in the statement that the system CM moves with constant velocity. This is a *first integral of motion* and will be used in Chapter 3. The next three equations of motion correspond to the Euler equations for a multibody system; if there is no manipulator on the spacecraft, they result in the Euler equations for a rigid body. If all external forces and torques are zero, these equations can be integrated to yield a *second integral of motion.* Again, this integral will be used in Chapter 3. The remaining N equations describe the motion of the manipulator, coupled to its spacecraft. If the spacecraft does not move, they result in equations of motion of a manipulator with a fixed base. Of course, in order to estimate a spacecraft's attitude expressed by the transformation matrix $\mathbf{T}_0$, Equations (2-22) and (2-36) must be used.

2.5 PLANAR SYSTEMS

The equations of motion of a space manipulator are complex. However, they simplify significantly for planar systems. This happens for the following reasons: First, all inertia matrices become scalars, equal to the inertia of a body around an axis perpendicular to the plane of motion. Second, the mixed inertia dyadics given by Equation (2-51) reduce to the product of two barycentric vectors, each one expressed in its home frame, times the cosine of the relative angle. If the center of mass of each individual link lies on the line that connects the two body joints, in other words if the barycentric vectors only have an x-component in their home frame, see Figure 2.4, then the ${}^0\mathbf{D}_{ij}$ matrices reduce to the d_{ij} scalars given by:

$$d_{ij} = -M r_i^* l_j^* \cos(\theta_j - \theta_i) = -M r_i^* l_j^* \cos(q_{i+1}+\ldots+q_j) \qquad i<j \qquad (2\text{-}64a)$$

$$d_{ii} = I_i + (m_0+\ldots+m_{i-1})(l_i^*)^2 + m_i (c_i^*)^2 + (m_i+\ldots+m_N)(r_i^*)^2 \qquad (2\text{-}64b)$$

$$d_{ij} = -M r_i^* l_j^* \cos(\theta_j - \theta_i) = -M l_i^* r_j^* \cos(q_{j+1}+\ldots+q_i) \qquad i>j \qquad (2\text{-}64c)$$

where, the left superscript was dropped for simplicity. It is obvious again that once the barycentric vectors are found, the required inertia matrices follow very easily. Using the parallel-axes theorem, it is easy to see that d_{ii} corresponds to the inertia of the augmented body. Third, cross products like the one in Equation (2-45) are zero.

In order to find the equations of motion of planar systems, Equations (2-62) can be used directly. However, additional compactness can be gained if the absolute angular velocities $\dot{\theta}_i$ are used in writting the nonlinear terms of planar systems, see Figure 2.4. Equations relating the absolute to the relative velocities, $\dot{q}_i$, can be introduced at a later stage. To this end, a slightly different procedure than the one used before is employed here.

The translational part of the Lagrangian yields trivial translational equations of motion for the system CM, and hence it is neglected temporarily. The rotational part of the Lagrangian of a planar system is written using Equations (2-56) and (2-64):

$$T = \frac{1}{2} \sum_{j=0}^{N} \sum_{i=0}^{N} d_{ij} \dot{\theta}_i \dot{\theta}_j \tag{2-65}$$

Lagrange's equations can be used directly. For simplicity, all external forces and torques are assumed temporarily equal to zero. From Figure 2.4, the net torque acting on link i is equal to $\tau_i - \tau_{i+1}$. Then, Lagrange's equations result in:

$$\frac{d}{dt}\left\{\frac{\partial T}{\partial \dot{\theta}_i}\right\} - \frac{\partial T}{\partial \theta_i} = \tau_i - \tau_{i+1} \qquad i = 0,\ldots,N \tag{2-66}$$

The first term in the above equation is written as:

$$\frac{d}{dt}\left\{\frac{\partial T}{\partial \dot{\theta}_i}\right\} = \frac{d}{dt}\sum_{j=0}^{N} d_{ij} \dot{\theta}_j = \sum_{j=0}^{N} d_{ij} \dot{\theta}_j - \sum_{j=0}^{N} \hat{d}_{ij} \dot{\theta}_j (\dot{\theta}_j - \dot{\theta}_i) \tag{2-67}$$

where $\hat{d}_{ij}$ are defined by:

$$\hat{d}_{ij} \equiv -M r_i^* l_j^* \sin(\theta_j - \theta_i) = -M r_i^* l_j^* \sin(q_{i+1}+\ldots+q_j) \qquad i<j \qquad (2\text{-}68a)$$

$$\hat{d}_{ii} \equiv 0 \qquad (2\text{-}68b)$$

$$\hat{d}_{ij} \equiv -M l_i^* r_j^* \sin(\theta_j - \theta_i) = M l_i^* r_j^* \sin(q_{j+1}+\ldots+q_i) \qquad i>j \qquad (2\text{-}68c)$$

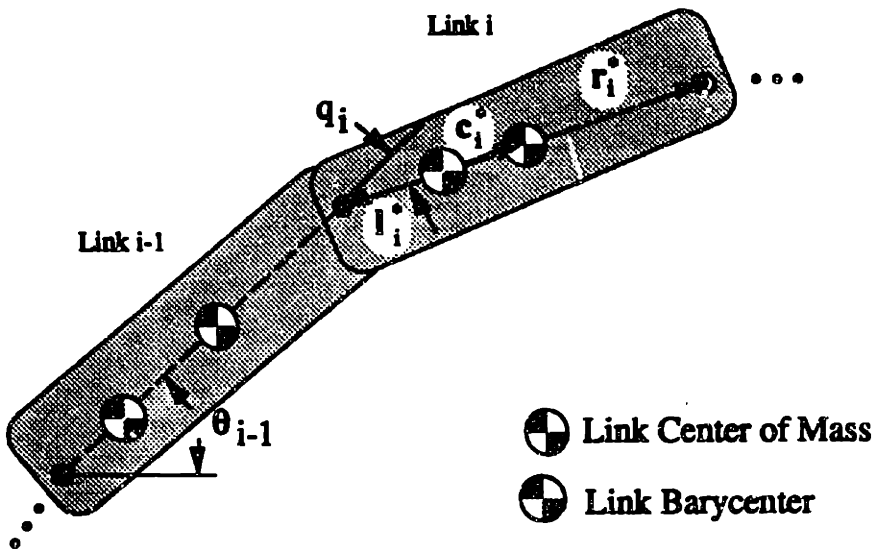

Figure 2.4. Definitions for planar systems.

The second term in Equation (2-66) is written as:

$$\frac{\partial T}{\partial \theta_i} = \frac{\partial}{\partial \theta_i} \sum_{j=0}^{N} \sum_{i>j}^{N} d_{ij} \dot{\theta}_i \dot{\theta}_j = \dot{\theta}_i \sum_{j=0}^{N} \hat{d}_{ij} \dot{\theta}_j \qquad (2\text{-}69)$$

Combining Equations (2-66), (2-67) and (2-69), the equation of motion for body i is written as:

$$\sum_{j=0}^{N} d_{ij} \ddot{\theta}_j - \sum_{j=0}^{N} \hat{d}_{ij} \dot{\theta}_j^2 = \tau_i - \tau_{i+1} \qquad i = 0,\ldots N \qquad (2\text{-}70)$$

The above equation is summed from i=k to i=N and the result is a set of N equations with inputs just the τ_i's:

$$\sum_{i=k}^{N}\sum_{j=0}^{N} d_{ij}\,\ddot{\theta}_j - \sum_{i=k}^{N}\sum_{j=0}^{N} \hat{d}_{ij}\,\dot{\theta}_j^2 = \tau_k \qquad k = 1,\ldots,N \qquad (2\text{-}71)$$

For k=0, a similar in form equation results. However, this is more important because it is actually the time derivative of the angular momentum of the system:

$$\sum_{i=0}^{N}\sum_{j=0}^{N} d_{ij}\,\ddot{\theta}_j - \sum_{i=0}^{N}\sum_{j=0}^{N} \hat{d}_{ij}\,\dot{\theta}_j^2 = 0 \qquad (2\text{-}72)$$

This equation could have been directly written using Equation (2-45). Indeed, the first term on its right side corresponds to the second term of Equation (2-72). The third term in the right side of Equation (2-45) is zero for a planar system, while its fourth term corresponds to the second term of Equation (2-72). Equations (2-70) and (2-71) can be easily written as a function of the q's. All ${}^{k}\mathbf{u}_k$ in Equation (2-24) are equal to $[0\ 0\ 1]^T$. Then, the ${}^{0}\mathbf{F}_k$ matrices are simplified to a 1×N matrix with k 1's and dropping the superscript (^{0}):

$$\mathbf{F}_k = [1, 1,\ldots, 1, 0,\ldots, 0] \qquad k = 1,\ldots,N \qquad (2\text{-}73)$$

where there are k 1's. Equation (2-23b) is then simplified to:

$$\dot{\theta}_k = \dot{\theta} + \mathbf{F}_k\,\dot{\mathbf{q}} = \dot{\theta} + \sum_{m=1}^{k} \dot{q}_m \qquad k = 1,\ldots,N \qquad (2\text{-}74)$$

where $\dot{\theta}$ is the spacecraft angular velocity. Equations (2-74) are substituted in Equations (2-71) and (2-72), and using the summation property used in Equation (C-5), the following results are obtained:

$$ {}^0D = D = \sum_{i=0}^{N} \sum_{j=0}^{N} d_{ij} \tag{2-75a} $$

$$ [{}^0D_q]_m = [D_q]_m = \sum_{i=m}^{N} \sum_{j=0}^{N} d_{ij} \qquad m = 1,\ldots,N \tag{2-75b} $$

$$ [{}^0D_{qq}]_{k,m} = [D_{qq}]_{k,m} = \sum_{i=k}^{N} \sum_{j=l}^{N} d_{ij} \qquad k,m = 1,\ldots,N \tag{2-75c)c} $$

$$ H^+(q) = \begin{bmatrix} M & 0 & 0 & 0 \\ 0 & M & 0 & 0 \\ 0 & 0 & D & D_q \\ 0 & 0 & D_q^T & D_{qq} \end{bmatrix} \tag{2-76} $$

where the symbol $[\bullet]_{m,n}$ stands for the k,m element of the matrix $\bullet$. The left superscript $({}^0)$ is dropped here because all the elements are independent of θ, the spacecraft attitude. Note that the inertia matrix of the system is just the matrix given by Equation (2-58), written for a planar system. For planar systems, $H^+(q)$ is a $(N+3)\times(N+3)$ matrix.

The nonlinear terms can be found explicitly using the same procedure as above. However, it is better to substitute Equation (2-74) in (2-71) and (2-72) without expanding the nonlinear terms, since such an operation is quite error-prone. Such an expansion is performed only in the worked examples. The nonlinear terms in the general Equation (2-62) are written by inspection from Equations (2-71) and (2-72):

$$ C_1^+ = c_1^+ = -\sum_{i=0}^{N} \sum_{j=0}^{N} \hat{d}_{ij} \dot{\theta}_j^2 \tag{2-77a} $$

$$ [C_2^+]_m = -\sum_{i=m}^{N} \sum_{j=0}^{N} \hat{d}_{ij} \dot{\theta}_j^2 \qquad m = 1,\ldots,N \tag{2-77b} $$

and:

$$C^+(q,\dot{\theta},\dot{q}) = \begin{bmatrix} 0 \\ c_1^+(q,\dot{\theta},\dot{q}) \\ C_2^+(q,\dot{\theta},\dot{q}) \end{bmatrix} \tag{2-77c}$$

Adding the generalized forces, the general equations of motion for a planar system follow:

$$H^+(q)\begin{bmatrix} {}^0\ddot{x}_{cm} \\ {}^0\ddot{y}_{cm} \\ \ddot{\theta} \\ \ddot{q} \end{bmatrix} + C^+(q,\dot{\theta},\dot{q}) = Q(\theta, q) \tag{2-78}$$

Two examples that demonstrate the kinematic and dynamic modeling of free-flying manipulators follow. A more detailed exposition of these examples can be found in Appendix E.

2.5.1 A one DOF manipulator example

A one DOF manipulator (N=1) on a three DOF spacecraft is assumed here, see Figure 2.5. Hence, the independent variables are the system CM position, $({}^0x_{cm}, {}^0y_{cm})$, the spacecraft attitude, θ, and the joint angle q. This example will be used to demonstrate the various forms that equations of motion can assume depending on the operating conditions.

As shown in Appendix E, the equations of motion for this system are:

$$M\,{}^0\ddot{x}_{cm} = Q_x \tag{2-79a}$$

$$M\,{}^0\ddot{y}_{cm} = Q_y \tag{2-79b}$$

$$D\ddot{\theta} + D_q\ddot{q} - (2\,\dot{\theta}\,\dot{q} + \dot{q}^2)\,\hat{d}_{01} = Q_\theta \tag{2-79c}$$

$$D_q\ddot{\theta} + D_{qq}\ddot{q} + \dot{\theta}^2\,\hat{d}_{01} = Q_q \tag{2-79d}$$

where $\dot{\theta}$ is the spacecraft angular velocity, M is the total mass, Q's are generalized forces, and all D-terms are inertia terms that depend on the joint angle q. Detailed definitions of all

terms involved are provided in Appendix E.

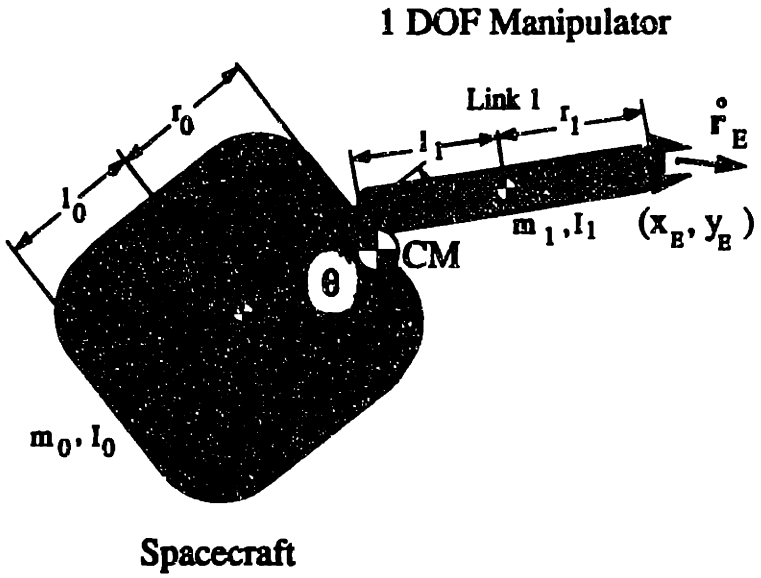

Figure 2.5. A one-DOF manipulator on a three-DOF spacecraft.

2.5.2 A two DOF manipulator example

In this section, the basic equations describing a two DOF system on a 3 DOF spacecraft are presented, see Figure 2.6. The independent variables are the system CM position, (${}^0x_{cm}$, ${}^0y_{cm}$), the spacecraft attitude, θ, and the manipulator joint angles q_1 and q_2. A detailed derivation can be found in Appendix E. This system is capable of demonstrating some interesting characteristics of space manipulators.

1. Kinematics. The end-effector position and orientation are written using Eq. (2-22):

$$x_E = x_{cm} + \alpha \cos(\theta) + \beta \cos(\theta+q_1) + \gamma \cos(\theta+q_1+q_2) \qquad (2\text{-}80a)$$

$$y_E = y_{cm} + \alpha \sin(\theta) + \beta \sin(\theta+q_1) + \gamma \sin(\theta+q_1+q_2) \qquad (2\text{-}80b)$$

$$\theta_E = \theta+q_1+q_2 \qquad (2\text{-}80c)$$

where α, β, γ, are lengths of barycentric vectors and are defined in Appendix E.

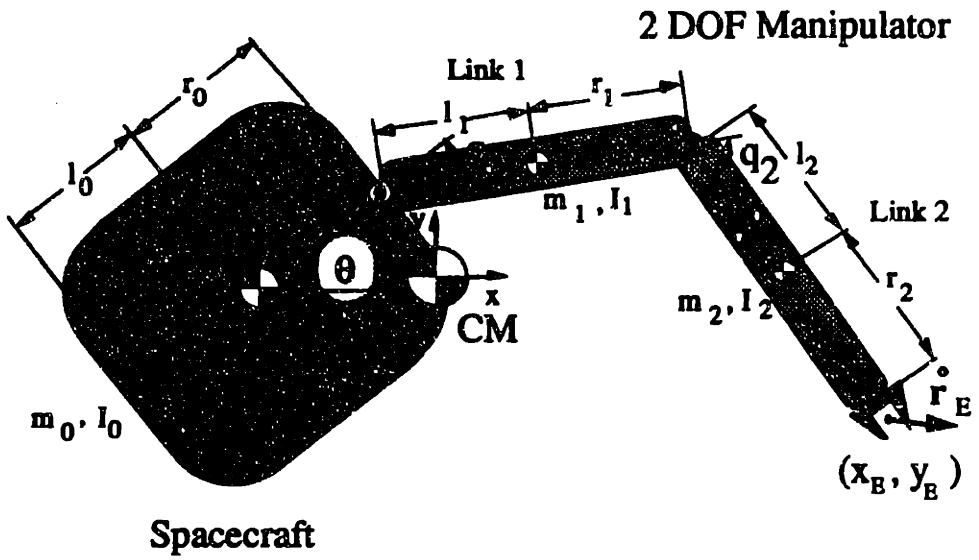

Figure 2.6. A two-DOF space manipulator system on a three-DOF spacecraft.

2. Differential kinematics. The Jacobian submatrices in Equation (2-33) are given by:

$$ {}^0\mathbf{J}_{11} = \begin{bmatrix} -\beta s_1 - \gamma s_{12} \\ \alpha + \beta c_1 + \gamma c_{12} \end{bmatrix} \quad {}^0\mathbf{J}_{12} = \begin{bmatrix} -\beta s_1 - \gamma s_{12} & -\gamma s_{12} \\ \beta c_1 + \gamma c_{12} & \gamma c_{12} \end{bmatrix} \quad {}^0\mathbf{J}_{22} = [1 \quad 1] \tag{2-81} $$

where $s_1 \equiv \sin(q_1)$, $c_{12} \equiv \cos(q_1+q_2)$ etc. The Jacobian $\mathbf{J}^+$ relating the end-effector motion to the controlled velocities is written using Equations (2-35):

$$ \mathbf{J}^+(\theta, \mathbf{q}) = \begin{bmatrix} \cos(\theta) & -\sin(\theta) & 0 \\ \sin(\theta) & \cos(\theta) & 0 \\ 0 & 0 & 1 \end{bmatrix} \begin{bmatrix} 1 & 0 & -\beta s_1 - \gamma s_{12} & -\beta s_1 - \gamma s_{12} & -\gamma s_{12} \\ 0 & 1 & \alpha + \beta c_1 + \gamma c_{12} & \beta c_1 + \gamma c_{12} & \gamma c_{12} \\ 0 & 0 & 1 & 1 & 1 \end{bmatrix} \tag{2-82} $$

In this case, it is desired to examine the effect of forces and torques acting on the spacecraft, due to jet actuators or momentum wheels. To this end, the Jacobian given by Equations (2-28) and (2-30) with k=0 and m=CM will be required. For simplicity, ${}^0\mathbf{J}_{12,S}$

is used instead of ${}^0J_{120,cm}$, etc.:

$$ {}^0J_{11,S} = \begin{bmatrix} -\varepsilon s_1 - \zeta s_{12} \\ \delta + \varepsilon c_1 + \zeta c_{12} \end{bmatrix} \quad {}^0J_{12,S} = \begin{bmatrix} -\varepsilon s_1 - \zeta s_{12} & -\zeta s_{12} \\ \varepsilon c_1 + \zeta c_{12} & \zeta c_{12} \end{bmatrix} \quad {}^0J_{22,S} = [0 \quad 0] \quad (2\text{-}83) $$

where ε, ζ, η, are lengths of barycentric vectors and are defined in Appendix E. The Jacobian ${}^0J_S^+$ relating the end-effector motion to the controlled velocities is written using Equations (2-30b), see also Equation (2-29):

$$ {}^0J_S^+(q) = \begin{bmatrix} 1 & 0 & -\varepsilon s_1 - \zeta s_{12} & -\varepsilon s_1 - \zeta s_{12} & -\zeta s_{12} \\ 0 & 1 & \delta + \varepsilon c_1 + \zeta c_{12} & \varepsilon c_1 + \zeta c_{12} & \gamma c_{12} \\ 0 & 0 & 1 & 0 & 0 \end{bmatrix} \quad (2\text{-}84) $$

3. Dynamics. It is assumed that a force f_E and a torque n_E (both fixed in inertial space) are applied at the manipulator end-effector. Also, a force ${}^0f_S$ and a torque ${}^0n_S$ are applied at the CM of the spacecraft and are measured in the spacecraft frame; these are due to the spacecraft jet actuators. The generalized forces are, see Appendix E:

$$ Q_x = {}^0f_{x,S} + \cos(\theta) f_{x,E} + \sin(\theta) f_{y,E} $$

$$ Q_y = {}^0f_{y,S} - \sin(\theta) f_{x,E} + \cos(\theta) f_{y,E} $$

$$ Q_\theta = {}^0n_S + n_E + {}^0J_{11,S}{}^T \begin{bmatrix} {}^0f_{x,S} \\ {}^0f_{y,S} \end{bmatrix} + (T_0\,{}^0J_{11})^T \begin{bmatrix} f_{x,E} \\ f_{y,E} \end{bmatrix} $$

$$ Q_q = \begin{bmatrix} Q_{q1} \\ Q_{q2} \end{bmatrix} = \begin{bmatrix} \tau_1 + n_E \\ \tau_2 + n_E \end{bmatrix} + {}^0J_{12,S}{}^T \begin{bmatrix} {}^0f_{x,S} \\ {}^0f_{y,S} \end{bmatrix} + (T_0\,{}^0J_{12})^T \begin{bmatrix} f_{x,E} \\ f_{y,E} \end{bmatrix} \quad (2\text{-}85) $$

where T_0 is given by:

$$T_0(\theta) = Rot(\theta) = \begin{bmatrix} \cos(\theta) & -\sin(\theta) \\ \sin(\theta) & \cos(\theta) \end{bmatrix} \tag{2-86}$$

Finally, the equations of motion are written as:

$$M\,{}^0\ddot{x}_{cm} = Q_x \tag{2-87a}$$

$$M\,{}^0\ddot{y}_{cm} = Q_y \tag{2-87b}$$

$$D\ddot{\theta} + D_q\ddot{q} + c_1^+ = Q_\theta \tag{2-87c}$$

$$D_q^T\ddot{\theta} + D_{qq}\ddot{q} + C_2^+ = Q_q \tag{2-87d}$$

where all the terms are defined in accordance to Equations (2-75), see also Appendix E. The matrix form of the equations of motion is given below:

$$H^+(q)\begin{bmatrix} \ddot{x}_{cm} \\ \ddot{y}_{cm} \\ \ddot{\theta} \\ \ddot{q} \end{bmatrix} + C^+(q,\dot{\theta},\dot{q}) = \begin{bmatrix} 0 \\ 0 \\ 0 \\ \tau \end{bmatrix} + J^+(\theta,q)^T\begin{bmatrix} f_E \\ n_E \end{bmatrix} + {}^0J_S^+(q)^T\begin{bmatrix} {}^0f_S \\ {}^0n_S \end{bmatrix} \tag{2-88}$$

2.6 EXTENSIONS OF THE FORMULATION

The formulation presented in this chapter can be easily extended to multi-manipulator systems. This extension is outlined here only.

Assume for simplicity that three manipulators with N_j DOF each, (j=1,2,3), are mounted on the spacecraft, see Figure 2.7. Assuming no closed loops, the total system has N DOF equal to the sum $N_1+N_2+N_3+6$. Equations for the individual link CM, like Equations (2-3) and (2-4) can be written, still. However, the notation must be changed to show to which manipulator a particular ρ_k belongs. To do this systematically, Hooker and

Margulies [29] used a tree topology. A similar approach, avoiding the use of topology, was proposed by Vafa [65]. If $\rho_{k,j}$ denotes the position of the CM of link k belonging to the j^{th} manipulator, then it is easy to show that Equation (2-9) can be written still, although there are $3(N_1+N_2+N_3+6)$ barycentric vectors, defined by equations similar to Eq. (2-10).

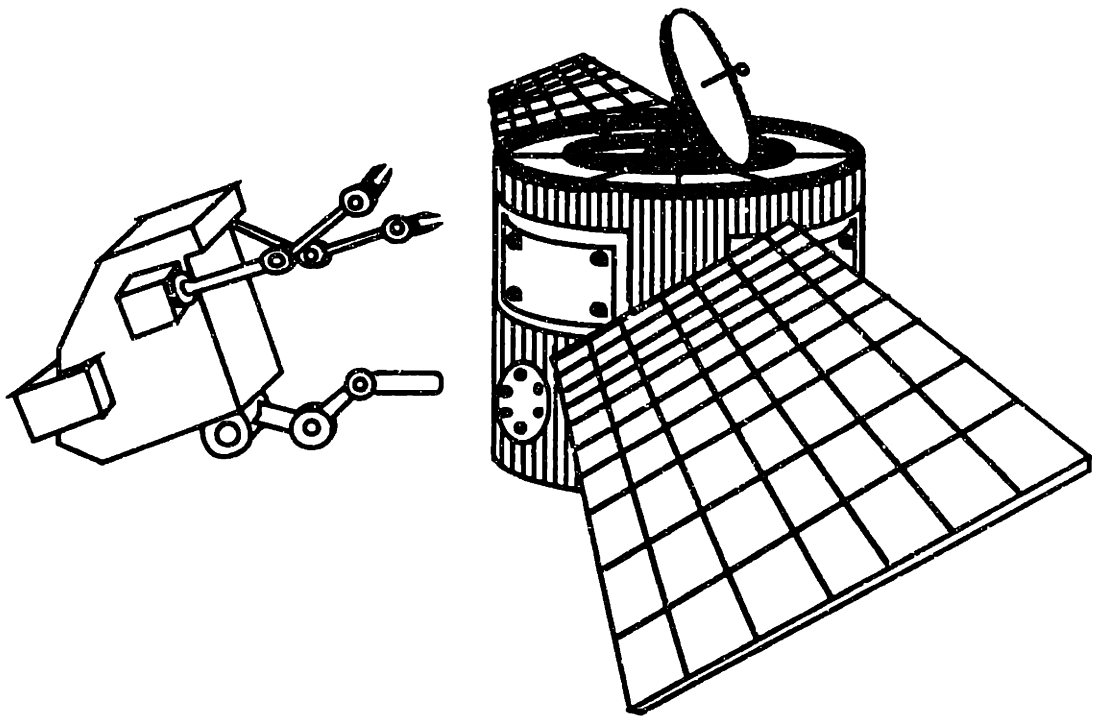

Figure 2.7. A three-arm space manipulator system.

Jacobians derived for such a system will have as input (independent) variables, the system CM linear velocity, the spacecraft angular velocity and the $N_1+N_2+N_3$ joint rates. Equations of motion will have the same form as Equation (2-62), however, the state vector will be augmented. In the absence of external forces or torques, the integrals of motion will be readily available. It is obvious that the complexity of such a system increases very much, and that some automated procedure must be employed to derive equations of motion.

2.7 SUMMARY

In this chapter a modeling methodology that describes the kinematics and dynamics of a free-flying space manipulator system was developed using an approach based on barycenters. The system CM coordinates, the spacecraft attitude and the joint angles vector of the manipulator were chosen as the independent variables. Closure equations and differential kinematical equations were derived. Equations of motion were formulated using a Lagrangian approach. This approach yielded an explicit and compact description of free-flying manipulator systems and will be used again in the subsequent chapters.

3 Free-Floating Manipulator Systems

3.1 INTRODUCTION

In this chapter, a free-floating manipulator system is analyzed. Such a system has an N DOF manipulator mounted on a 6 DOF uncontrolled spacecraft; in other words, spacecraft position and attitude control is turned off. As mentioned in Chapter 1, this may be desired for the following reasons. First, a substantial amount of jet (control) fuel can be consumed for station keeping of the spacecraft. Jet fuel consumption increases further when flexibilities in the system are excited and interact with the spacecraft controller [55]. Turning off a spacecraft's control system may extend a system's life. Second, space manipulators will be required to handle extremely fragile payloads or work in areas in which EVA astronauts may be present. End-effector jerky motions that may occur when jet actuators are turned on suddenly are not desirable; turning off a spacecraft's control system reduces those problems.

It must be noted here that turning off a spacecraft's controller is feasible only in the absence of large external forces or torques and initial momentum. If these effects are present, the spacecraft will drift in space. However, space is an ideal environment in which sources of external disturbances can be ignored for extended time intervals. Disturbances like solar pressure, atmospheric drag, or gravitational forces are negligible for the purposes of this thesis, see [65, 71, p.241]. Of course, from time to time a spacecraft's control system should take action to correct for any accumulated momentum.

The assumption of an uncontrolled spacecraft has an important result: the position of the system CM and the spacecraft attitude are *dependent* variables, the *independent* being

the manipulator joint angles which are controlled by the joint motors. In order to control such a system, it is desired to eliminate any dependent variables and have a *minimal* description of the system "plant." This is the main focus for this chapter. Once such a minimal description, or system *reduction*, is achieved, it is possible to examine its characteristics and possible limitations.

The methods developed in Chapter 2 are adapted in this chapter to describe free-floating manipulators. Section 3.2 investigates the existence of integrals of motion in the absence of external forces and torques. The non-integrability of the angular momentum is proved and its consequences are discussed. In Section 3.3, a free-floating system's differential kinematics are formulated and a system's Jacobian is constructed. This Jacobian is used in Section 3.4 to investigate the extent of feasible motions for free-floating manipulators and to define and quantify the notion of dynamic singularities. It is shown that dynamic singularities are functions of the dynamic properties of the system and that points in the workspace may or may not be singular, depending on the path taken by the end-effector in inertial space. In Section 3.5 a systematic exposition of the nature of free-floating manipulator workspaces is presented. Path independent workspaces, in which no dynamic singularities occur are defined. Section 3.6 deals with the issue of minimizing the negative effects of dynamic singularities. In Section 3.7 equations of motion for free-floating manipulators are written, based on the methods of Chapter 2. Section 3.8 deals with the consequence of non-zero system momentum, and Section 3.9 illustrates the key ideas in this chapter using an example. Finally, Section 3.10 concludes this chapter.

3.2 INTEGRALS OF MOTION

The first step in eliminating dependent variables from a dynamic system is the search for integrals of motion [51]. In the absence of external forces and torques, the system linear and angular momentum is conserved. However, it is not clear what is the effect of the

existence of those integrals to the capabilities of free-floating systems. Hence, in this section the nature of the conservation equations is examined in detail.

3.2.1 Linear Momentum

Consider the free-floating space manipulator shown in Figure 3.1. In the absence of external forces, the linear momentum of the system, $\underline{\mathbf{p}}$ is equal to a constant $\underline{\mathbf{p}}_0$, see Equation (2-38):

$$\underline{\mathbf{p}} = M\dot{\underline{\mathbf{r}}}_{cm} = \underline{\mathbf{p}}_0 \tag{3-1}$$

This is a first integral of motion. It follows that system CM velocity, $\dot{\underline{\mathbf{r}}}_{cm}$, is also constant and equal to $\dot{\underline{\mathbf{r}}}_{cm,0}$. Equation (3-1) can be integrated once more to yield an expression for the position of the system CM as a function of time t, which is a second integral of motion:

$$\underline{\mathbf{r}}_{cm} = \dot{\underline{\mathbf{r}}}_{cm,0}\, t + \underline{\mathbf{r}}_{cm,0} \tag{3-2}$$

The constants $\underline{\mathbf{p}}_0$ and $\underline{\mathbf{r}}_{cm,0}$ are determined by the initial conditions. Equations (3-1) and (3-2) could be obtained immediately from the equations of motion of the whole system, see Equation (2-62). Indeed, the three first scalar equations correspond to the time derivative of the linear momentum of the system. When no external forces are present, these equations decouple and can be integrated to yield the position of the system CM, as above. Hence, there are just N+3 dynamic equations. In other words, the effect of these integrations is to reduce the order of the system from an N+6 order system to an N+3 order system. This reduction also can be achieved by applying the Virtual Manipulator method proposed by Vafa [64].

Since the motion of the system CM is known, it can be substituted into all the kinematic equations, for example to Equation (2-11). The same is true for $\dot{\underline{\mathbf{r}}}_{cm}$, see Equation (2-15). However, Equation (3-2) describes a system that drifts with time. It will be assumed that the system is initially at rest, or equivalently that $\underline{\mathbf{p}}_0$ is zero. As was

mentioned in the previous section, when this assumption is violated, the spacecraft controller must eliminate any accumulated momentum. The effects of nonzero momentum will be examined in more detail in Section 3.8. The other constant, $\underline{r}_{cm,0}$, is not important because it represents a constant offset to all system positions. Without loss of generality, $\underline{r}_{cm,0}$ will be assumed zero, which is equivalent to locating the inertial origin, O, at the system CM.

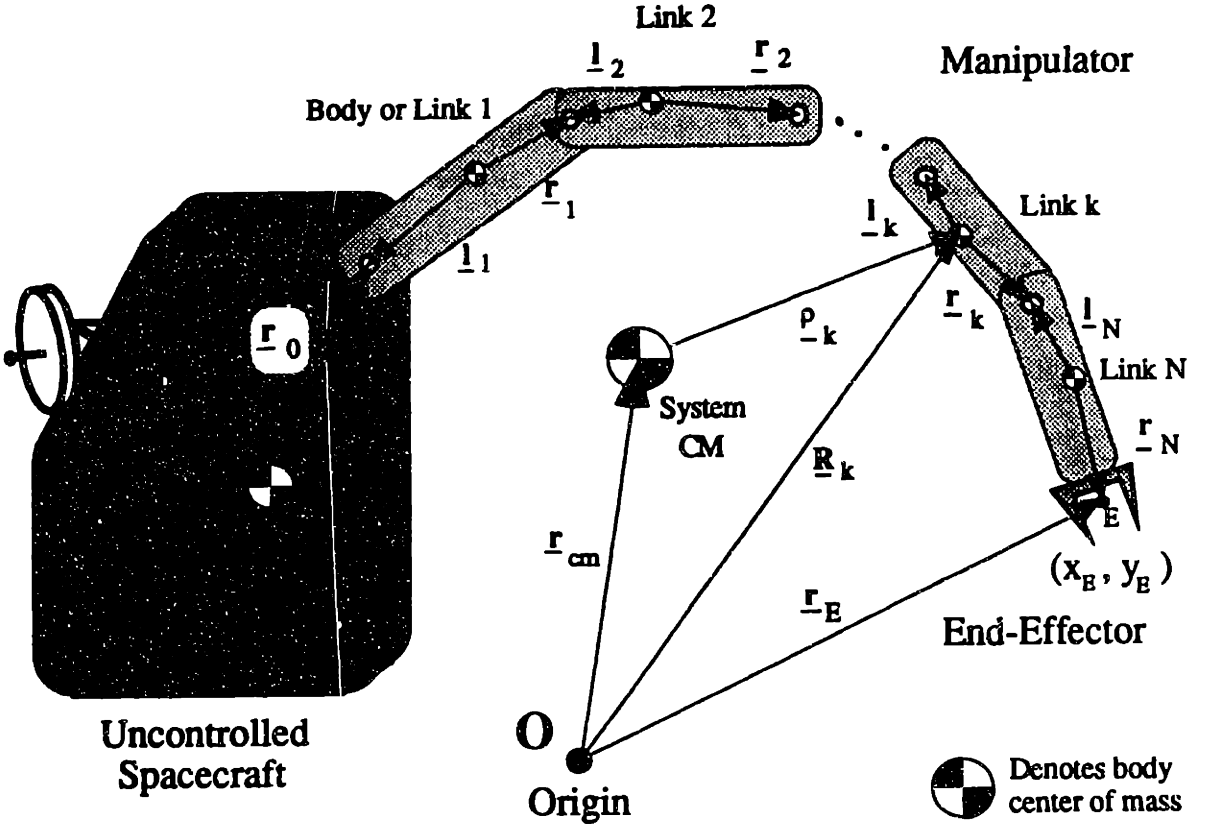

Figure 3.1. A Free-floating space manipulator system.

3.2.2 Angular Momentum

The time derivative of the angular momentum of the system with respect to its CM, $\mathbf{h}_{cm}$, given by Equation (2-54), or equivalently by the second set of three equations in the system

equations of motion (2-62), is zero in the absence of external forces and torques. Hence, Equation (2-54) can be integrated to a constant $\mathbf{h}_{cm,0}$, see also Equation (2-49):

$$\mathbf{h}_{cm} = \mathbf{T}_0 \left({}^0\mathbf{D}\, {}^0\boldsymbol{\omega}_0 + {}^0\mathbf{D}_q\, \dot{\mathbf{q}} \right) = \mathbf{h}_{cm,0} \tag{3-3}$$

In other words, the angular momentum with respect to the system CM, $\mathbf{h}_{cm}$, is a conserved quantity, or a third integral of motion. If the above is solved for ${}^0\boldsymbol{\omega}_0$, then it provides a spacecraft's angular velocity as a function of its manipulator rates, $\dot{\mathbf{q}}$.

It would be desirable to integrate Eq. (3-3) once more to obtain a spacecraft's attitude as a function of manipulator angles and possibly of time. In such a case, spacecraft attitude could be substituted in the kinematic and dynamic equations and thus be eliminated. Spacecraft attitude is described by matrix[1] $\mathbf{T}_0$, and it is well known that [30]:

$$\dot{\mathbf{T}}_0 = \mathbf{T}_0\, {}^0\boldsymbol{\omega}_0^{\times} \tag{3-4}$$

Combining Equations (3-3) and (3-4), yields the following differential equation for $\mathbf{T}_0$:

$$\dot{\mathbf{T}}_0 = \mathbf{T}_0 \left\{ {}^0\mathbf{D}^{-1} \left(\mathbf{T}_0^{\mathrm{T}}\, \mathbf{h}_{cm,0} - {}^0\mathbf{D}_q\, \dot{\mathbf{q}} \right) \right\}^{\times} \tag{3-5}$$

${}^0\mathbf{D}^{-1}$ is always non-singular because it represents the inertia of the whole system. Equation (3-5) is a generalized Pfaffian equation, see [54,70]. Integrability conditions were given by Frobenius and can be used to prove that Equation (3-5) is non-integrable. However, these conditions are very hard to apply, see [54]. Similar conditions in a more general setting involving vector fields, Lie brackets and distributions can be used, although the required computations are quite involved [46]. In both cases, no general results can be

---

[1]There are many ways to describe the attitude of a body, for example Euler angles, Euler parameters, direction cosines, etc. An excellent treatment of this subject can be found in [30]. Euler parameters are used mainly in this thesis. However, Equation (3-4) implies the use of direction cosines. This is preferred here because Equation (3-4) is the basic form from which all others can be derived and provides a more understandable and compact form. Alternatively, the Euler parameters equivalent, see Equations (2-36) and (2-21), could have been used instead.

obtained because applying these methods can be done in association to specific systems only.

Here, the non-integrability[2] of Equation (3-5) is proved using physical arguments. Assume that one can integrate Equation (3-5) and obtain an expression of the form:

$$\mathbf{T}_0(\mathbf{e}, \mathbf{n}) = \mathbf{T}_0(\mathbf{q}) = \mathbf{T}(\mathbf{q})\,\mathbf{T}_0(\mathbf{0}) \tag{3-6}$$

where $\mathbf{T}(\mathbf{q})$ is a transformation matrix satisfying $\mathbf{T}(\mathbf{0}) = \mathbf{1}$. This expression, implies that a spacecraft's attitude (e,n) is a function of $\mathbf{q}$ only, or in other words that the final attitude of a spacecraft is *independent* of the path taken in joint space, (the space with axes $q_1,\ldots,q_N$). Partition the joint angle vector $\mathbf{q}$ in two sub-vectors and (abusing somehow the notation), write: $\mathbf{q} = (\mathbf{q}_1, \mathbf{q}_2)$. Construct first a path in joint space that starts from point $\mathbf{q} = \mathbf{0}$ and moves first to point $(\mathbf{q}_{1f}, \mathbf{0})$ and then to the final point $(\mathbf{q}_{1f}, \mathbf{q}_{2f})$. Then $\mathbf{T}_0$ is given by:

$$\mathbf{T}_0(\mathbf{q}_f) = \mathbf{T}(\mathbf{0}, \mathbf{q}_{2f})\mathbf{T}(\mathbf{q}_{1f}, \mathbf{0})\mathbf{T}_0(\mathbf{0}) \tag{3-7}$$

Consider now a second path that passes first from point $(\mathbf{0}, \mathbf{q}_2)$ and then moves to the final point. Then $\mathbf{T}_0$ is given by:

$$\mathbf{T}_0(\mathbf{q}_f) = \mathbf{T}(\mathbf{q}_{1f}, \mathbf{0})\mathbf{T}(\mathbf{0}, \mathbf{q}_{2f})\mathbf{T}_0(\mathbf{0}) \tag{3-8}$$

Since both paths have same initial and final $\mathbf{q}$, the following must be true:

$$\mathbf{T}(\mathbf{0}, \mathbf{q}_{2f})\mathbf{T}(\mathbf{q}_{1f}, \mathbf{0}) = \mathbf{T}(\mathbf{q}_{1f}, \mathbf{0})\mathbf{T}(\mathbf{0}, \mathbf{q}_{2f}) \tag{3-9}$$

However, it is well known that finite rotations do *not* commute, see for example [21], that is Equation (3-6) does *not* hold. In other words, the attitude of the spacecraft is not only a function of the joint angles $\mathbf{q}$, but also of the *path* taken in joint space; different paths in the manipulator joint space will result in different final attitudes for the spacecraft; closed paths

---

[2]Clearly, Equation (3-5) always can be integrated *numerically*. But numerical integration implies a path, that is a succession of joint angles as a function of time. Integrability deals with the question of whether the final attitude is a function of the path or not.

in joint space will result in changes in spacecraft's attitude[3]. Because of this path dependency, which is solely due to the non-integrability of the angular momentum, some researchers attributed a "non-holonomic nature" or "structure" to free-floating manipulators, see [45]. However, a free-floating manipulator is a perfect example of a *holonomic* system; no physical constraints of any form limit its motion.

As shown in Appendix D, Section D.4, the only non-trivial case in which the angular momentum *can* be integrated, is that of the one-DOF example described in Section 2.5.1. This is because all rotations in this system occur around the same and only axis, a case in which rotation matrices do commute. As a demonstration of the more general case, it is proved in Appendix D that the angular momentum of the two-DOF example of Section 2.5.2, can *not* be integrated.

In this section it was shown that free-floating manipulators possess three integrals of motion which can be used in simplifying their kinematic and dynamic description. Also shown was that the conservation of angular momentum cannot be integrated to give a spacecraft's attitude as a function of its manipulator joint angles. This results in a system with path *dependency*, a characteristic that will be used later on. In the next section, the above results are used to analyze the behavior of free-floating manipulator systems.

3.3 KINEMATICS OF FREE-FLOATING SYSTEMS

In the previous section, free-floating manipulators were shown to possess three integrals of motion. In this section, those results will be used to provide expressions for the motion of the manipulator's end-effector as a function of the controlled (independent) variables, $\mathbf{q}$ and $\dot{\mathbf{q}}$. This is required for investigating the kind of feasible motions one can expect from a free-floating system and for control design, the theme of the next chapter.

---

[3]This property allowed Vafa to propose small joint space cyclic motions that can result in simultaneous control of the spacecraft and the manipulator, see [63,65].

It was shown above that spacecraft attitude cannot be written solely as a function of manipulator joint angles. For the same reason, no expression for the end-effector *orientation* can be written; such orientation depends on spacecraft attitude. Also, under the assumptions of Section 3.2.1, the system CM does not move, and hence, an expression for the end-effector *position* can be written according to Equation (2-22) as:

$$\mathbf{r}_E = \mathbf{T}_0(e,n) \sum_{i=0}^{N} {}^0\mathbf{T}_i(q_1,\ldots, q_i)\, {}^i\mathbf{v}_{iN,E} \tag{3-10}$$

In fixed-based systems, closure equations like the above can be inverted, in principle, to yield a map between end-effector positions and joint manipulator angles. In order to achieve a certain end-effector position, it suffices to move the joint angles of the manipulator to a pre-programmed set of desired angles. However in free-floating systems, end-effector position depends upon a spacecraft's attitude described by $\mathbf{T}_0$. This attitude depends upon the *history* of system motion. Hence, Equation (3-10) can not be inverted and no map between the joint angles $\mathbf{q}$ and the end-effector position $\mathbf{r}_E$ exists. Hence, Equation (3-10) cannot be used for planning or control purposes. Next, the differential kinematics of free-floating systems are considered.

As mentioned above, in free-floating systems the system CM does not move and hence, Equations (2-31) result in expressions for the end-effector linear and angular velocity:

$$\dot{\mathbf{r}}_E = \mathbf{T}_0 \{ {}^0\mathbf{J}_{11}\, {}^0\boldsymbol{\omega}_0 + {}^0\mathbf{J}_{12}\, \dot{\mathbf{q}} \} \tag{3-11a}$$

$$\boldsymbol{\omega}_E = \mathbf{T}_0 \{ {}^0\boldsymbol{\omega}_0 + {}^0\mathbf{J}_{22}\, \dot{\mathbf{q}} \} \tag{3-11b}$$

where the J-terms are linear functions of the barycentric vectors and of the system configuration $\mathbf{q}$; they are given by Equations (2-33). Similar expressions can be written for any point or body of the free-floating manipulator, as done in Chapter 2. Equations (3-11)

reflect the fact that the motion of the end-effector is the vector sum of two partial velocities. One is due to the motion of the joints, the second to the resulting motion of the spacecraft caused by dynamic coupling. Since no expression relating the spacecraft attitude to manipulator joint angles can be written, the dependence of $\mathbf{T}_0$ on the spacecraft attitude cannot be removed.

Equations (3-11) do not permit the construction of a system's Jacobian, because ${}^0\omega_0$ is a dependent variable. To this end, the conservation of angular momentum can be used. Indeed, if a system is initially at rest, Equation (2-49) results in:

$$\mathbf{0} = {}^0\mathbf{D}\,{}^0\omega_0 + {}^0\mathbf{D}_\mathbf{q}\,\dot{\mathbf{q}} \tag{3-12}$$

where the D-terms are quadratic functions of the barycentric vectors, the system inertias and the configuration $\mathbf{q}$, and are given by Equations (2-50). Since ${}^0\mathbf{D}$ is the system inertia calculated with respect to the system CM, it is always a positive definite symmetric matrix and thus it is always invertible. Hence, Equation (3-12) can be solved to provide ${}^0\omega_0$ as follows:

$${}^0\omega_0 = -\,{}^0\mathbf{D}^{-1}\,{}^0\mathbf{D}_\mathbf{q}\,\dot{\mathbf{q}} \tag{3-13}$$

The above can be substituted in equation (3-12) to yield expressions for the end-effector velocities and for the free-floating system Jacobian, called a *generalized Jacobian* by [60]:

$$\dot{\mathbf{x}} = [\,\dot{\mathbf{r}}_E\,,\,\omega_E\,]^T = \mathbf{J}^*\,\dot{\mathbf{q}} \tag{3-14}$$

where:

$$\mathbf{J}^*(\mathbf{e},\mathbf{n},\mathbf{q}) \equiv \mathrm{diag}(\mathbf{T}_0,\mathbf{T}_0)\begin{bmatrix} -{}^0\mathbf{J}_{11}\,{}^0\mathbf{D}^{-1}\,{}^0\mathbf{D}_\mathbf{q} + {}^0\mathbf{J}_{12} \\ -{}^0\mathbf{D}^{-1}\,{}^0\mathbf{D}_\mathbf{q} + {}^0\mathbf{J}_{22} \end{bmatrix} \tag{3-15a}$$

$$= \mathrm{diag}(\mathbf{T}_0,\mathbf{T}_0)\,{}^0\mathbf{J}^*(\mathbf{q}) \tag{3-15b}$$

with:

$$ {}^{0}\mathbf{J}^{*}(\mathbf{q}) \equiv \begin{bmatrix} -{}^{0}\mathbf{J}_{11}\,{}^{0}\mathbf{D}^{-1}\,{}^{0}\mathbf{D}_{\mathbf{q}} + {}^{0}\mathbf{J}_{12} \\ -{}^{0}\mathbf{D}^{-1}\,{}^{0}\mathbf{D}_{\mathbf{q}} + {}^{0}\mathbf{J}_{22} \end{bmatrix} \tag{3-15c} $$

Note that unlike to fixed-based manipulator Jacobians, ${}^{0}\mathbf{J}^{*}$ is a function of the dynamic properties of the system. Both $\mathbf{J}^{*}$ and ${}^{0}\mathbf{J}^{*}$ are 6×N matrices. If N is equal to six, then $\mathbf{J}^{*}$ is square and, if not singular, can be inverted. Note also that $\text{diag}(\mathbf{T}_0,\mathbf{T}_0)$ is always non-singular, because $\mathbf{T}_0$ is always non-singular. If N is less than six, it is not possible to follow any given end-effector trajectory while, if N is greater than six, the manipulator is redundant and a generalized inverse technique can be used. Here, it will be assumed that N is equal to six (no redundancy) unless it is otherwise noted. It will be shown in Chapter 4, that unlike the kinematic Equation (3-10), $\mathbf{J}^{*}$ can be used for planning and control purposes. In the next section, the invertibility conditions for $\mathbf{J}^{*}$ are investigated.

3.4 DYNAMIC SINGULARITIES

In the previous section a Jacobian $\mathbf{J}^{*}$ that provides the motion of the end-effector as a function of the manipulator's controlled rates $\dot{\mathbf{q}}$ was found in spite of the uncontrolled motions of the spacecraft. That Jacobian's explicit structure was revealed. In this section, the important question of when the Jacobian becomes singular is addressed. This is important for both physical and control reasons. The physical reason is that for a manipulator position, the system Jacobian must be invertible or of full rank in order *physically to move* the manipulator end-effector in all directions at that point in space. Also, since nearly all planning algorithms as well as all resolved rate or acceleration control algorithms need to invert a Jacobian, it is important to examine when this is possible.

Singularities occur for fixed-base non-redundant manipulators when end-effector velocity due to the motion of one joint is parallel to the velocity due to the motion of some other joint. At such points, at least one degree of freedom is lost and the rank of the manipulator Jacobian J is reduced accordingly, becoming singular. Singular points for fixed-

base manipulators occur at workspace boundaries or when there is alignment of joint axes. Given the kinematic structure of a manipulator, we can find all its singular configurations by solving the equation det[J(q)]=0. The literature usually describes singular points in terms of fixed-base manipulator workspace positions instead of singular configurations or of singularities in the joint space because at any singular set of joint angles $\mathbf{q}_s$, there corresponds a singular point in the six DOF workspace. The obvious benefit is that the manipulator path planner or controller can be designed to avoid these workspace points. Singularities of fixed-base manipulators are *kinematic*, because it is sufficient to analyze the *kinematic structure* of the manipulator in order to identify them.

The singularities of $\mathbf{J}^*$ for a free-floating space system are obtained by examining Equation (3-15). First, it can be seen that the term $\text{diag}(\mathbf{T}_0,\mathbf{T}_0)$ is always square and invertible. Thus, any singular points of $\mathbf{J}^*$ are due to singular points of ${}^0\mathbf{J}^*(\mathbf{q})$ which can be found from the condition, (N=6):

$$\det[{}^0\mathbf{J}^*(\mathbf{q})] = 0 \tag{3-16}$$

Equation (3-16) proves that all singularities are functions of the manipulator *configuration* with respect to its spacecraft, $\mathbf{q}$, not to the spacecraft attitude. These singularities correspond to singular points in the manipulator's *joint space*, in other words, singularities are fixed in joint space.

As mentioned in connection to Equation (3-10), no direct map from the configuration $\mathbf{q}$ to end-effector workspace points exists. Hence, singular points in joint space cannot be mapped into unique points in the workspace. In general, each end-effector workspace point can be reached with infinite system configurations $\mathbf{q}$ and spacecraft attitudes (e,n), satisfying Equation (3-10). The set of (e,n,$\mathbf{q}$) that will actually result during some motion of the end-effector depends on the path taken by the end-effector in inertial space. This can be explained as follows: Assume that in some region Equation (3-14) is invertible, that is a smooth map between $\dot{\mathbf{q}}$ and $\dot{\mathbf{x}}$ exists. Since Equation (3-5) is not integrable, the same

holds if $\dot{\mathbf{x}}$ is substituted for $\dot{\mathbf{q}}$. This proves that spacecraft attitude depends upon the *path* taken by the end-effector in inertial space. Due to Equation (3-10), the joint configuration $\mathbf{q}$ that is needed to reach a workspace point also depends upon the path taken to reach that point. In other words, the set of $(\mathbf{e},\mathbf{n},\mathbf{q})$ that results at the end of a motion during which the end-effector reaches a particular workspace point, depends upon the *path* taken by the end-effector in reaching that point. Therefore, a workspace point can be singular or not depending on whether the manipulator reaches this point in a singular configuration. In other words, free-floating manipulator singularities in the end-effector workspace are path *dependent.*

In addition, ${}^0\mathbf{J}^*(\mathbf{q})$ in Equation (3-15c) depends on the kinematic, mass and inertia properties of both the manipulator and the spacecraft. Since the ${}^0\mathbf{D}_{ij}$ matrices that represent the inertia properties of the system are functions of the configuration, singular configurations cannot be predicted by examining the kinematic structure of the manipulator alone. Since the singularities of $\mathbf{J}^*$ depend on the system's dynamic parameters, its mass and inertia properties, they are called *dynamic singularities*, see also [48,49].

The dynamic singularities of a free-floating manipulator space manipulator system can be explained physically by noting that the end-effector velocity $\dot{\mathbf{x}}$, given by Equation (3-11), can be decomposed in two parts. The first part is due to the motion of the manipulator joints, the second is due to spacecraft motion. This second motion occurs because of the dynamic coupling of the spacecraft and the manipulator and is a function of the system masses and inertias. The matrix $\mathbf{J}^*$ becomes singular when the end-effector velocity $\dot{\mathbf{x}}$, produced by the combined joint-spacecraft motion caused by the motion of a manipulator joint, is parallel to another $\dot{\mathbf{x}}$ produced by the by the same means by some other joint and the spacecraft. If the mass and inertia of the vehicle becomes very large, approximating a fixed-base manipulator, then all the dynamic terms in Equation (3-14) vanish and $\mathbf{J}^*$ reduces to the fixed-base manipulator Jacobian, while the dynamic singularities reduce to the ordinary kinematic singularities.

The conclusion of this analysis is that if the spacecraft of a space manipulator system is not actively controlled but is free-floating, then dynamic singularities can occur. All resolved rate or resolved acceleration control schemes will fail because at these points, Equation (3-14) has no inverse. Control schemes that compute the desired joint torques by using a transposed Jacobian will fail to keep the desired end-effector velocity because dynamic singularities represent an inherent *physical* limitation. The manipulator will move with a velocity that is the projection of the desired velocity on the allowed direction: the result may be large end-effector errors.

3.5 FREE-FLOATING MANIPULATOR WORKSPACES

Space manipulators have more complex workspace characteristics than fixed-base manipulators, as was shown by using the concept of the Virtual Manipulator. Vafa describes a *constrained* workspace, one where all points can be reached if the attitude of the spacecraft is controlled, but not its position [65]. This workspace is a sphere with its center at the system's CM. To show this, note first that the orientation matrix $\mathbf{T}_0$ does not change the length of a vector; hence, the distance R of the end-effector location from the system CM can be written using Equation (3-10) as a function of the system's configuration $\mathbf{q}$ only:

$$R = R(\mathbf{q}) = \left\| \sum_{i=0}^{N} {}^{0}\mathbf{T}_i (q_1, \ldots, q_i)\, {}^{i}\mathbf{v}_{iN,E} \right\| \tag{3-17}$$

The symbol $\|\cdot\|$ denotes a vector's norm (length). Equation (3-17) also defines a spherical shell in inertial space with its center at the system CM and of a radius R. The reachable workspace is constrained between the spherical shells of radii (R_{min}, R_{max}) given by:

$$R_{min} = \min_{\mathbf{q}} R(\mathbf{q}) \tag{3-18a}$$

$$R_{max} = \max_{q} R(q) \qquad (3\text{-}18b)$$

However, due to the non-integrability of the angular momentum discussed in Section 3.1, infinite many spacecraft attitudes[4] can be achieved by choosing appropriate joint space paths[5]. Hence, even if the attitude is not controlled, points in the constrained space can still be reached by selecting a suitable path. For this reason in this thesis it is preferred to call this workspace the *reachable*[6] workspace. What follows below shows that the nature of this workspace is related to a system's dynamic singularities.

It was proven already that a system's dynamic singularities are a unique function of the configuration and that their occurrence at a particular inertial workspace location is path dependent. For practical reasons, it is desirable to find regions in the reachable workspace in which dynamic singularities never occur. Recall that dynamically singular configurations can be found from Equation (3-16). Its solution represents a family of hypersurfaces $Q_{s,i}$ (i=1,2,...) in the manipulator *joint space*. These hypersurfaces are collections of points q_s that result in dynamically singular configurations. Each singular configuration q_s is mapped according to Equation (3-17) to a spherical shell in inertial space. By the same token, each hypersurface $Q_{s,i}$ is mapped according to Equation (3-17) to a volume contained within the spherical shells with radii:

$$R_{min,i} = \min_{q \in Q_{s,i}} R(q) \qquad (i=1,2,...) \qquad (3\text{-}19a)$$

---

[4]This is a similar characteristic to the one found in systems with non-holonomic constraints, which also are non-integrable. It is well known that these constraints do not reduce the dimensionality of the configuration space; all of it is available to the system, see [54]. However, reaching a particular configuration requires a particular path, like the one required to park a car.

[5]This fact induced research in path planning for free-floating manipulators with the goal to find appropriate inertial workspace paths that will move the end-effector to a desired location *and* control the spacecraft attitude at the same time, see [45]. So far, success in doing so is arguable.

[6]Some authors make a distinction between *dextrous* and *reachable* workspaces [14]. The reachable workspace is that volume of space which the end-effector can reach in *at least one* orientation. The dextrous workspace is that volume of space which the end-effector can reach with *any* orientation. This thesis will not be concerned with the latter.

$$R_{max,i} = \max_{q \in Q_{s,i}} R(q) \qquad (i=1,2,...) \qquad (3\text{-}19b)$$

All workspace points that belong in this volume can be singular if they are reached in singular configurations q_s. As shown earlier, this may happen or not depending on the path taken by the manipulator's end-effector. If there is more than one singular hypersurface, then there are more such volumes containing points that can lead to singular configurations. The union of all these volumes is called a *Path Dependent Workspace (PDW)*. The Path Dependent Workspace contains all reachable workspace locations that may be reached in singular configurations, depending upon the path taken by the end-effector. It follows that locations in the PDW can be reached with some paths but not with others; this justifies their name. In order to reach points belonging to the PDW, carefully selected paths must be employed.

Subtracting the PDW from the reachable workspace results in the *Path Independent Workspace (PIW)*. Due to its construction, this workspace region contains all reachable workspace locations that will *never* lead to dynamically singular configurations. It follows that all points in the Path Independent Workspace can be reached by any path, assuming that this path lies entirely in the PIW.

Another workspace defined by Vafa is the *free workspace* [65]. This is the workspace volume that can be reached with *any* spacecraft *attitude*. Probably, the main reason for defining such a workspace is that it simplifies the problem of finding a path to a point in it with uncontrolled spacecraft attitude, because the problem reduces to a search of paths in joint space. As shown in Section 3.9, the PIW is a subset of the free workspace.

It is interesting to analyze the effects of payloads to system workspaces, because it has been proposed that space manipulator systems should be able to manipulate objects of size and mass comparable to theirs. Since a payload increases the mass of the last link, as

well as the total system mass, its effect is to decrease the size of all the barycentric vectors[7] ${}^{i}v_{iN,E}$, because all barycenters move closer to the joint closer to the payload, see Figure 2.2. This results in a reduction of the reachable workspace as given by Equations (3-17) and (3-18). This means that although a space manipulator may be able to handle big payloads due to the absence of gravity, still it will not be able to manipulate them in any desired way; feasible motions will be restricted in a small region that will shrink with the size of the load. This fact makes sense: if a system attempts to move an object of size comparable to its own, it is not clear which is going to move which!

The PIW or PDW spaces may reduce to zero depending on the case. A clear goal for the designer is to reduce the PDW and increase the PIW. This is the theme of the next section.

3.6 REDUCING THE EFFECT OF DYNAMIC SINGULARITIES

Maximizing the PIW clearly reduces the impact of dynamic singularities on a system's effectiveness. One way to achieve this is to keep the spacecraft attitude constant, because then ${}^{0}\omega_{0}$ is zero, and the only singular points are of kinematic nature. Indeed, if ${}^{0}\omega_{0}$ is zero then only the terms ${}^{0}J_{12}\dot{q}$ and ${}^{0}J_{22}\dot{q}$ remain in Equations (3-11). In these equations, the columns of the sub-Jacobians, ${}^{0}J_{12}$ and ${}^{0}J_{22}$, are columns of a fixed-based manipulator Jacobian where instead of real manipulator link lengths, barycentric vectors are substituted. These barycentric vectors are real manipulator lengths scaled by mass ratios of the form m_i/M, see Equations (2-33), (2-12), (2-10) and (2-7). Since linear scaling does not change topological properties, kinematic singularities of a fixed-based manipulator are transformed

---

[7]It must be noted that the system CM after picking up a payload is instantly moved to a new location; obviously, the end-effector is in the reachable workspace before and after the acquisition of the payload. However, for comparison reasons, the dashed circle in Figure 2.2 is shown as having its center at the new CM.

to kinematic singularities[8] of the free-floating one. This means that if for example a two-DOF fixed-base manipulator has a singularity which depends on q_2 only, the same will be true for the free-floating one, when its spacecraft attitude is constant. Also, if the fixed-based manipulator does not have interior singularities the same will be true for the free-floating one, etc. This does not necessarily imply that, for example, a two-DOF free-floating manipulator will be singular at q_2=0°, ±180°. It may be singular at some other q_2, but still this singularity will correspond to reachable workspace limits[9] and will be independent of q_1. The problem with this method is that requires active control of spacecraft attitude which can increase cost and reduce a system's useful life.

Another method to reduce the effect of dynamic singularities is to increase the inertia of the spacecraft. Indeed, in such a case ${}^0\mathbf{I}_0$ and ${}^0\mathbf{D}_0$ become large, and, ${}^0\omega_0$ is almost zero. Therefore, the PIW is maximized for the reasons mentioned above. Although it is desirable in most cases to make a spacecraft as light as possible for a number of reasons, such as launch weight, a system's designer has the freedom to increase a system's inertia keeping its mass constant. Such a design would result in an increase in the system's PIW.

The PIW also can be maximized by using manipulator redundancy. If a manipulator is at a singular configuration, redundant degrees of freedom may be used to achieve the necessary end-effector velocity. This is an area which requires additional research and will not be explored in this thesis.

Finally, for the case where the manipulator acts in a plane, it can be shown that if the manipulator is mounted at a spacecraft's center of mass, the PIW is equal to the reachable workspace and the PDW is eliminated. This occurs because in this case the effect of

---

[8]In the Virtual Manipulator setting, singular points that occur when the spacecraft attitude is fixed correspond to a kinematically singular VM whose first link is fixed. See also the interpretation of ${}^0\mathbf{J}_{12}$ and ${}^0\mathbf{J}_{22}$, after Equation (2-33).

[9]It can be shown that if the CM of each link is along the line connecting two joints, then not only the topological properties are conserved, but also a free-floating and a fixed-based manipulator have exactly the same singular configurations. For example, a two-DOF free-floating manipulator with constant spacecraft attitude is singular when q_2=0°, ±180°.

spacecraft rotations due to dynamic coupling is the same to the effect of first manipulator joint motion. In such a case, system singularities are due to joint axes alignments or to workspace extremums, in other words they are of kinematic nature.

To prove the above statement, assume first that r_0 is zero, that is a manipulator is mounted at its spacecraft's CM. Then $v_{0N,E}$, and c_0^* are zero, too. Also, ${}^0D_{00} = {}^0I_0$ while ${}^0D_{i0}$ and ${}^0D_{0j}$ (i=1,...,N) are zero. The absolute inertial velocity of the end-effector produced by the motion of the k^{th} joint, $\dot{r}_{E,k}$, is written using Equations (2-23) and (2-31) and setting all ω_j^0 (j≠k) equal to zero:

$$\dot{r}_{E,k} = -\sum_{i=k}^{N} [T_i\, {}^i v_{iN,E}]^{\times}\, \omega_k^0 - \sum_{i=1}^{N} [T_i\, {}^i v_{iN,E}]^{\times}\, \omega_0 \qquad (3\text{-}20)$$

Recall that ω_k^0 is the inertial velocity of the k^{th} link with respect to the spacecraft. Then, Equation (3-20) represents the contribution in end-effector inertial velocity by the motion of the k^{th} joint. Setting k equal to 1, it is clear that ω_1^0 and ω_0 are multiplied by exactly the same matrix. If ω_1^0 and ω_0 are parallel vectors, both sums in Equation (3-20) correspond to parallel vectors differing only by a constant, c. Thus, the second sum in Equation (3-20) can be replaced by the first one, with k equal to 1, times the constant c. In such a case, Equation (3-20) can be rewritten as:

$$\dot{r}_{E,k} = -\sum_{i=k}^{N} [T_i\, {}^i v_{iN,E}]^{\times}\, \omega_k^0 - \sum_{i=1}^{N} [T_i\, {}^i v_{iN,E}]^{\times}\, \omega_1^0\, c \qquad (3\text{-}21)$$

Note that all ω_k^0 (k=1,...,N) are relative to the spacecraft inertial angular velocities and that ω_0 does not appear in Equation (3-21). Hence, end-effector inertial velocity does not depend on a spacecraft's angular velocity, in which case, all dynamic singularities reduce to kinematic singularities, and the PDW is eliminated.

It remains to examine when ω_1^0 and ω_0 can be parallel vectors. If only the first joint is driven, the conservation of angular momentum equation can be written as, see Equations (2-43), and (2-18):

$$\left\{\sum_{j=1}^{N}\sum_{i=1}^{N} \mathbf{D}_{ij}\right\}\omega_1^0 + \left\{\mathbf{I}_0 + \sum_{j=1}^{N}\sum_{i=1}^{N} \mathbf{D}_{ij}\right\}\omega_0 = \mathbf{0} \qquad (3\text{-}22)$$

and shows that ω_1^0 and ω_0 are indeed parallel only in the planar case, where all inertia sums are scalars and all angular velocities are perpendicular to the plane of motion. In general, adding $\mathbf{I}_0$ to the double sum in Equation (3-22) will result in a matrix with different principal axes and the angular velocities ω_1^0 and ω_0 will not be parallel. However, the planar case can be quite important in some designs and this guideline can help in reducing or eliminating dynamic singularities.

In some cases it may be possible to use combinations of the various techniques discussed. For example, a system may be designed to have a large moment of inertia about one axis while the manipulator arm is mounted near the spacecraft CM in the other two dimensions. Hence, a system's properties can be enhanced by thoughtful design.

The previous sections have examined the nature of feasible motions of free-floating manipulators. In the next section, the nature of their dynamics is analyzed.

3.7 DYNAMICS OF FREE-FLOATING MANIPULATORS

As mentioned in Chapter 2, development of equations of motion is important not only for simulations but also for designing controllers. In this section equations of motion for free-floating manipulator systems are developed. It is shown that under the assumptions of free-floating systems, the equations of motion developed in Section 2.4 can be *reduced* from N+6 to just N, that is as many as the manipulator DOF. This reduction will be

achieved using a *Routhian* function [21,51]. This method[10] shares characteristics from both the Lagrangian and Hamiltonian formulations, and can be used when some generalized momentum is conserved in a system in which the corresponding coordinate is *ignorable*, that is the Lagrangian is *not* a function of that coordinate.

The first step in deriving equations of motion is to express the system kinetic energy as a function of the generalized coordinates and the corresponding velocities. The system CM of the free-floating system shown in Figure 3.1 does not move in the absence of external forces. Following the same reasoning as in Section 2.4, the system kinetic energy is equal to the system's Lagrangian. The symbol T is used for the Lagrangian also. The kinetic energy, T, can be written as, see Equation (2-57a):

$$T = \frac{1}{2} {}^0\omega_0{}^T \, {}^0\mathbf{D} \, {}^0\omega_0 + {}^0\omega_0{}^T \, {}^0\mathbf{D}_\mathbf{q} \, \dot{\mathbf{q}} + \frac{1}{2} \dot{\mathbf{q}}^T \, {}^0\mathbf{D}_{\mathbf{qq}} \, \dot{\mathbf{q}} \tag{3-23}$$

Note that T is a function of ${}^0\omega_0$, $\dot{\mathbf{q}}$ and $\mathbf{q}$ only, since the **D**-terms above were shown to be functions of the configuration $\mathbf{q}$ and not of the spacecraft attitude; spacecraft attitude coordinates are ignorable. Next examine the generalized momentum that corresponds to spacecraft angular velocity, ${}^0\omega_0$. This can be obtained by differentiating the Lagrangian given above. Due to the conservation of angular momentum in the system, see Equation (3-3), this generalized momentum is given by:

$$\frac{\partial T}{\partial {}^0\omega_0} = {}^0\mathbf{D} \, {}^0\omega_0 + {}^0\mathbf{D}_\mathbf{q} \, \dot{\mathbf{q}} = \mathbf{T}_0^T \, \mathbf{h}_{cm,0} = {}^0\mathbf{h}_{cm,0} \tag{3-24}$$

This momentum can be recognized as the system angular momentum calculated with respect to the spacecraft frame, located at the CM. Although $\mathbf{h}_{cm,0}$ is a constant, $\mathbf{T}_0^T$ is not, so the momentum given by the above expression, is not constant in direction, and a

---

[10]Reduction of equations of motion also can be achieved by the highly mathematical and abstract methods of theoretical mechanics, using Hamiltonians and symmetry arguments. An excellent reference for these methods is [1], while an example application can be found in [59].

Routhian function cannot be constructed, in general. However, if the system is initially at rest, $\mathbf{h}_{cm,0}$ is zero and angular momentum is conserved in both the inertial and spacecraft frames. The same is also true for planar systems, even if $\mathbf{h}_{cm}$ is nonzero, because both $\mathbf{h}_{cm,0}$ and ${}^0\mathbf{h}_{cm,0}$ are perpendicular to the plane of motion. Under those conditions, one can use a Routhian to reduce a system's dynamic equations. In the case of zero angular momentum, the Routhian is equal to the Lagrangian given by Equation (3-23), in which ${}^0\omega_0$ is eliminated using Equation (3-13). The result of this operation is given below:

$$T = \frac{1}{2}\dot{\mathbf{q}}^T \mathbf{H}^*(\mathbf{q})\,\dot{\mathbf{q}} \tag{3-25}$$

where $\mathbf{H}^*(\mathbf{q})$ is the system inertia matrix, given by:

$$\mathbf{H}^*(\mathbf{q}) \equiv {}^0\mathbf{D}_{qq} - {}^0\mathbf{D}_q^T\,{}^0\mathbf{D}^{-1}\,{}^0\mathbf{D}_q \tag{3-26}$$

As shown in Appendix F, $\mathbf{H}^*$ is an N×N positive definite symmetric inertia matrix, which depends upon the configuration $\mathbf{q}$ and the system mass and inertia properties. These properties of $\mathbf{H}^*$ will be exploited in Chapter 4. Equation (3-26) shows how to construct the inertia matrix efficiently. One just needs to find the barycentric vectors of the system, compute the inertia matrices ${}^0\mathbf{D}_{ij}$ using these barycentric vectors, find the D-inertia terms using definitions (2-50), and finally assemble $\mathbf{H}^*$.

The expression for T given by Equation (3-25) is the system Routhian, which is the appropriate Lagrangian function for this system. Clearly, T is a function of $(\mathbf{q}, \dot{\mathbf{q}})$, the manipulator joint angles and velocities, only. Lagrange's equations, for this system are written as:

$$\frac{d}{dt}\left\{\frac{\partial T}{\partial \dot{\mathbf{q}}}\right\} - \frac{\partial T}{\partial \mathbf{q}} = \tau \tag{3-27}$$

where τ is the generalized force vector which, in this case, is equal to the applied torque vector $[\ \tau_1, \tau_2, \ldots, \tau_N\ ]^T$. Applying Equation (3-27) to the Routhian given by Equation (3-25) results in a set of N dynamic equations of the form:

$$\mathbf{H}^*(\mathbf{q})\,\ddot{\mathbf{q}} + \mathbf{C}^*(\mathbf{q},\dot{\mathbf{q}})\,\dot{\mathbf{q}} = \tau \tag{3-28}$$

where $\mathbf{C}^*(\mathbf{q},\dot{\mathbf{q}})\,\dot{\mathbf{q}}$ contains the nonlinear Coriolis and centrifugal terms. As shown in Appendix F, $\dot{\mathbf{H}}^* - 2\mathbf{C}^*$ can be written as a skew-symmetric matrix. Note that the above equations of motion do no depend upon a spacecraft's attitude or position variables. A spacecraft's contribution to the kinetic energy, T, appears through the presence of the inertia matrices ${}^0\mathbf{D}_{0i}$ (i=0,...,N), which are functions of a spacecraft's mass m_0 and inertia $\mathbf{I}_0$.

Equations (3-28) describe the dynamics of free-floating systems. Note that a space manipulator system has N+6 DOF, while the derived equations are only N. In other words, the dynamics of a space manipulator system with uncontrolled spacecraft can be reduced to the dynamics of an N DOF system[11]. The dependent variables were eliminated completely. As said earlier, the motion of the system CM is completely known; the CM does not move. This accounts for three more DOF. Spacecraft attitude coordinates are controlled by Equation (3-5), or by Equations (3-4), (2-36) and (2-21). In both cases, given a joint rate vector $\dot{\mathbf{q}}$, spacecraft angular velocity and spacecraft attitude follow, see Equations (3-4) and (3-5), or (2-36) and (2-21). This accounts for the last three DOF of the system.

The above analysis has certain important implications for the control of free-floating systems and will be used as a building block in Chapter 4. In the next section, examples are used to demonstrate the theory that was developed in this chapter.

---

[11] A similar case is the one where two carts interact through a force acting between them. This system can be described with just *one* dynamic equation, although two masses are involved. In *bond-graph* terminology, the mass of one of the two carts would be a *dependent* mass. The *reduced* mass defined in such a case is the equivalent of the inertia matrix $\mathbf{H}^*$ here. Off course, the two carts problem is much simpler because it is linear and not configuration dependent.

3.8 EXAMPLES

Example 1. For the one-DOF system of Section 2.5.1, the system inertia matrix H^* and the nonlinear term C^* are 1×1 scalars given by:

$$H^*(q) \equiv D_{qq} - D_q^T D^{-1} D_q$$

$$= \frac{d_{00}d_{11} - d_{01}^2}{D} \tag{3-29a}$$

$$C^*(q, \dot{q}) = \frac{(d_{00}+d_{01})(d_{01}+d_{11})}{D^2} \hat{d}_{01} \dot{q} \tag{3-29b}$$

where all the terms are defined by Equations (E-5) and (E-7). The only equation of motion for this example is:

$$H^*(q) \ddot{q} + C^*(q, \dot{q}) \dot{q} = \tau \tag{3-30}$$

Example 2. The planar two link system shown in Figure 2.6 assumes the two coordinates of the end-effector, x and y, are controlled by the two manipulator joint angles, q_1 and q_2. System parameters are given in Table I. End-effector orientation is not controlled for this two DOF system (N=2), hence Equation (3-14) for this system is simply:

$$\dot{x} = \dot{r}_E = \frac{d}{dt}[x_E, y_E]^T = J^* \dot{q} \tag{3-31}$$

where:

$$x = r_E = [x_E, y_E]^T \tag{3-32}$$

$$q = [q_1, q_2]^T \tag{3-33}$$

Table I. System parameters for the two-DOF manipulator example.

Body	l_i (m)	r_i (m)	m_i (Kg)	I_i (Kg m^2)
0	.5	.5	40	6.667
1	.5	.5	4	0.333
2	.5	.5	3	0.250

The free-floating Jacobian $\mathbf{J}^*$ given by Equation (3-15), becomes:

$$\mathbf{J}^*(\theta,\mathbf{q}) = \mathbf{T}_0(\theta)\,{}^0\mathbf{J}^*(\mathbf{q}) = \mathbf{T}_0\,[-{}^0\mathbf{J}_{11}\,\mathbf{D}^{-1}\,\mathbf{D}_\mathbf{q} + {}^0\mathbf{J}_{12}] \tag{3-34}$$

where θ denotes the spacecraft attitude, as shown in Figure 2.6. The left superscript in the D-terms was dropped as done previously. For this example, the total inertia D and the inertia matrix $\mathbf{D}_\mathbf{q}$ are given by Equations (E-24), and ${}^0\mathbf{J}_{11}$ and ${}^0\mathbf{J}_{12}$ are given by Equation (E-26). By direct substitution in Equation (3-34), the following Jacobian is obtained:

$$\mathbf{J}^*(\theta,\mathbf{q}) = \begin{bmatrix} \cos(\theta) & -\sin(\theta) \\ \sin(\theta) & \cos(\theta) \end{bmatrix} {}^0\mathbf{J}^*(\mathbf{q}) \tag{3-35a}$$

$${}^0\mathbf{J}^*(\mathbf{q}) = \begin{bmatrix} -(\beta s_1+\gamma s_{12})+(\beta s_1+\gamma s_{12})\dfrac{D_1+D_2}{D} & -\gamma s_{12}+(\beta s_1+\gamma s_{12})\dfrac{D_2}{D} \\ (\beta s_1+\gamma s_{12})-(\alpha+\beta s_1+\gamma s_{12})\dfrac{D_1+D_2}{D} & \gamma c_{12}-(\alpha+\beta s_1+\gamma s_{12})\dfrac{D_2}{D} \end{bmatrix} \tag{3-35b}$$

where $s_1 = \sin(q_1)$, $c_{12} = \cos(q_1+q_2)$, etc. The inertia scalar sums D, D_0, D_1 and D_2 are defined by Equations (E-24), and $\alpha \equiv r_0^* = 0.426$ m, $\beta \equiv r_1^* = 0.894$ m, and $\gamma \equiv c_2^* + r_2 = 0.968$ m.

In order to invert $\mathbf{J}^*$ given by Equation (3-35), the 2x2 ${}^0\mathbf{J}^*(\mathbf{q})$ must be inverted. This is not possible when its determinant becomes zero. In this case, the condition $\det\{{}^0\mathbf{J}^*(\mathbf{q})\}$ results in the following:

$$\alpha\beta D_2(q_1,q_2)\sin(q_1) + \beta\gamma D_0(q_1,q_2)\sin(q_2) - \alpha\gamma D_1(q_1,q_2)\sin(q_1+q_2) = 0 \tag{3-36}$$

When the above condition is satisfied, the system is in a dynamically singular configuration. The values of q_1 and q_2 which satisfy Equation (3-36) are plotted in joint space as shown in Figure 3.2. This figure also shows that conventional kinematic singularities like $q_1=k\pi$, $q_2=k\pi$, $k=0,\pm1,\ldots$ still satisfy Equation (3-36). These correspond to the boundaries of the reachable workspace. However, infinitely more dy-

namically singular configurations exist which cannot be predicted from the kinematic structure of the manipulator. These are *interior* singularities which do not exist if the same manipulator has a fixed base; only singularities which occur at workspace boundaries exist in this case. Note that there are two singular hypersurfaces, called $Q_{s,1}$ and $Q_{s,2}$. This is because to each q_1 correspond two angles q_2 for which the system becomes dynamically singular. Since the joint space is two-dimensional in this case, those surfaces are lines, that is one-dimensional spaces.

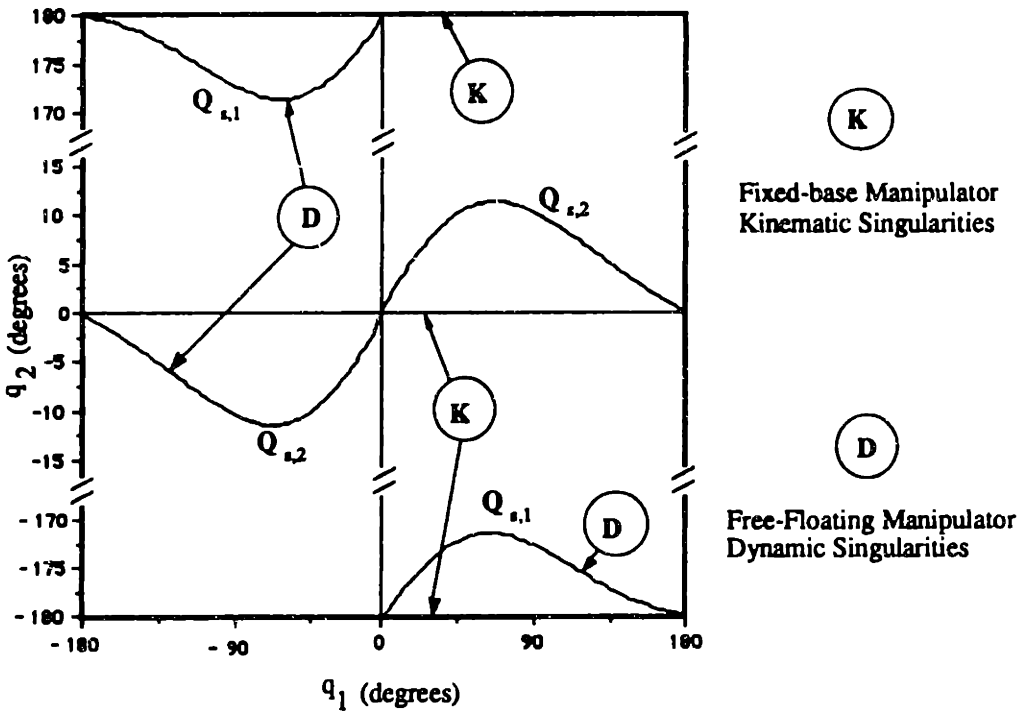

Figure 3.2. Dynamic singularities in joint space.

Figure 3.3 shows the manipulator in the singular configuration at q_1=-65°, q_2=-11.41°; the spacecraft attitude is θ=40°. This figure also shows the only available direction for the end-effector motion. The inertial motion of the end-effector in this configuration will be the shown, no matter how the joint actuators are driven. The best a control algorithm can do is to follow the available direction. *All* algorithms that use a Jacobian

inverse, such as the resolved rate or resolved acceleration control algorithms, fail at such a point. Ones that use a pseudoinverse Jacobian or a Jacobian transpose will likely follow the available direction, but may result in large errors.

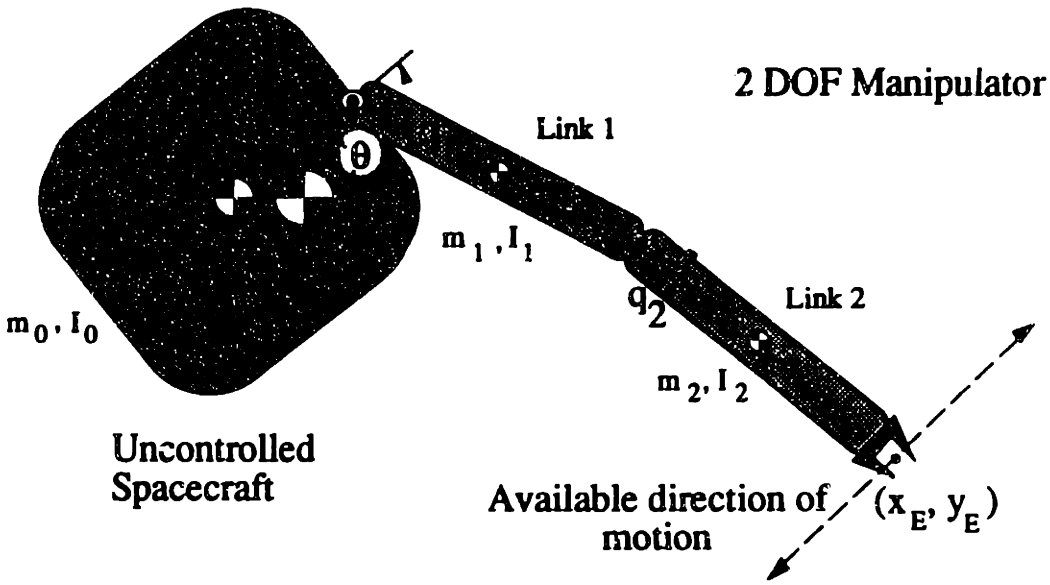

Figure 3.3. A dynamically singular configuration at q_1=-65° and q_2=-11.41°.

It is instructive to examine what exactly happens at a singular configuration. Figure 3.4 shows the two components of velocities that contribute to generate the end-effector velocity. Assume first that only the first joint is operated; the second remains fixed. Referring to Figure 3.4, the end-effector velocity is the vectorial sum of two components. Component v_1 is a velocity perpendicular to line AE and equal to the size of AE times $\dot{q}_1$, where AE corresponds to sub-Jacobian ${}^0J_{12}$ in Equation (3-11a). Component v_2 is a velocity perpendicular to line (CM)E and equal to the length of (CM)E times $\dot{\theta}$, where (CM)E corresponds to sub-Jacobian ${}^0J_{11}$. Of course, the magnitude of $\dot{\theta}$ is set by Equation (3-12). The vectorial sum of v_1 and v_2 gives the partial end-effector velocity due to joint 1, called $\dot{r}_{E,1}$, see Figure 3.4.

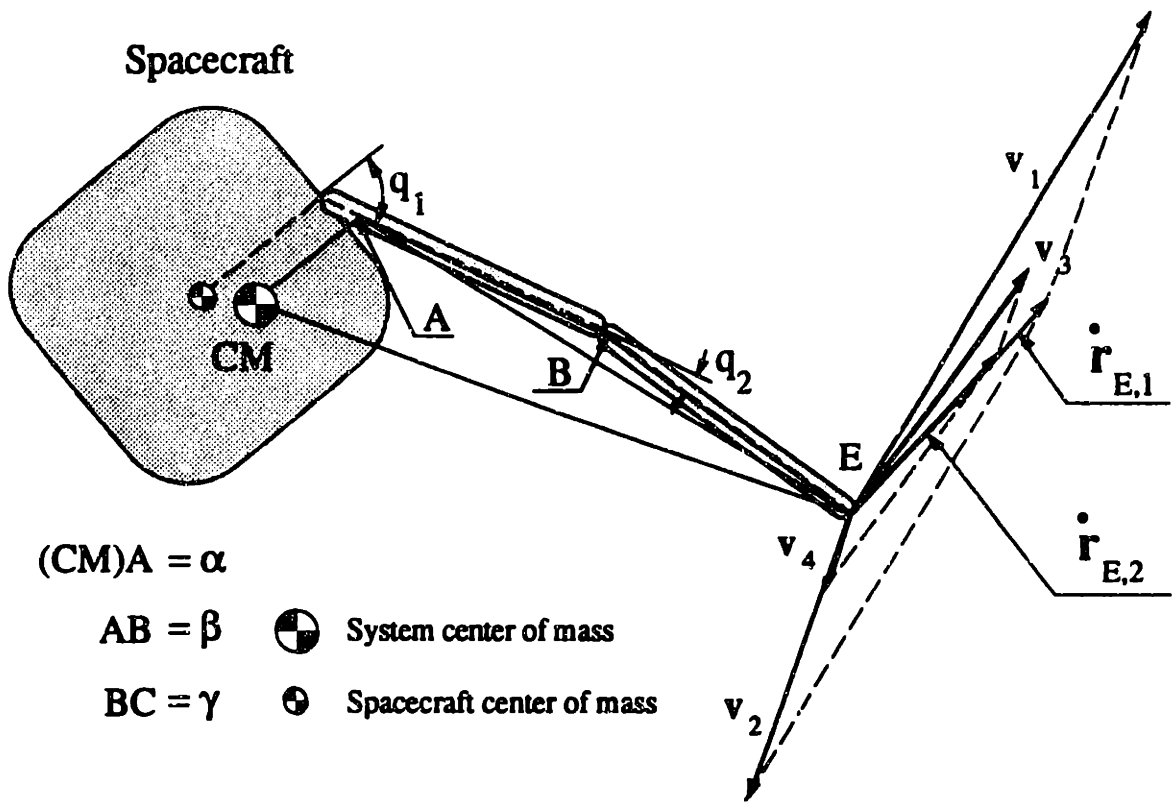

Figure 3.4. Velocity components at a singular configuration.

Similarly, if joint 1 is fixed and joint 2 is operated, another partial velocity, called $\dot{r}_{E,2}$, is obtained. In the general case where both joint operate, end-effector velocity is the vectorial sum of the two partial velocities, $\dot{r}_{E,1}$ and $\dot{r}_{E,2}$. If these are *not* parallel, the end-effector can move in any direction by adjusting the magnitudes of the joint rates, $\dot{q}_1$ and $\dot{q}_2$. When these two partial velocities *are* parallel, a degree of freedom is lost and the system is dynamically singular. Clearly, the available direction of motion is set by the only possible direction of the end-effector velocity.

Next, the nature and size of the workspaces is examined. The distance R of the end-effector E from the system CM, see Figure 3.4, is given by Equation (3-17) and written as:

$$R = R(q) = \sqrt{x_E^2 + y_E^2} \qquad (3\text{-}37a)$$

$$= \sqrt{\alpha^2+\beta^2+\gamma^2+2\alpha\beta\cos(q_1)+2\alpha\gamma\cos(q_1+q_2)+2\beta\gamma\cos(q_2)} \quad (3\text{-}37b)$$

Also see Equation (E-25). Applying Equations (3-18), the boundaries of the reachable workspace are found to be:

$$R_{min} = 0.352 \text{ m} = \alpha+\beta-\gamma \quad (3\text{-}38a)$$

$$R_{max} = 2.288 \text{ m} = \alpha+\beta+\gamma \quad (3\text{-}38b)$$

Therefore, the reachable workspace is a disk with a hole in it, see Figure 3.5. To construct the PIW and PDW workspaces for this example, note from Figure 3.2 that there are two hypersurfaces $\mathbf{Q}_s$ which are lines in the joint space. These hypersurfaces are found according to Equation (3-36). Each of these lines corresponds to pairs of q_1 and q_2, which are substituted in Equation (3-37). Then, conditions (3-19) result in two Path Dependent Workspaces, constrained by $(R_{min,1}, R_{max,1})$ and $(R_{min,2}, R_{max,2})$ respectively:

$$R_{min,1} = 0.352 \text{ m} = \alpha+\beta-\gamma \quad (3\text{-}39a)$$

$$R_{max,1} = 0.500 \text{ m} = \alpha+\gamma-\beta \quad (3\text{-}39b)$$

$$R_{min,2} = 1.436 \text{ m} = \beta+\gamma-\alpha \quad (3\text{-}39c)$$

$$R_{max,2} = 2.288 \text{ m} = \alpha+\beta+\gamma \quad (3\text{-}39d)$$

The PIW is then found by subtracting the two PDW regions defined above from the reachable workspace, see Figure 3.5. In general, the PIW is smaller than the free workspace defined in [65], although in this case it is equal to it. For example, consider a system with mass properties given by Table II. In this case, the same procedure yields the following boundaries for the workspaces:

$$R_{min,1} = 1.941 \text{ m} = \alpha+\beta-\gamma \quad (3\text{-}40a)$$

$$R_{max,1} = 2.756 \text{ m} > \alpha+\beta-\gamma \quad (3\text{-}40b)$$

$$R_{min,2} = 3.734 \text{ m} < -\alpha+\beta+\gamma \quad (3\text{-}40c)$$

$$R_{max,2} = 4.568 \text{ m} = -\alpha+\beta-\gamma \quad (3\text{-}40d)$$

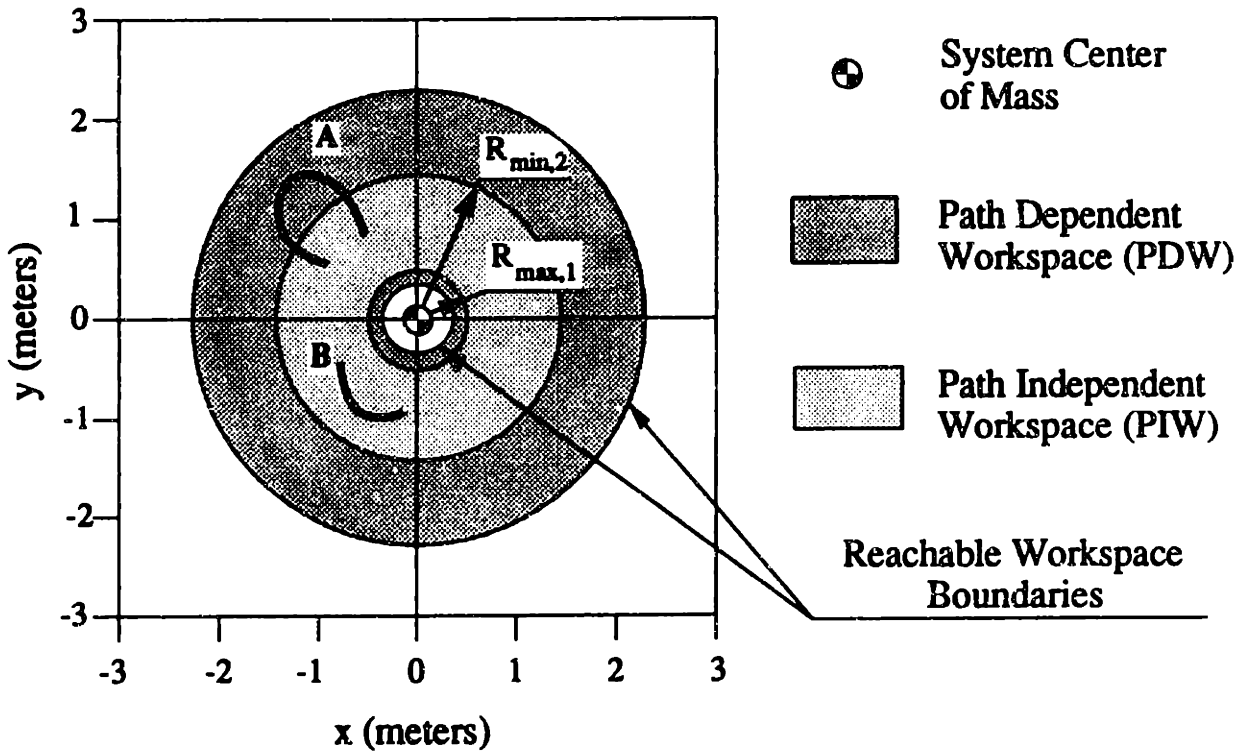

Figure 3.5. The Reachable, Path Independent and Path Dependent Workspaces.

Table II. Alternative system parameters for the two-DOF manipulator example.

Body	l_i (m)	r_i (m)	m_i (Kg)	I_i (Kg m^2)
0	.5	.5	40	6.667
1	2.0	2.0	16	21.333
2	.5	.5	3	0.250

The boundaries of the free workspace are constrained by $\alpha+\beta-\gamma = 2.618$ m, and $-\alpha+\beta+\gamma = 3.890$ m. These boundaries correspond to points $q_2=0^\circ, \pm 180^\circ$ which always belong to PDW/PIW boundary. Therefore the PIW is equal or smaller than the free workspace (a

subset). For example, point (x_E,y_E) = (3.8,0.0) is singular when (θ,q_1,q_2) = (236.06°,118°,45.29°) although it can be reached with any spacecraft orientation.

When the end-effector path has points belonging to the PDW, such as path A in Figure 3.5, the manipulator may assume a dynamically singular configuration because points in the PDW region can be dynamically singular, depending on the path. On the other hand, paths totally within the PIW region, such as path B, can never lead to dynamically singular configurations, because these cannot be reached in singular configurations.

Consider next the effect of a payload on the workspaces. It is assumed that the payload is a disk with mass 20 kg, that is half of the spacecraft's mass, and its radius is 0.30 m; the payload is grasped at its center of mass. The net effect of this payload can be described by modifying the mass and inertia properties of the last link of the system. The new system parameters are given in Table III.

In Figure 3.6, the dashed circle shows the boundaries of the reachable workspace if no load is present. When the load is captured, the system of mass changes position and the new workspace boundaries are the ones shown in Figure 3.6. By direct computation, one can find that in this case, $R_{min,1}$ = 0.246 m, $R_{max,1}$ = 0.421 m, $R_{min,2}$ = 1.01 m, $R_{max,1}$ = 1.605 m. Obviously, the region in which the load can be manipulated effectively has shrunk dramatically. At the limit, if the payload is very massive, all workspaces will reduce to zero; motions of the manipulator will result in spacecraft motions only!

Table III. System parameters for the two-DOF manipulator example, manipulating a load.

Body	l_i (m)	r_i (m)	m_i (Kg)	I_i (Kg m^2)
0	.5	.5	40	6.667
1	.5	.5	4	0.333
2	.5	.5	23	1.802

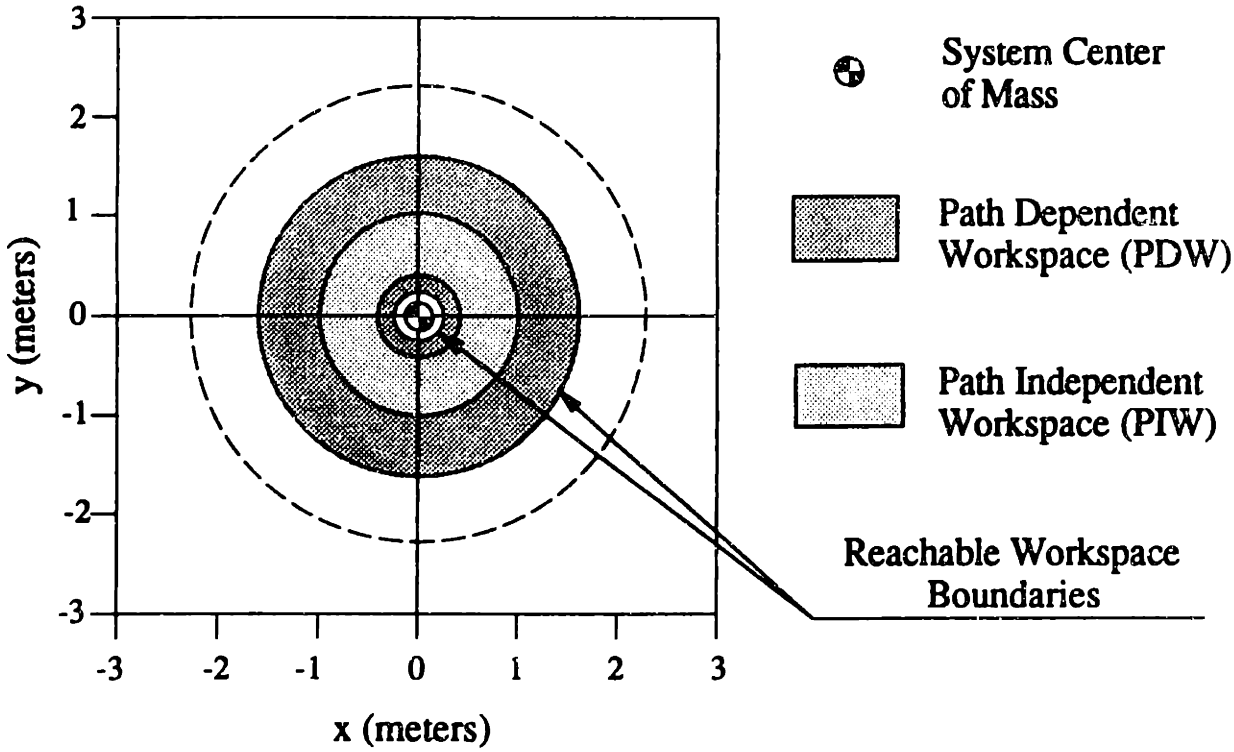

Figure 3.6. The effect of a payload on workspaces.

As discussed earlier, it is desired to reduce the effect of dynamic singularities. Applying the results of Section 3.6, first assume that spacecraft inertia, I_0, approaches infinity. Then, d_{00}, D_0 become very large and the only significant term in Equation (3-36) is $I_0\sin(q_2)$. Therefore, singular configurations in this case are the usual kinematic ones ($q_2=0^\circ, \pm 180^\circ$). In other words, as the inertia of the spacecraft becomes larger, the effects of dynamic singularities are reduced and and PIW is increased, approaching the reachable workspace limits.

Another method discussed in Section 3.6 is to mount the manipulator at the CM of the spacecraft. Indeed, if r_0 is zero, then r_0^* and α are zero, and the only singular configuration that exists is at $q_2=0^\circ, \pm 180^\circ$, see Equation (3-36). Again, this is a kinematic singularity and corresponds to reachable workspace boundaries. As r_0^* or α approach zero, $R_{max,1}$ approaches R_{min} and $R_{min,2}$ approaches R_{max}. Therefore, the two circles that define PIW,

shown in Figure 3.5, approach the reachable workspace boundaries, and dynamic singularities become less important.

In deriving equations of motion for this example, the system inertia matrix must be found. This is accomplished using Equation (3-26) and definitions (E-24). The result is:

$$\mathbf{H}^*(q) = \begin{bmatrix} d_{11}+2d_{12}+d_{22} - \dfrac{(D_1+D_2)^2}{D} & d_{12}+d_{22} - \dfrac{D_2(D_1+D_2)}{D} \\ d_{12}+d_{22} - \dfrac{D_2(D_1+D_2)}{D} & d_{22} - \dfrac{D_2^2}{D} \end{bmatrix} \tag{3-41}$$

The system inertia matrix, $\mathbf{H}^*$, is a 2×2 positive definite symmetric matrix whose elements are functions of the joint angles q_1 and q_2, only. Note that D represents the inertia of the whole system with respect to its CM and thus, is always a positive number. Using $\mathbf{H}^*$ and Lagrange's equations, the system's equations of motion are obtained in the form (3-28).

3.9 NON-ZERO INITIAL MOMENTUM

In the previous sections, it was assumed that the system is initially at rest, or equivalently, that the system linear and angular momentum is zero. Here the consequences of non-zero momentum are examined.

Using Equations (2-31), (2-32), (3-1), and (3-3), an expression for the end-effector velocity can be written still as:

$$\dot{\mathbf{x}} = \mathbf{J}^* \dot{\mathbf{q}} + \begin{bmatrix} \mathbf{M}^{-1}\mathbf{1} & \mathbf{T}_0{}^0\mathbf{J}_{11}{}^0\mathbf{D}^{-1}\mathbf{T}_0^T \\ \mathbf{0} & \mathbf{T}_0{}^0\mathbf{D}^{-1}\mathbf{T}_0^T \end{bmatrix} \begin{bmatrix} \mathbf{p}_0 \\ \mathbf{h}_{cm,0} \end{bmatrix} . \tag{3-42}$$

In the above, $\mathbf{J}^*$ is the free-floating system Jacobian defined by equation (3-15), $\mathbf{p}_0$ is the constant linear momentum and $\mathbf{h}_{cm,0}$ is the constant angular momentum about the system CM. The 6×6 matrix in Equation (3-42) is a function of both the spacecraft attitude and the system configuration. Multiplying this matrix with the constant momentum vector results

in an end-effector *drift* term, which is non-zero even when the manipulator does not move ($\dot{\mathbf{q}} = 0$). From the above, it is clear that no Jacobian can be written in this case. However, Equation (3-42) can be inverted to result in a set of $\dot{\mathbf{q}}$ as a function of $\dot{\mathbf{x}}$ and the drift term, and hence it is possible to drive the manipulator joints appropriately. Clearly, this can be done for small momentum and/or for relatively short periods of time. To see this, imagine that the end-effector must stay at some fixed inertial point, ($\dot{\mathbf{x}} = 0$). Then, because of Equations (2-22) and (3-2), the configuration $\mathbf{q}$ will be changing continuously to keep $\mathbf{x}$ at $\mathbf{x}_{des}$. After some time, $\mathbf{J}^*$ will become singular and hence, there will be no $\dot{\mathbf{q}}$ that can result in $\dot{\mathbf{x}} = 0$. Even if no dynamic singularities occur, as the reachable workspace drifts in inertial space, $\mathbf{J}^*$ will become singular when $\mathbf{x}_{des}$ reaches the boundaries of the reachable workspace. At this point, it will not be possible to compensate for the momentum vector any more and the end-effector will drift away from $\mathbf{x}_{des}$. Although this is a problem, it may not be a fatal one; the system may be able to function for some time till this happens. Thereafter, spacecraft actuators must eliminate any accumulated momentum.

The effect of initial momentum to the equations of motion must be examined also. As was mentioned above, in general, a Routhian function cannot be found for a spatial system. To avoid this difficulty, Equation (2-54) is solved for ${}^0\dot{\omega}_0$ and Equation (3-3) for ${}^0\omega_0$, (recall that no external forces or torques are present). The results are substituted to the general equations of motion given by Equations (2-62) which yield:

$$\mathbf{H}^*(\mathbf{q})\,\ddot{\mathbf{q}} + \mathbf{C}^*(\mathbf{q},\dot{\mathbf{q}})\,\dot{\mathbf{q}} + \mathbf{G}^*(\mathbf{q},\mathbf{e},\mathbf{n},\mathbf{h}_{cm,0}) = \tau \qquad (3\text{-}43)$$

where $\mathbf{H}^*$ and $\mathbf{C}^*$ were defined earlier and $\mathbf{G}^*$ is an extra term which is a function of $\mathbf{q}$, $\mathbf{e}$, $\mathbf{n}$, and $\mathbf{h}_{cm,0}$. This extra term vanishes when $\mathbf{h}_{cm,0}$ is zero, but not when the manipulator stops moving. The symbol $\mathbf{G}^*$ was selected because this term exhibits similar characteristics to those of gravity terms in fixed-based manipulators, if $\mathbf{g}$, the gravity vector, is substituted for $\mathbf{h}_{cm,0}$. Note that the dynamic equations are still N, but coupled to the first order momentum equations because $\mathbf{G}^*$ is a function of the spacecraft attitude.

In planar systems, it is easy to find the exact form of $\mathbf{G}^*$ by constructing a Routhian function R, given below without proof[12]:

$$R(\mathbf{q},\dot{\mathbf{q}}) = \frac{1}{2}\dot{\mathbf{q}}^T \mathbf{H}^*(\mathbf{q})\,\dot{\mathbf{q}} + h_{cm,0}\, D^{-1}\mathbf{D}_q\dot{\mathbf{q}} - \frac{1}{2}h_{cm,0}^2\, D^{-1} \tag{3-44}$$

Note that the second term of R is linear in the joint velocities and that the third term depends only on the configuration $\mathbf{q}$, hence, it acts like a potential term. Applying Lagrange's equations on R, the following equations of motion result:

$$\mathbf{H}^*(\mathbf{q})\,\ddot{\mathbf{q}} + \mathbf{C}^*(\mathbf{q},\dot{\mathbf{q}})\,\dot{\mathbf{q}} + \frac{1}{2}h_{cm,0}^2\frac{\partial D^{-1}}{\partial \mathbf{q}} = \boldsymbol{\tau} \tag{3-45}$$

The above shows that for planar systems, $\mathbf{G}^*$ is independent of the spacecraft attitude and therefore the reduced equations of motion are truly decoupled. However, $(\mathbf{q},\mathbf{0})$ points are not equilibria any more; in general[13] some torque must be applied to cancel $\mathbf{G}^*$, which acts like a *disturbance* to the system. This disturbance can be cancelled under the provisions mentioned above.

Example. For the one-DOF system of Section 2.5.1, the only equation of motion is:

$$H^*(q)\,\ddot{q} + C^*(q,\dot{q})\,\dot{q} + \frac{\hat{d}_{01}}{D^2}h_{cm,0}^2 = \tau \tag{3-46}$$

where all terms are by Equations (3-29), (E-5) and (E-7). Since the term $\hat{d}_{G1}$ is proportional to sin(q), the system equilibria are q=0°, ±180°. The disturbance term is configuration dependent, like a gravity term in fixed-based systems, and can be cancelled similarly.

---

[12]The Routhian can be found by subtracting $h_{cm,0}\dot{\theta}$ from the kinetic energy of the unreduced system given by Equation (3-23a) and by substituting $\dot{\theta}$ in the expression that will result, as a function of the joint rates and the constant momentum, see Equation (3-3).

[13]When Equation (3-32) reaches an equilibrium, the whole system revolves around the CM without deforming. Equilibria of Equation (3-32) are not infinite, but rather countable. A reader interested in such equilibria is refereed to some recent theoretical studies, for example to [9].

The conclusion of this section is that although non-zero momentum is a problem for free-floating systems, it can be handled for some period of time. Eventually, once momentum is detected, jet actuators and/or momentum wheels must eliminate it.

3.10 SUMMARY

Integrals of motion that exist in space manipulator systems where spacecraft position and attitude are not controlled, are found and analyzed. It was shown that the non-integrability of the angular momentum results in a system with path dependencies; a closed path in joint or end-effector space does change a spacecraft's attitude.

The system Jacobian was derived and shown to be singular in configurations that are distinct from the usual kinematically singular configurations: these are due to the dynamic coupling between manipulator motions and its spacecraft. These singularities are called *dynamic singularities* and can be a serious problem for all planning and control algorithms that do not assume active control of spacecraft attitude. Consequently, their effects must be considered in the design of such systems. Additionally, a workspace point may be singular or not depending on the end-effector path used to reach this point. A manipulator's reachable workspace is defined and is divided in two regions. In the first, called a Path Independent Workspace (PIW), no dynamic singularities can occur; in the second, called a Path Dependent Workspace (PDW), dynamic singularities may occur depending on the path taken by the end-effector in the inertial space. Some notions are presented that may help in maximizing the PIW. Finally, the effect of non-zero momentum was shown to degrade a system's performance gracefully, but spacecraft actuators must eliminate periodically any accumulated momentum.

In this and the previous chapter, the characteristics and capabilities of free-flying and free-floating systems were analyzed. The next chapter deals with the problem of controlling such systems.

4 Motion Control Algorithms for Space Manipulators

4.1 INTRODUCTION

It is well known that one generally needs three basic elements in order to control a fixed-based manipulator. These are, first, an invertible representation of manipulator kinematics, which can be in the form of a closure equation or a Jacobian. Second, one may need a set of dynamic equations describing the response of manipulator joint angles to actuator torques or forces. Third, one must design a control algorithm using internally or externally provided sensory information in order to calculate torques or forces required to achieve a desired task.

In most cases, the two first elements are in direct correspondence to a system's "plant," that is to an input-output description of the dynamical system to be controlled. This description for space manipulator systems was obtained in the two previous chapters where their kinematics and dynamics were analyzed from a fundamental point of view. In this chapter, a fundamental approach is taken to the question of what kind of control algorithms can be applied to the motion control of space manipulators; control algorithm design will be based on the obtained description of the plant. Further, the analysis of the previous chapters will be used as a guideline of what is feasible in controlling space systems. The main issues that will be covered are controllability, controller structure, sensory requirements, and controller robustness.

Section 4.2 analyzes the various modes of operation of space manipulator systems and identifies the appropriate plant description for each mode. In Section 4.3, state and output controllability of free-floating systems is investigated. In Section 4.4, the kinematic

and dynamic description of free-floating systems is compared to the one for fixed-based systems: the same structure between fixed-based and free-floating systems is shown, with some exceptions. From this analysis it is deduced that nearly any control algorithm can be applied in the control of free-floating systems, provided that some mild conditions are observed. Also in the same section the issue of required sensory capabilities and of robustness to disturbances and parameter variations is discussed. Section 4.5 illustrates these results with an example of control law design for a free-floating system. Section 4.6 generalizes the above methods, treating a free-flying manipulator as a MIMO mechanical system with redundancy. This redundancy is used to control the spacecraft and the manipulator in a coordinated way. In Section 4.7 Coordinated Control for a free-flying system is demonstrated using an example and Section 4.8 closes this chapter.

4.2 CONTROL MODES FOR SPACE MANIPULATOR SYSTEMS

In this section, the appropriate system description with respect to some control objective is prescribed. As shown in Figure 4.1, the system to be controlled is described by some dynamical equations which correspond to the "dynamics" block of the figure. The input to this block is a control vector, for example actuator torques, and the output is a state of the system, for example joint rates and joint angles. This state vector does not necessarily represent variables to be controlled; the "kinematics" block represents a map[1] from the state of the system to its output. This block is not always the same; what it really is depends upon the task which sets the command (or set-point).

Usually two modes of motion control are implemented in fixed-based systems. In the first mode, joint angles of a manipulator are commanded to some desired angles

---

[1]Consider the linear system described by: $\dot{x} = Ax + Bu$, $y = Cx$, where x is the system state, u the input and y the output. Then, the dynamics block is equivalent to the "A" matrix in linear systems, or to the pair (A,B), and the kinematics block to the "C" matrix.

(command), in other words, the manipulator is controlled in its *joint space*. Kinematics do *not* play any role in this case; the kinematics block in Figure 4.1 is just an integrator, assuming that the dynamics block output is a set of joint positions and rates. Knowledge of the system dynamics may improve this mode of control, although a simple PD joint controller is in many cases adequate for this task. In the second mode, the end-effector is commanded to move with respect to some fixed coordinate frame; the end-effector is controlled in some *cartesian or operational space* [33], and the command is some cartesian space position and/or velocity.

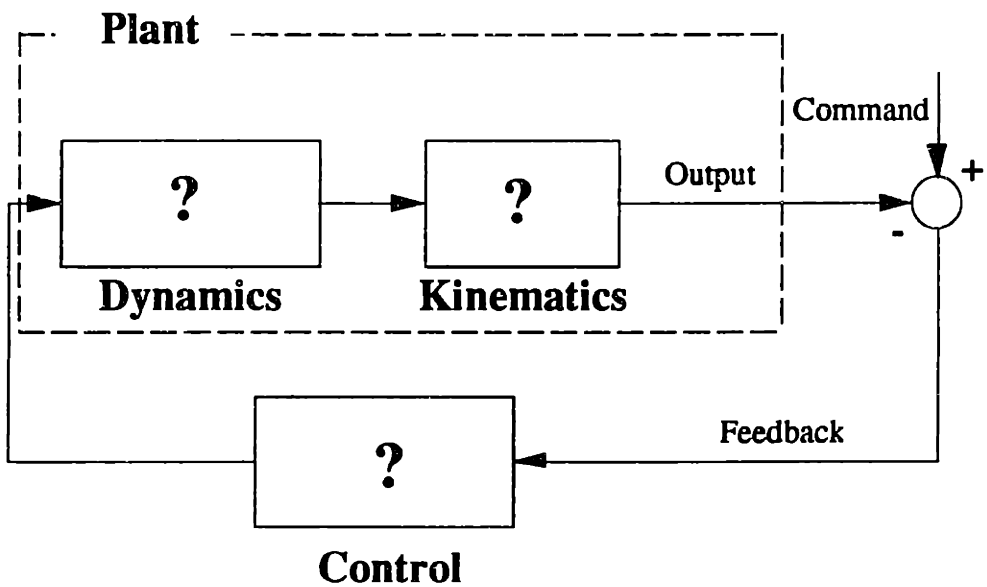

Figure 4.1. General block diagram for closed-loop control.

The kinematics block contains either a Jacobian matrix that maps joint rates to end-effector velocities, or a set of closure equations that map joint angles to cartesian space points[2], or both. Inversion of manipulator kinematics, either in the form of closure equations or in the

[2]If Euler angles are used to represent the orientation of the end-effector, then end-effector position/orientation is described by a 6×1 column vector, $x \in \mathbf{R}^6$. This description is valid locally only, since Euler angles cannot provide a global description of orientation; four parameter descriptions, for example Euler parameters, are required to avoid singularities in the description. Also see [34,36,43].

form of a Jacobian is *required* for planning or control purposes. Note that the two "plant" blocks in Figure 4.1, are part of the actual *physical system*, as defined from an input-output point of view and cannot be removed or altered; this is why it is important to have this picture in mind. Planners or controllers invert a part or the whole of a plant, and hence must use an available representation of these blocks. Although this is straightforward in fixed-based systems, it needs clarification in space systems.

4.2.1 Joint Space Motion Control

Similarly to fixed-based systems, a space manipulator may operate under different modes, differing by the control objective. In some cases, the only objective may be to command a simple *joint motion*, such as when the manipulator is to be driven at its stowed position. As in the fixed-based case, kinematics are not needed to achieve this task; simple PD joint controllers are in general enough. If it is desired to predict the motion of the entire system, or if a computed torque algorithm is used, one needs the appropriate equations of motion. In the case of a free-flying system, these will be characterized by the full system inertia matrix $\mathbf{H}^+$ while in the case of a free-floating system by $\mathbf{H}^*$, see Equations (2-62) and (3-28). The "dynamics" block in Figure 4.1 contains precisely these equations.

Unlike fixed-based systems, there are two types of cartesian space motion control: Spacecraft-Referenced End-Point Motion Control and Inertially-Referenced End-Point Motion Control. These are discussed below.

4.2.2 Spacecraft-Referenced End-Point Motion Control

Spacecraft-Referenced End-Point Motion Control is the mode of control where the manipulator end-point is commanded to move to a location *fixed to its own spacecraft.* That is, the position of the target or the reference trajectory is defined with respect to *the moving spacecraft.* For example, in Figure 4.2 the task is to move the end-effector close to the screw which is fixed with respect to the spacecraft. The appropriate dynamics are the

same as mentioned in Section 4.2.1, depending on whether the system is free-flying or free-floating. However in this mode, system kinematics are important to achieve the task. Since motion of the space manipulator is controlled with respect to its own base, the appropriate Jacobian in this mode of operation is identical to that of a fixed-based manipulator, called **J**. If the manipulator structure is solvable[3], closure equations can be equally well used to yield set-points for the joint angle control systems. Of course, since the dynamics are different from the fixed-based case, control torques of different magnitudes will be required. But this is a trivial difference, and one can use any controller designed for a fixed-based system; if a computed torque method is used [43], the appropriate dynamics must be used.

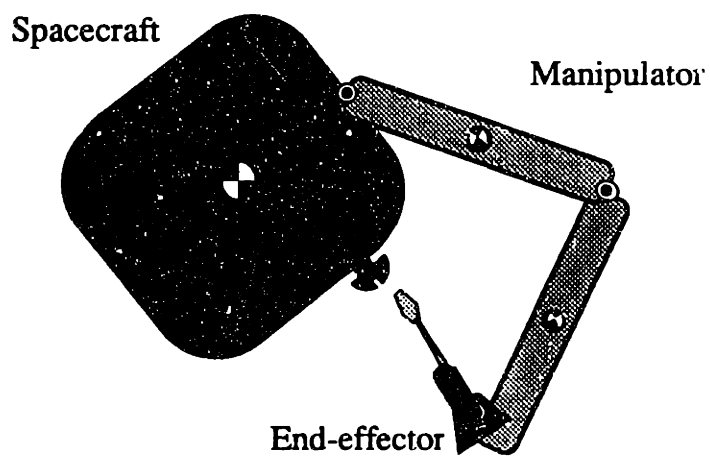

Figure 4.2. Spacecraft-Referenced End-Point Motion Control.

4.2.3 Inertially-Referenced End-Point Motion Control

Inertially-Referenced End-Point Motion Control, is the mode where the manipulator end-point is commanded to move with respect to *inertial space*. Kinematic descriptions that apply to this mode were developed in the two previous chapters.

---

[3]A kinematic structure is called *solvable* if a closed-form inverse solution, (a map from end-effector positions/orientations to joint angles), exists, see [5, p.46].

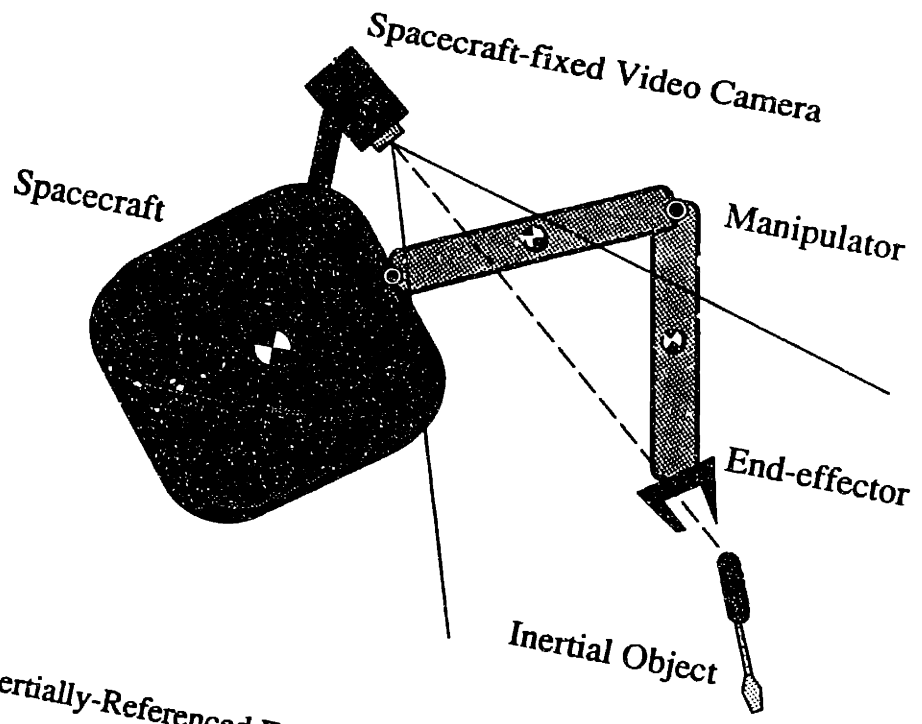

Figure 4.3. Inertially-Referenced End-Point Motion Control. Camera spacecraft-fixed.

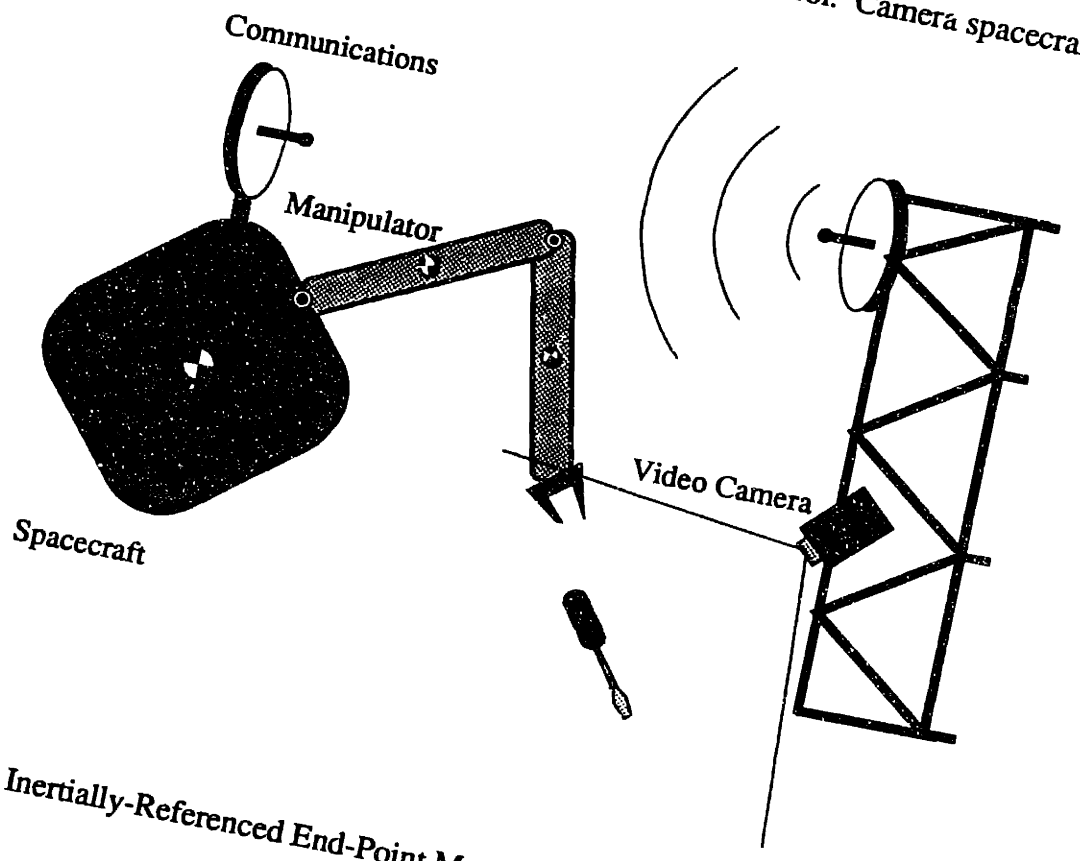

Figure 4.4. Inertially-Referenced End-Point Motion Control. Camera inertially-fixed.

Two cases may be distinguished here. The first is the one where a desired trajectory is fixed in inertial space, but the controller receives *feedback* from instrumentation *fixed on the spacecraft*, for example from a spacecraft-fixed camera, see Figure 4.3. Then, the available feedback is the end-effector position as seen from the moving spacecraft, ${}^0\mathbf{x}$, and hence, the appropriate Jacobians are just ${}^0\mathbf{J}^+$ or ${}^0\mathbf{J}^*$, given by Equations (2-35) and (3-15c). Note that these Jacobians are functions of the configuration $\mathbf{q}$ only. This fact will be used later again.

One problem with a spacecraft-fixed camera is that the target may move out of the camera's range. Some absolute inertial measurement may be preferred in such cases. This can be provided for example, by an inertially-fixed camera mounted on some space structure, see Figure 4.4.

Here the appropriate Jacobians are $\mathbf{J}^+$ or $\mathbf{J}^*$, depending on whether the system is free-flying or free-floating. As mentioned above, the dynamic equations are always the same, described by either $\mathbf{H}^+$ or $\mathbf{H}^*$. Note that in this mode of control, Jacobians are in addition functions of a spacecraft's attitude. By far, this is the most interesting case of motion control, and hence, in the next sections it will be assumed that the task is to follow an inertially fixed path in a six dimensional space.

4.3 STATE/OUTPUT CONTROLLABILITY OF FREE-FLOATING SYSTEMS

In the previous section, emphasis was placed in identifying the right plant description, according to various control objectives. Assuming that this description is determined, the next step is to check whether a system is controllable; a free-floating system is assumed. Two types of controllability are considered here, *state* and *output* controllability. These can be defined for any type of system, linear or nonlinear, [47, p.762]. First, state controllability of a free-floating system is examined.

4.3.1 State Controllability

A system is *state controllable* if it is possible to transfer the system state from an initial state to any other state in a finite interval of time. As will be seen later, state controllability is related to whether joint-space control is possible. To examine state controllability for a free-floating system, its input-output description will be used; for convenience it is summarized here using Equations (3-28), (3-13) and (3-4):

$$\mathbf{H}^*(\mathbf{q})\,\ddot{\mathbf{q}} + \mathbf{C}^*(\mathbf{q},\dot{\mathbf{q}})\,\dot{\mathbf{q}} = \boldsymbol{\tau} \tag{4-1a}$$

$$\mathbf{r}_{cm} = \mathbf{r}_{cm,0} \tag{4-1b}$$

$${}^0\boldsymbol{\omega}_0 = -\,{}^0\mathbf{D}^{-1}\,{}^0\mathbf{D}_q\,\dot{\mathbf{q}} \tag{4-1c}$$

$$\dot{\mathbf{T}}_0 = \mathbf{T}_0\,{}^0\boldsymbol{\omega}_0^{\times} \tag{4-1d}$$

These equations are represented in block diagram form in Figure 4.5, where θ denotes the spacecraft's attitude, and the trivial linear equations are not included. The system is initially at rest. Since the objective is to control a manipulator's configuration $\mathbf{q}$, θ is not part of the feedback-loop and not controlled.

The form of Equation (4-1a) suggests that it is trivial to transfer state $(\mathbf{q}, \dot{\mathbf{q}})$ to any other by an appropriate control law. To show this it suffices to consider a decoupling law which includes a feedforward nonlinear term and an auxiliary control input $\mathbf{u} \in \mathbf{R}^N$:

$$\boldsymbol{\tau} = \mathbf{C}^*(\mathbf{q},\dot{\mathbf{q}})\,\dot{\mathbf{q}} + \mathbf{H}^*(\mathbf{q})\,\mathbf{u} \tag{4-2}$$

The inverse of $\mathbf{H}^*$ always exists since it was proven to be positive definite and therefore, Equations (4-1a) and (4-2) result in a linear decoupled and *controllable* system of the form:

$$\ddot{\mathbf{q}} = \mathbf{u} \tag{4-3}$$

Note that any state $(\mathbf{q},\dot{\mathbf{q}}) = (\mathbf{q}_{des},\mathbf{0})$ is an asymptotically stable equilibrium.

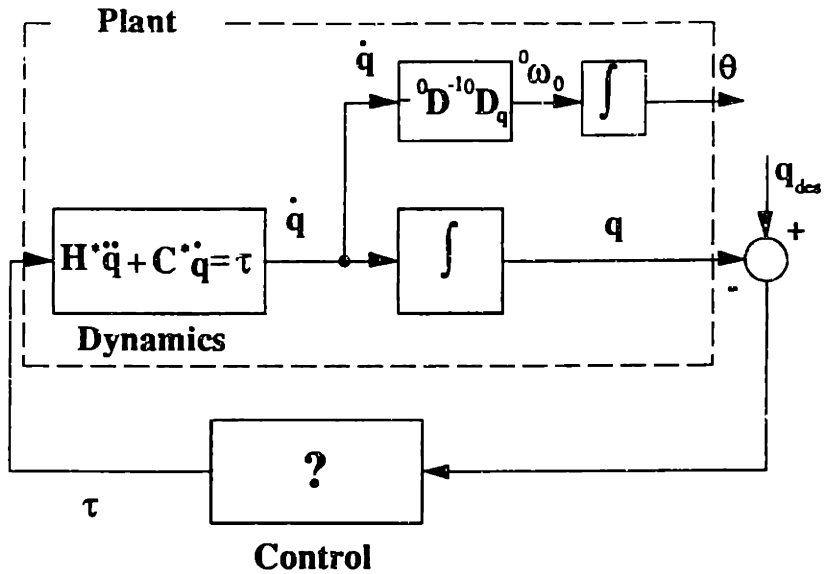

Figure 4.5. Block diagram of a free-floating system in Joint Space Control mode.

To draw conclusion about the behavior of the whole system, the remaining system states must be examined. Since it is not possible to control the position or velocity of the system CM with internal forces, such as manipulator joint torques, $\mathbf{r}_{cm}$ and $\dot{\mathbf{r}}_{cm}$ are uncontrollable. These states correspond to a double integrator system, with zero inputs and zero initial conditions, that is to a marginally stable system. The states left are the spacecraft angular velocity and attitude. Obviously, one cannot set ${}^0\omega_0$ independently of $\dot{\mathbf{q}}$ because of Equation (4-1c), but for exactly the same reason, when $\dot{\mathbf{q}}\rightarrow\mathbf{0}$ asymptotically ${}^0\omega_0\rightarrow\mathbf{0}$ asymptotically. Then due to Equation (4-1d), $\mathbf{T}_0\rightarrow\mathbf{T}_{0,ss}$, that is the attitude assumes a constant but unknown value[4]; stability in the motion of the spacecraft is assured. This analysis proves that under the assumptions of free-floating systems, the uncontrollable states of the system span a stable space; the subspace that corresponds to the manipulator states is controllable and possesses infinite equilibria of the form $(\mathbf{q}_{des},\mathbf{0})$[5]. Note that if the

[4]As mentioned in Chapter 3, this value also can be manipulated by using an appropriate path in the joint space. This is due to the non-integrability of the angular momentum equation. However, the focus here is in controlling the manipulator configuration and not the spacecraft's attitude.

[5]This corresponds to the notion of *stabilizability* in linear systems, where one requires that the unstable subspace of a system is controllable; in other words, the uncontrollable part must be stable, [37].

system has nonzero momentum, the uncontrollable space is unstable. However as noted earlier, spacecraft actuators should remove any momentum, because otherwise the system becomes unpractical.

4.3.2 Output Controllability

In the previous section it was proved that the subspace spanned by $(\mathbf{q},\dot{\mathbf{q}})$ is controllable. However, when a system operates under one of the end-point control modes, the system output is the end-effector position and/or velocity. Hence, the focus here is to check if the system is *output controllable*, that is if the output can be taken from any initial state to any other state in finite time. Below it is assumed that the system operates under Inertially-Referenced End-Point Control mode.

First, the appropriate block diagram is constructed using results from Chapter 3 and depicted in Figure 4.6. It is clear that the same remarks that were made above about the motion of the system CM and the spacecraft hold here, too. The main difference with the previous case is the existence of a kinematics block, described by Equations (3-14) and (3-15), and repeated here:

$$\dot{\mathbf{x}} = \mathbf{J}^* \dot{\mathbf{q}} \tag{4-4a}$$

$$\mathbf{J}^* = \mathrm{diag}(\mathbf{T}_0, \mathbf{T}_0)\, {}^0\mathbf{J}^*(\mathbf{q}) \tag{4-4b}$$

where $\dot{\mathbf{x}} \in \mathbf{R}^6$ is the end-effector velocity. Kinematic equations relating attitude variables to angular velocities also must be used; these equations are represented here by an integrator block, see Figure 4.6. Next, the effect of this Jacobian on a system's output controllability is analyzed.

As done above, one can use the control law (4-2) to linearize and decouple the system. Also, Equation (4-4a) can be differentiated once more to yield the end-effector acceleration as a function of $\ddot{\mathbf{q}}$ and $\dot{\mathbf{q}}$:

$$\dot{\mathbf{x}}^{\cdot} = \mathbf{J}^{*}\ddot{\mathbf{q}} + \dot{\mathbf{J}}^{*}\dot{\mathbf{q}} \tag{4-5}$$

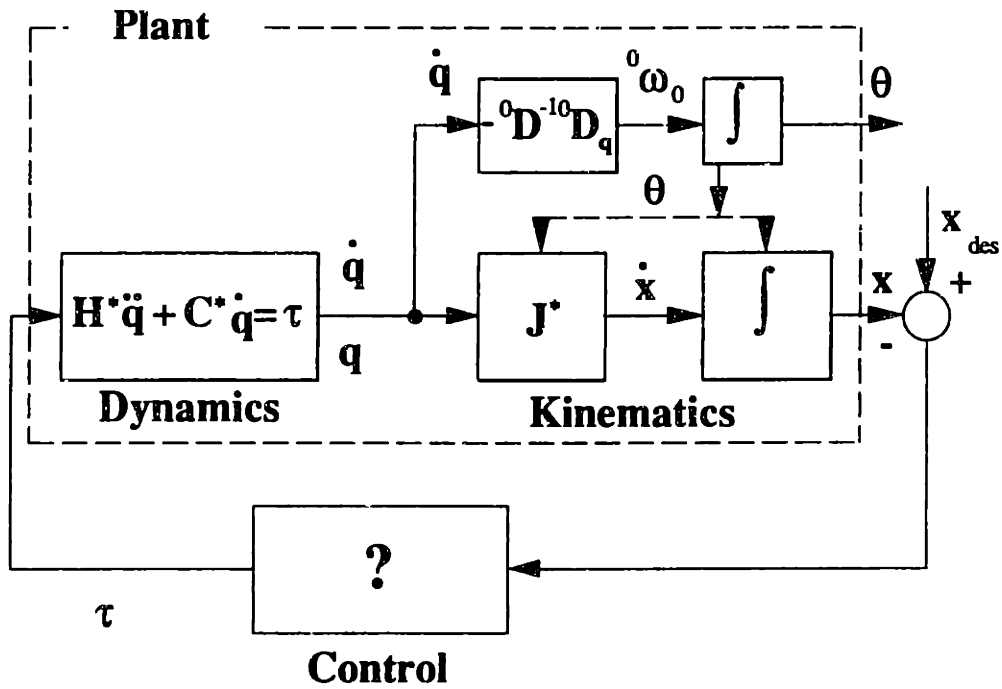

Figure 4.6. Block diagram of a free-floating system operating in Inertially-Referenced End-Point Control mode.

Assume that the system is linearized around an equilibrium point, for example around ($\mathbf{q}$, $\mathbf{0}$). Then $\mathbf{J}^{*}$ is almost a constant and the above can be written as $\ddot{\mathbf{x}} = \mathbf{J}^{*}\ddot{\mathbf{q}}$. Multiplying the two sides of Equation (4-3) by $\mathbf{J}^{*}$ and substituting $\ddot{\mathbf{x}}$ for $\mathbf{J}^{*}\ddot{\mathbf{q}}$, the following linearized equations of motion are obtained:

$$\dot{\mathbf{x}}^{\cdot} = \mathbf{J}^{*}\mathbf{u} \tag{4-6}$$

This system can be written in the standard form for linear systems as:

$$\frac{d}{dt}\begin{bmatrix}\mathbf{x}\\ \dot{\mathbf{x}}\end{bmatrix} = \begin{bmatrix}\mathbf{0} & \mathbf{1}\\ \mathbf{0} & \mathbf{0}\end{bmatrix}\begin{bmatrix}\mathbf{x}\\ \dot{\mathbf{x}}\end{bmatrix} + \begin{bmatrix}\mathbf{0}\\ \mathbf{J}^{*}\end{bmatrix}\mathbf{u} \tag{4-7a}$$

$$= \mathbf{A}\begin{bmatrix}\mathbf{x}\\ \dot{\mathbf{x}}\end{bmatrix} + \mathbf{B}\,\mathbf{u} \qquad (4\text{-}7b)$$

where the state of the linear system is a 12×1 vector. Applying the controllability rank condition to this system, one can easily see that unless $\mathbf{J}^*$ has rank 6, the system described by Equation (4-7) is *uncontrollable*. If this rank is r<6, then the controllable subspace has order 2r<12, in other words only r coordinates and the corresponding velocities can be controlled. If the manipulator is not redundant (N=6), $\mathbf{J}^*$ is square, and hence it must be nonsingular. However, in Chapter 4 it was shown that $\mathbf{J}^*$ can become dynamically singular at some configuration. Then, at these points the system is *output uncontrollable*. As shown in Chapter 4, this problem can be avoided by working at the Path Independent Workspace, because there $\mathbf{J}^*$ is guaranteed of full rank.

It has been noted that reaching a point in the Path Dependent Workspace may or may not be possible, depending on the path taken by the end-effector. This is not in disagreement with this analysis, since this is local by nature. Some global technique may yield a path that conceivably can take any initial state to any desired one; such a path may be feasible for a nonlinear system although it is not for a linear one. Finally, note that a similar analysis can be done for the other modes of control, discussed in Section 4.2, with similar results. The next section deals with the nature of control algorithms for free-floating manipulators.

4.4 THE NATURE OF CONTROL ALGORITHMS FOR FREE-FLOATING SYSTEMS

In the above section, state and output controllability of a free-floating system was assessed. Assuming that the system operates in a domain where it is controllable, the next question is what kind of controllers one can use and what kind of feedback is needed to accomplish this task.

It can be argued that if a free-floating space manipulator and a fixed-base manipulator have the same dynamic and kinematic structure, then a control law which can be used for that fixed-based manipulator is theoretically suitable for the space manipulator. Hence, the structures of the dynamic and kinematic equations of free-floating manipulators are compared to the ones corresponding to fixed-based manipulators. By structure it is meant that the matrices of the dynamic equations and the Jacobian of the two manipulators have the same order and symmetry and depend upon the same variables. Of course, the numerical values of the elements of the matrices of the free-floating space system will have different values. For example, the elements of the dynamic matrices $\mathbf{H}^*$ and $\mathbf{C}^*$, will be different from those of the similar matrices of the fixed-base manipulator, $\mathbf{H}$ and $\mathbf{C}$, since $\mathbf{H}^*$ and $\mathbf{C}^*$ depend in part on a spacecraft's mass properties. As a result, the same torque vector τ will produce different joint accelerations in the two systems. Also, since the applicability of fixed-base controllers does not depend upon the existence of gravity, it can be neglected for the purposes of this comparison. Here it is assumed that the control mode is the one described in Section 4.2.3, that is inertial motion of the end-effector. Similar results hold for the other modes, see also [48,50].

4.4.1 Comparison of fixed-based and free-floating systems

This comparison is rather straightforward; it is only required to compare $\mathbf{J}^*$ and $\mathbf{H}^*$ to $\mathbf{J}$ and $\mathbf{H}$, that is to the Jacobian and inertia matrix of the same manipulator with a fixed base.

It has been shown, see Chapter 3, that the minimum number of equations describing the dynamics of the N+6 DOF system is N for an N DOF manipulator, the same as for a fixed-base N DOF manipulator. As proved in Appendix F, $\mathbf{H}^*$ is an N×N symmetric positive definite matrix, function of the system configuration $\mathbf{q}$ only, that is it has the same structure as the inertia matrix $\mathbf{H}$ of the same manipulator with a fixed base. A slight difference, important to some adaptive controllers, will be discussed in section 4.4.2. Finally, since $\mathbf{C}^*$ is derived from $\mathbf{H}^*$, it will have the same form as the fixed-base $\mathbf{C}$ which

is derived from **H**, see also Appendix F. Hence, the dynamic equations of both systems have the same *structure* as defined above.

If the spacecraft becomes very large, m_0 and $\mathbf{I}_0$ approach infinity, and $\mathbf{H}^*$ and $\mathbf{C}^*$ converge to **H** and **C**. To show this, note that in such a case ${}^0\mathbf{D}$, the total system inertia becomes large. Then the second term in the defining equation for $\mathbf{H}^*$ becomes zero. Also, M, the total system mass becomes large and all μ_i in Equation (2-6) are equal to 1 (i=1,...N+1) and barycenters move to the joint closer to the spacecraft. It is easy to show that in such a case, ${}^0\mathbf{D}_{qq}$ (=$\mathbf{D}_{qq}$), converges to **H**. This should be expected, because a very large spacecraft will not react to its manipulator's motions and the system will behave essentially as a fixed-base system. Further, the order of the system remains fixed and equal to N, independent of the size of m_0 and $\mathbf{I}_0$.

Also in Chapter 4 was shown that ${}^0\mathbf{J}^*(\mathbf{q})$ is a 6×N Jacobian which is a function of both the manipulator configuration, **q**, and of the system mass and inertia properties. If N=6, then ${}^0\mathbf{J}^*(\mathbf{q})$ becomes a square matrix. $\mathbf{T}_0$ depends on the spacecraft attitude, which can be measured or estimated using Equations (4-1c,d). It is unnecessary to use spacecraft attitude where the inertial motion is measured with respect to the spacecraft frame, see Section 4.2.3. In that case the Jacobian required is simply ${}^0\mathbf{J}^*(\mathbf{q})$.

It is well known that the Jacobian, **J**, of a fixed-base manipulator is a 6×N matrix that depends on **q** and the link lengths of the manipulator. $\mathbf{J}^*$ or ${}^0\mathbf{J}^*(\mathbf{q})$ has the same dimensions as **J** and also depends on **q** as well as on the ${}^0\mathbf{v}_{ik}$ vectors, scaled by the ${}^0\mathbf{D}_{ij}$ (i,j=0,...,N) inertia matrices. This means that the free-floating system differential kinematics, although complicated, have the same structure as the kinematics of the same manipulator with a fixed base.

If a spacecraft's mass and inertia, m_0 and $\mathbf{I}_0$, are large, $\mathbf{T}_0$ approaches a constant matrix and $\text{diag}(\mathbf{T}_0,\mathbf{T}_0){}^0\mathbf{J}^*(\mathbf{q})$ results in the normal fixed-based manipulator Jacobian. Mass and inertia dependencies vanish. This can be shown using the same as above arguments, in connection to Equation (3-15).

The above analysis confirms that the kinematics and dynamics of free-floating and fixed-based systems are essentially the same, with some minor exceptions. These are summarized below:

1. Terrestrial fixed-base manipulator Jacobians depend on the joint angles $\mathbf{q}$, only. In space, system Jacobians also depend on spacecraft orientation. This orientation can be calculated, or measured on-line by additional sensors. No such procedure is needed for fixed-base systems.
2. In general, the knowledge of kinematic parameters, such as link lengths, is enough for fixed-based manipulator control purposes. In space, this is not enough. The Jacobian of free-floating space system depends on its dynamic properties, such as the masses and inertias of its spacecraft, and on its manipulator's link lengths. In addition, system dynamics are more complicated and depend on products of inertias which increase the error in obtaining the mass matrix. External sensing or on/off-line parameter identification, see [7,68], can be very important for space systems.
3. Singularities are functions of the kinematic structure of the terrestrial fixed-base manipulator only. In space, dynamic singularities exist that depend on the mass and inertia distribution. A point in a free-floating system's workspace can be singular or not depending upon the path taken to reach it. These singularities represent physical limitations and render a system uncontrollable; hence they must be avoided. Terrestrial and space workspace sizes and structures are not the same.
4. Many controllers implemented in fixed-based terrestrial systems, use an invertible closure equation to map desired workspace points to manipulator joint angles. These joint angles are fed to the servo of a manipulator as set-points. The path from one point to another may not be known, but the final point will be the desired one. This type of control is called "point to point" control by [15]. However, in the case of free-floating manipulators, such a map between $\mathbf{q}$ and $\mathbf{x}$ does not exist,

because workspace locations are functions not only of the configuration $\mathbf{q}$ but also or the spacecraft attitude, which depends on the system's history, see Equation (3-10). This characteristic does not allow the use of "point to point" control.

So far it has been shown that the dynamics and kinematics of free-floating systems are described by equations that are same in structure with their counterparts in fixed-based systems, see Equations (4-1a) and (4-4). Also it has been shown that the matrices in these equations have the same structure to the matrices that correspond to fixed-based systems, with some minor exceptions. Hence, this analysis confirms that nearly any control algorithm that can be used for fixed-base manipulators can also be used for free-floating manipulators, provided, of course, that the appropriate matrices are used. For example, laws like resolved rate [69], resolved acceleration [43], impedance control [25], or simple PD and PID algorithms [4], including adaptive control [13,57], can be used if one uses the appropriate Jacobian and inertia matrix.

4.4.2 Sensory requirements and robustness issues

Required Measurements. The statement that nearly any control law can be used in free-floating systems has certain implications upon the kind of sensory information required. Assuming absolute knowledge of geometry, mass and inertia properties, measurement of $\mathbf{q}$ and $\dot{\mathbf{q}}$ is in general enough, as is for fixed-based systems. For example, if spacecraft attitude is needed, see Section 4.2, it can be estimated using Equations (4-1c,d) if a system's properties are known.

Attitude Measurement. The requirement for an exact knowledge of a system's parameters can be relaxed by allowing measurement of additional variables. Since it is harder to identify inertia properties than mass properties, spacecraft attitude can be measured instead of being estimated. In such a case, measurement of attitude and

knowledge of mass and geometry properties is in general enough. This information is in general available in space system.

End-point feedback. If system parameters are not known with sufficient accuracy, end-point position and/or velocity for closed-loop control in the cartesian space is required. Note that the same is true for fixed-based systems, when the kinematic properties of the system are not known with sufficient accuracy; exact knowledge of mass and inertia properties is desirable but not absolutely necessary.

Some authors have suggested that end-point feedback is essential to free-floating systems due to either the existence of a "nonholonomic constraint," or to "history" dependence of the end-effector location, [3,44]. However end-effector position and attitude can be known to a system's controller even if it relies entirely upon internal measurements, see Equations (3-10) and (2-20a); the only requirement is that geometry, mass and inertia properties of the system must be known with high accuracy. Hence, one can conclude that end-point sensing is needed for *robustness* reasons and is not due to the nature of the problem. This observation is important in view of the fact that it is very difficult to have inertial end-point-feedback in six DOF throughout a system's workspace. Until effective sensing techniques are developed, end-point sensing will remain a research issue.

Adaptive Control. Some advanced adaptive controllers for manipulators rely on two "extra" properties [13,57]. First, matrix $\dot{\mathbf{H}}^* - 2\mathbf{C}^*$ must be skew-symmetric. As shown in Appendix F, the first property holds. The second property requires that dynamic matrices are linear in the unknown geometry, mass and inertia parameters. This property allows one to write:

$$\mathbf{H}^*(\mathbf{q})\,\ddot{\mathbf{q}} + \mathbf{C}^*(\mathbf{q},\dot{\mathbf{q}})\,\dot{\mathbf{q}} = \mathbf{Y}(\mathbf{q},\dot{\mathbf{q}},\ddot{\mathbf{q}})\,\mathbf{a} \tag{4-8}$$

where $\mathbf{a}$ is a vector that contains all unknown parameters; the equations of motion are written in a linear parameter space. However, due to the definition of $\mathbf{H}^*$, see Equation (3-

26), this property does not hold. Nevertheless, an adaptive controller can still be applied, if one uses the last N equations of the unreduced system, given by Equations (2-62), because these are linear in the unknown parameters:

$$\mathbf{H}^*(\mathbf{q})\,\ddot{\mathbf{q}} + \mathbf{C}^*(\mathbf{q},\dot{\mathbf{q}})\,\dot{\mathbf{q}} = {}^0\mathbf{D}_{\mathbf{q}}(\mathbf{q})^T\,{}^0\dot{\omega}_0 + {}^0\mathbf{D}_{\mathbf{qq}}(\mathbf{q})\ddot{\mathbf{q}} + \mathbf{C}_2^+(\mathbf{q},\,{}^0\omega_0,\,\dot{\mathbf{q}}) = \mathbf{Ya} \tag{4-9}$$

In the above, the spacecraft angular velocity is *not* eliminated, and therefore, ${}^0\omega_0$ must be measured in addition to $\mathbf{q}$, $\dot{\mathbf{q}}$. (Some algorithms require additional measurement of accelerations, for example [13]). These conditions are enough for designing an adaptive algorithm capable of tracking in the joint space. To guarantee tracking in the inertial workspace, system Jacobians must be known accurately. Since $\mathbf{J}^*$ is a function of the mass properties of the system, algorithms which assume perfect knowledge of the $\mathbf{J}^*$ may not track in inertial workspace. This limitation may be solved by writting the end-effector velocities as functions of the spacecraft linear and angular velocities and not of those of the system CM, and by measuring the spacecraft coordinates and velocities.

Robustness to disturbances. As noted earlier, turning off a spacecraft's controller is only viable in the absence of external disturbances. Although the system may not fail fatally if a disturbance occurs, jet actuators must take over in such a case, and therefore the system will not satisfy the definition of a free-floating one any more.

In conclusion, if system parameters are sufficiently known, internally provided feedback is enough to control a system, using any controller. Additional measurements are required if this assumption does not hold. These measurements include either a spacecraft's attitude and angular velocity or end-point feedback, depending on the algorithm used. Finally, to eliminate the effect of disturbances (external forces/torques) spacecraft actuators must be used.

4.5 EXAMPLES

Here the five-DOF example system of Section 3.8 is used to illustrate the key results of the previous sections. System parameters are given in Table I. First, the structure of the Jacobian and inertia matrices are compared against the same matrices, derived for a fixed-based manipulator. As shown in Section 3.8, $\mathbf{J}^*$ is given by:

$$\mathbf{J}^*(\theta,\mathbf{q}) = \begin{bmatrix} \cos(\theta) & -\sin(\theta) \\ \sin(\theta) & \cos(\theta) \end{bmatrix} {}^0\mathbf{J}^*(\mathbf{q}) \tag{4-10a}$$

$${}^0\mathbf{J}^*(\mathbf{q}) = \begin{bmatrix} -(\beta s_1+\gamma s_{12})+(\beta s_1+\gamma s_{12})\dfrac{D_1+D_2}{D} & -\gamma s_{12}+(\beta s_1+\gamma s_{12})\dfrac{D_2}{D} \\ (\beta s_1+\gamma s_{12})-(\alpha+\beta s_1+\gamma s_{12})\dfrac{D_1+D_2}{D} & \gamma c_{12}-(\alpha+\beta s_1+\gamma s_{12})\dfrac{D_2}{D} \end{bmatrix} \tag{4-10b}$$

Since the inertia terms D_i (i=0,1,2) and D are functions of $\mathbf{q}$, the Jacobian elements are more complicated functions of the $\mathbf{q}$ than their fixed-based counterparts. $\mathbf{J}^*$ should be compared to the fixed-based manipulator $\mathbf{J}$ which is given by:

$$\mathbf{J}(\mathbf{q}) = \begin{bmatrix} -(l_1+r_1)s_1-(l_2+r_2)s_{12} & -(l_2+r_2)s_{12} \\ (l_1+r_1)c_1+(l_2+r_2)c_{12} & (l_2+r_2)c_{12} \end{bmatrix} \tag{4-11}$$

It can be seen that $\mathbf{J}^*$ and $\mathbf{J}$ have the same structure, as defined above.

$\mathbf{H}^*$ is given by Equation (3-41) and repeated here for convenience:

$$\mathbf{H}^*(\mathbf{q}) = \begin{bmatrix} d_{11}+2d_{12}+d_{22}-\dfrac{(D_1+D_2)^2}{D} & d_{12}+d_{22}-\dfrac{D_2(D_1+D_2)}{D} \\ d_{12}+d_{22}-\dfrac{D_2(D_1+D_2)}{D} & d_{22}-\dfrac{D_2^2}{D} \end{bmatrix} \tag{4-12}$$

Direct examination of all the terms in $\mathbf{H}^*$ shows that it has the same structure as the fixed-base inertia matrix $\mathbf{H}$, whose elements are given by:

$$\mathbf{H(q)} = \begin{bmatrix} h_{11} & h_{12} \\ h_{12} & h_{22} \end{bmatrix} \tag{4-13a}$$

$$h_{11} = I_1+m_1l_1^2+m_2(l_1+r_1)^2+2m_2l_2(l_1+r_1)\cos(q_2)+I_2+m_2l_2^2$$

$$h_{12} = h_{21} = m_2l_2(l_1+r_1)\cos(q_2)+I_2+m_2l_2^2$$

$$h_{22} = I_2+m_2l_2^2 \tag{4-13b}$$

At the limit, when both m_0 and I_0 approach infinity, it is easy to see that $m_0/M\rightarrow 1$, $m_1/M\rightarrow 0$, $m_2/M\rightarrow 0$, $\beta\rightarrow(l_1+r_1)$, $\gamma\rightarrow(l_2+r_2)$, i.e., they approach the manipulator link lengths, $D_0/D\rightarrow 1$, $D_1/D\rightarrow 0$ and $D_2/D\rightarrow 0$; $\mathbf{T}_0$ becomes a constant transformation from the manipulator base frame to the inertial frame, usually the unit matrix; and hence, $\mathbf{J}^*\rightarrow\mathbf{J}$, the fixed-base manipulator Jacobian, and $\mathbf{H}^*\rightarrow\mathbf{H}$, the mass matrix of the fixed-base manipulator, as given by Equations (4-11) and (4-13).

Next, the attention is focused on control. Inertially-Referenced End-Point Control is assumed here. One can select any control algorithm that can be used for fixed-base manipulators, using the two matrices $\mathbf{H}^*$ and $\mathbf{J}^*$. In this case, the Transpose Jacobian Control will be used, augmented by a velocity feedback term for increased stability margins [14]. The end-point position and velocity, $\mathbf{x}$ and $\dot{\mathbf{x}}$, can be calculated or measured directly. Assuming $\mathbf{x}$ and $\dot{\mathbf{x}}$ are measured, the control law is:

$$\tau = \mathbf{J}^{*T}\{\mathbf{K}_p(\mathbf{x}_{des}-\mathbf{x})-\mathbf{K}_d\dot{\mathbf{x}}\} \tag{4-14}$$

where $\mathbf{x}_{des}$ is the inertial desired point location. The matrices $\mathbf{K}_p$ and $\mathbf{K}_d$ are diagonal. Note that this algorithm drives the end-point to a desired location, but does not specify a path. If the control gains are large enough, then the motion of the end-point will be a straight line. First, the end-point path will be restricted to the PIW part of the workspace, and hence dynamic singularities will be avoided.

Figure 4.7 shows the path of the end-point from the initial location (1,0) to the final (0.8,0.8). The control gain matrices are $\mathbf{K}_p$ = diag(5,5) and $\mathbf{K}_d$ = diag(15,15), and the initial conditions are $(\theta, q_1, q_2) = (39.6^\circ, -134.2^\circ, 134.4^\circ)$. The end-effector path, shown with a heavy line, is almost a straight line and converges to the desired location. Shown also is the end-point path that results when the control law given by Equation (4-14) uses the fixed-base Jacobian given by Equation (4-11). In this case, the end-effector diverges from the straight line because it does not resolve the error term correctly; it still converges to the desired point due to end-point feedback. Depending on the situation, the use of the fixed-base Jacobian can create stability problems [44].

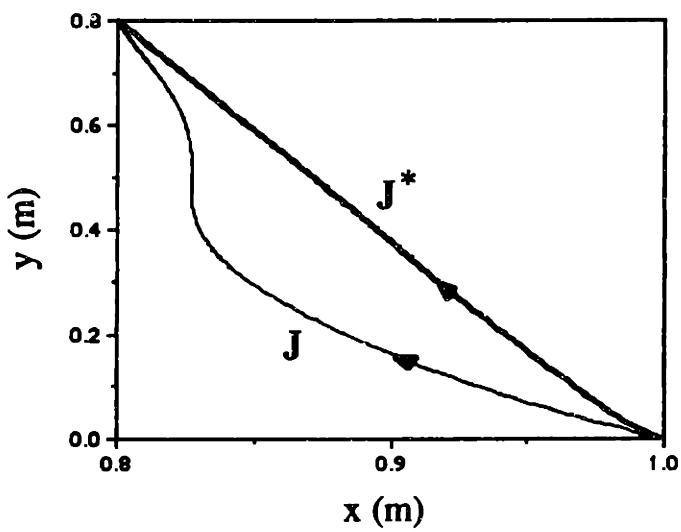

Figure 4.7. End-effector path in inertial PIW space, using $\mathbf{J}^*$ and $\mathbf{J}$.

Figure 4.8 shows the spacecraft attitude θ and the joint angles as a function of time, during the end-point motion depicted in Figure 4.7, when $\mathbf{J}^*$ is used. Note that although the spacecraft attitude changes by about 35°, the end-point converges to the desired inertial location as it would do if its base were fixed. Figure 4.9 shows the system in inertial space. The origin is fixed at the system's CM. The spacecraft is depicted as a square and the initial and final manipulator configurations are shown in bold lines. The end-effector

moves from point A to point B and the path is as shown in Figure 4.7. Note that during the manipulator motion the spacecraft translates and rotates.

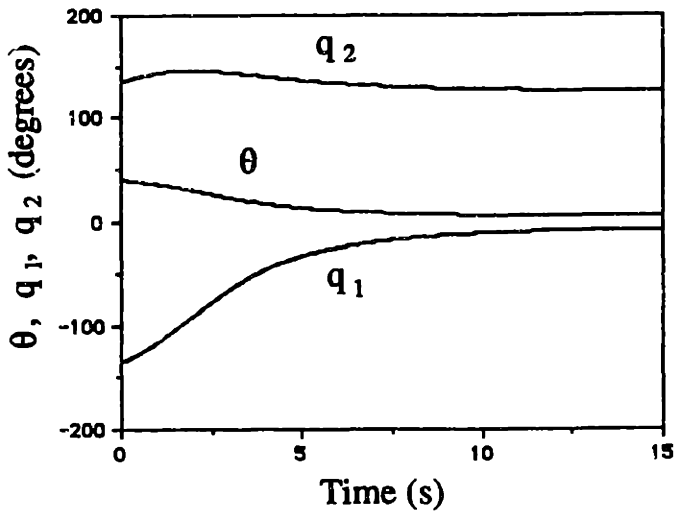

Figure 4.8. Spacecraft attitude θ and joint angles q_1 and q_2 during a motion in the PIW.

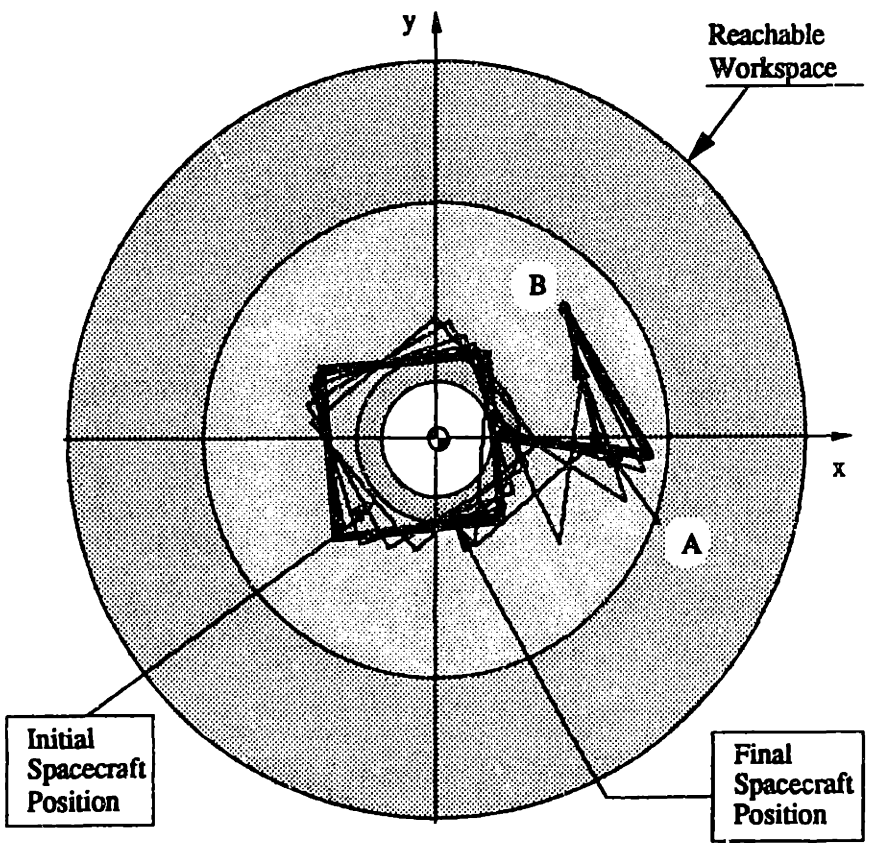

Figure 4.9. System configurations following a path in PIW .

Next, the same control algorithm is used but this time the path lies in the PDW. The manipulator end-effector is commanded to reach workspace point D(1.5,1.5) starting from the initial location of A(2,0) with initial attitude $(\theta, q_1, q_2) = (21^\circ, -58^\circ, 60.3^\circ)$. As shown in Figure 4.10, the end-effector initially moves along a straight line in the reachable workspace, leading to point D. However, at point B a dynamic singularity occurs and the end-effector fails to keep on line AD; instead it diverges to point C where it stops.

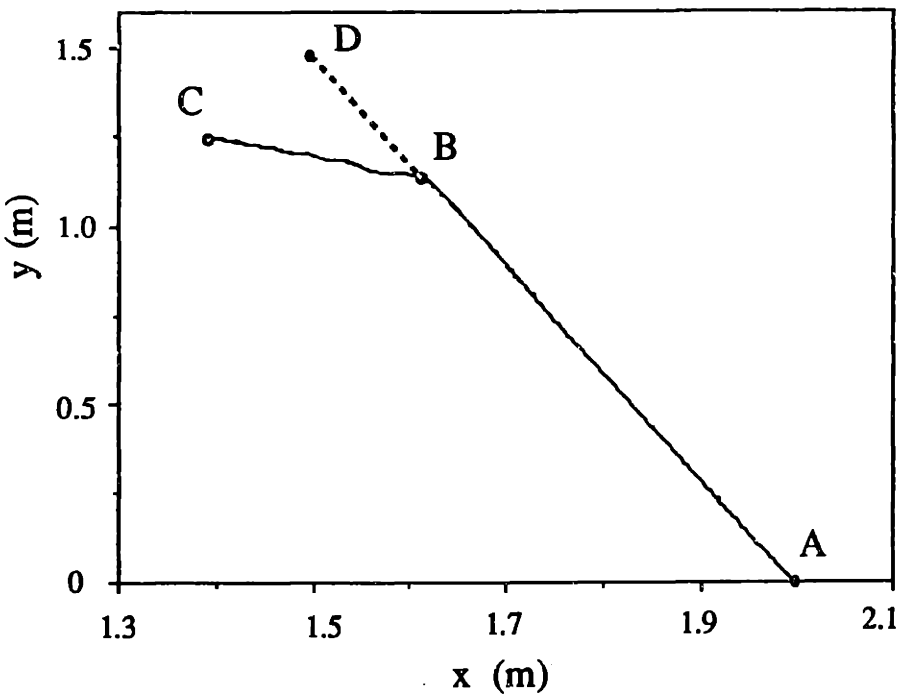

Figure 4.10 Dynamic singularity at point B results in large unrecoverable end-point errors.

By looking at the slopes of joint angles in Figure 4.11, it can be seen that the joint rates increase as the configuration **q** moves closer to a singular one. Note that the first singularity occurs in about t = 5 sec, at a point where $(\theta, q_1, q_2) = (-32.38^\circ, 74.24^\circ, 10.60^\circ)$. This configuration is indeed singular as can be seen with the help of the singular configurations plot, given by Figure 3.2.

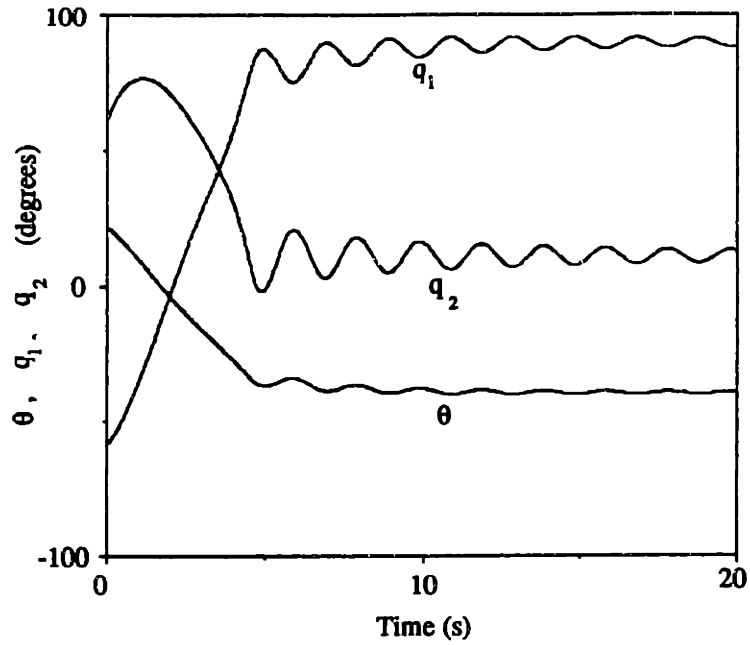

Figure 4.11. Spacecraft attitude θ and joint angles q_1 and q_2 during a motion in the PDW.

At point B, the system is output uncontrollable and the end-effector follows the only available direction whose slope is -25.34° to the horizontal. Note that the end-effector does not stop at point B because its acceleration at this point is still parallel to line AD. Trying to get back to its track towards point D, another singularity occurs and the joint angles oscillate around their steady state values which are $(\theta, q_1, q_2) = (-39.29^\circ, 88.81^\circ, 10.60^\circ)$, see Figure 4.11. This effect can be explained by transforming the equations of motion in the cartesian domain. Indeed, Equations (4-14), (4-5) and (4-4a) are substituted in Equation (4-1a) and assuming for simplicity that the control gains are larger compared to the nonlinear velocity terms, the following error equation can be written:

$$\ddot{\mathbf{e}} + (\mathbf{J}^{*}\mathbf{H}^{*-1}\mathbf{J}^{*T})\mathbf{K}_d\dot{\mathbf{e}} + (\mathbf{J}^{*}\mathbf{H}^{*-1}\mathbf{J}^{*T})\mathbf{K}_p\mathbf{e} = \mathbf{0} \qquad (4\text{-}15)$$

where $\mathbf{e} = \mathbf{x}_{des}-\mathbf{x}$. If the configuration and the joint angles do not change much, this is a linear second order system. This system has not only the obvious equilibrium $\mathbf{e} = \mathbf{0}$, but also any other $\mathbf{e}$ which belongs in the null space of $\mathbf{J}^{*}\mathbf{H}^{*-1}\mathbf{J}^{*T}\mathbf{K}_p$. Such points do exist

because it was proven in Chapter 3 that $\mathbf{J}^*$ is not of full rank in dynamically singular configurations. Recall that $\mathbf{K}_p$ and $\mathbf{H}^{*-1}$ are positive definite and therefore are always of full rank. Hence, the end-effector is attracted by the equilibrium at point C, see Figure 4.10. At point C motion stops because $\mathbf{K}_p\mathbf{e}$ is in the null space of $\mathbf{J}^{*T}$ and the torque input is zero; the end-effector is stuck at point C.

Figure 4.12 shows the motion of the whole system in cartesian space; the path is the same as in Figure 4.10. Note that the path is in the PDW and that q_2 at the separation point B is approximately 10.60°. An algorithm using a Jacobian inverse either for planning or for closed-loop control would fail computationally at a location like point B. This problem cannot be overcome because dynamic singularities represent a physical limitation.

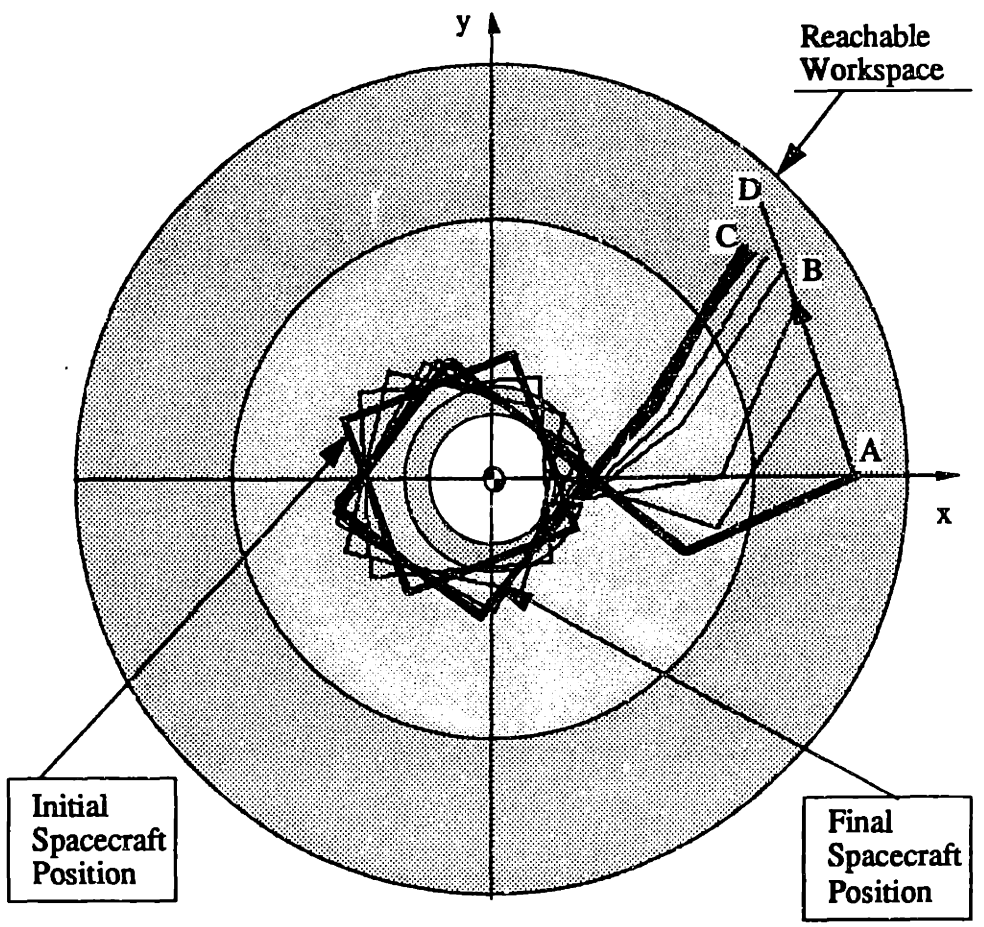

Figure 4.12. A path in PDW results in a dynamic singularity at point B.

To prove that point D is still accessible from point A, one can work as follows: First, since point D is in the reachable workspace, start by any configuration that corresponds to point D and command some desired location lying in the PIW; such a path can always be found. Then move from point A to the same point in the PIW; this will in general result in a different system configuration than that during the previous motion. Since the end-effector is in the PIW no singularities will occur if one moves the end-effector along a small cyclical path around that common point in the PIW, see also [65]. This cyclical motion will change the spacecraft's attitude and after some time the configuration that resulted from one of the two motions will be identical to the one that resulted from the other. Then, working backwards, the end-effector will move to point D without any problems. Of course, this method is not efficient, but it is described here to show that paths from A to D do exist.

Following the above procedure, any control algorithm that employs the system's $\mathbf{H}^*$ and $\mathbf{J}^*$ can be designed. However, control methods that depend on cancellation of terms, e.g. computed torque methods, require the exact system inertia matrix $\mathbf{H}^*$, and thus emphasis must be placed in its computation. This can be done by either off-line or on-line identification or by using adaptive control.

4.6 COORDINATED CONTROL FOR FREE-FLYING MANIPULATORS

In the previous sections the fundamental nature of control algorithms for free-floating systems was studied. In this section it is assumed that the spacecraft is using its actuators which are capable of applying a force at its CM as well as a torque around it. Forces can be generated by thruster (jet) actuators, while torques may be generated by thruster actuators, momentum gyros or reaction wheels. The two last methods have the advantage of using electric power that can be available from solar panels; their drawback is that they have limited torque capabilities; momentum wheels may saturate, revolving at the maximum angular velocity and momentum gyros may reach their maximum control angles (90°). In

those cases *momentum dump maneuvers* must be performed using spacecraft thruster actuators. For more details on this subject, the reader is referred to [71].

Spacecraft actuators are required for the following reasons: (a) To keep a spacecraft's attitude and/or position fixed, since in some cases it may not be desired to let a spacecraft move, (for communications or safety reasons). A fixed spacecraft greatly simplifies manipulator control but has the drawbacks that were pointed out in Chapter 3. (b) To move the entire system freely in space (free-flying system). (c) To compensate for external disturbances. (d) To apply useful forces to other bodies or structures or to prepare for docking.

The approach taken in the previous sections can be extended and used here, too; controllers will be designed based on a system's kinematic and dynamic description[6], obtained in Chapter 2. This is quite straightforward, although one should provide some way of resolving a system's redundancy.

4.6.1 Dynamic Models for Control

For simplicity, it will be assumed that external forces on the system are due to spacecraft thrusters and to forces acting at the end-effector. Of course, any other forces or torques can be modelled in the same way. Since thrusters are fixed with respect to the spacecraft frame ${}^0\mathbf{J}_S^+(\mathbf{q})$ must be used in the equations of motion. Forces at the end-effector tip are assumed fixed in inertial space. Using Equations (2-61), (2-62), (2-30b), (2-34) and (2-35) the equations of motion for a free-flying system are written as:

$$\mathbf{H}^+(\mathbf{q})\,\ddot{\mathbf{z}}_0 + \mathbf{C}^+(\mathbf{q}, {}^0\boldsymbol{\omega}_0, \dot{\mathbf{q}}) = \mathbf{Q} \tag{4-16}$$

---

[6]The formulation presented in Chapter 2 is well suited for free-floating systems because in the absence of external forces the equations of motion are naturally decoupled. This is not always the case in the presence of forces and torques, since these affect both the translation of the system and its change of configuration. It should be noted that some other kinematic and dynamic description of the system can be used to design controllers for a free-flying system. For example, instead of using the system CM to describe the system's translation, one can use a fixed point on the spacecraft. Which formulation is better is not clear; sometimes it is a matter of preference.

where $\dot{z}_0$ is a vector that contains the independent velocities and is given by:

$$\dot{z}_0 \equiv \begin{bmatrix} {}^0\dot{r}_{cm} \\ {}^0\omega_0 \\ \dot{q} \end{bmatrix} \tag{4-17}$$

Equation (4-16) describes in the most general way the motion of a free-flying manipulator system under the effect of external forces and torques and internal actuator torques. The generalized forces Q are decomposed into the unknown disturbance forces, Q_d, and the control forces, Q_c:

$$Q = Q_c + Q_d \tag{4-18}$$

The control forces include the spacecraft's thruster forces and the manipulator's joint torques. To simplify the notation, S is used to represent for the CM of the spacecraft, see also Equation (2-30). Then, the control forces can be written as:

$$Q_c = J_q^T \begin{bmatrix} {}^0f_S \\ {}^0n_S \\ \tau \end{bmatrix} = \begin{bmatrix} 1 & {}^0J_{11,S} & {}^0J_{12,S} \\ 0 & 1 & 0 \\ 0 & 0 & 1 \end{bmatrix}^T \begin{bmatrix} {}^0f_S \\ {}^0n_S \\ \tau \end{bmatrix} \tag{4-19}$$

where ${}^0f_S$ and ${}^0n_S$ are the thuster forces and torques applied to the spacecraft, expressed in its frame. Forces can be generated by thruster actuators, while torques may be generated by thruster actuators, momentum gyros or reaction wheels. Note that J_q is square and always invertible.

Similarly, the disturbances can be modeled using Equations (2-62). For simplicity, it is assumed here that disturbances act on the end-effector only. Then, these are given by:

$$Q_d = J^+(e,n,q)^T \begin{bmatrix} f_E \\ \\ n_E \end{bmatrix} \tag{4-20}$$

Equation (4-16) is the "engine" that can be used in any type of control: it describes the way accelerations depend on inputs (${}^0\mathbf{f}_S, {}^0\mathbf{n}_S, \tau$) and unknown disturbances, ($\mathbf{f}_E, \mathbf{n}_E$). A controller must calculate a required set of thruster forces and torques and a set of manipulator joint torques that will move the end-effector along a desired path and reduce the effect of disturbances. Disturbances in space are generally very small, [65]. However, when a manipulator system is docking to some object, interaction forces will result and then they must be compensated for by a spacecraft's thrusters.

4.6.2 Coordinated Motion Control

The similarity between Equation (4-16) and the equations of motion that correspond to a fixed-based manipulator leads to an investigation of whether control laws that are applicable in the latter case also can be used in the control of space robotic systems. However, two differences between the two situations must be pointed out. The first is that an appropriate representation of a spacecraft's attitude is needed, e.g. Euler angles, Euler parameters, etc. The second difference is that, due to a spacecraft's mobility, a space robotic system is inherently redundant. This redundancy can be used to achieve additional tasks; here it will be used to control a spacecraft's location and attitude by augmenting the system output. This has the advantage that the location and attitude of the spacecraft can be controlled to follow some prescribed plan, and hence, impacts can be avoided. In addition, by planning a spacecraft's motion, the end effector can reach a point while its manipulator assumes some desired configuration. For example, this scheme may allow a manipulator to be in a configuration suitable for applying some forces or to avoid singularities.

Equation (2-34) is used to control the end-effector position and orientation, an important task in free-flying manipulation. As noted in Chapter 2, even when the manipulator has six DOF, (N=6), $\mathbf{J}^+$ is not square and therefore is not invertible, although its rank is always six. If N=6, then $\mathbf{J}^+$ is a 6×12 matrix. The additional control requirements of controlling the spacecraft location and attitude are introduced by adding

${}^0J_S^+$, the Jacobian relating $\dot{z}_0$ to spacecraft linear and angular velocity, $\dot{R}_S$, and $\omega_S = \omega_0$. This Jacobian is obtained from Equation (10) by setting the subscript S to stand for the spacecraft's CM, (k=0 and m=CM).

$$\dot{z}_1 = \begin{bmatrix} \dot{r}_E \\ \omega_E \\ \dot{R}_S \\ \omega_S \end{bmatrix} = \mathrm{diag}(T_0, T_0, T_0, T_0) \begin{bmatrix} 1 & {}^0J_{11} & {}^0J_{12} \\ 0 & 1 & {}^0J_{22} \\ 1 & {}^0J_{11,S} & {}^0J_{12,S} \\ 0 & 1 & 0 \end{bmatrix} \dot{z}_0 = J_z \dot{z}_0 \qquad (4\text{-}21)$$

where $\dot{z}_1$ is the vector of output velocities. The Jacobian J_z is an invertible 12×12 matrix, unless the manipulator is kinematically singular, and relates input to output velocities providing a basis for controlling a free-flying system. Different control requirements can be appended in the same way.

Equations of motion (4-16) and Jacobians given by Equation (4-21) can be used to apply various standard motion control techniques, in a way similar to Khatib's "operational" approach [33], where a Jacobian map relating generalized joint velocities to operational velocities is used to design controllers in the cartesian space. In this case, Equation (4-21) is used as a map between the selected state variables $\dot{z}_0$ and the output variables $\dot{z}_1$. Then, based on this map, a controller operating in the z_1 domain can be designed.

Here, a Transposed-Jacobian type controller with inertial feedback is designed to demonstrate this technique. The equations of motion in the z_1 domain can be found by substituting Equation (4-21) into Equation (4-16) to obtain the form:

$$\tilde{H}\,\ddot{z}_1 + \tilde{C} = (J_z^{-1})^T Q_c \qquad (4\text{-}22)$$

where $\tilde{C}$ contains the nonlinear terms and $\tilde{H}$ is given by:

$$\tilde{H} = (J_z^{-1})^T H^+ J_z^{-1} \qquad (4\text{-}23)$$

This inertia matrix is positive definite if J_z is nonsingular. An error e is defined in the output domain z_1 as:

$$e \equiv z_{1,des} - z_1 \tag{4-24}$$

where z_1 is provided by inertial feedback, and $z_{1,des}$ is the desired inertial point. It is assumed here that inertial measurements of the position and orientation of the spacecraft and the end-effector are available. Then, if the input Q_c is taken to be:

$$Q_c = J_z^T \{ \hat{H} (K_p e + K_d \dot{e} + \ddot{z}_{1,des}) + \hat{C} \} \tag{4-25}$$

where K_p, K_d are positive definite diagonal matrices, then the error dynamics are given by:

$$\ddot{e} + K_d \dot{e} + K_p e = 0 \tag{4-26}$$

and therefore the error converges asymptotically to zero. Equation (4-25) is a modification of the operational space controller, [33]. If high enough gains are used, the simpler Transposed Jacobian controller can be used, [14]:

$$Q_c = J_z^T (K_p e + K_d \dot{e}) \tag{4-27}$$

Note that if a singularity is encountered, the controllers given by Equations (4-25) and (4-27) will result in errors but will not fail fatally. If some small disturbance acts on the system, a small steady state error is expected, because these controllers are basically PD controllers. Finally, the reaction jet forces and torques and the joint torques can be found by inverting Equation (4-19). Assuming that Equation (4-27) is used, these are given by:

$$\begin{bmatrix} {}^0f_S \\ {}^0n_S \\ \tau \end{bmatrix} = (J_q^T)^{-1} J_z^T (K_p e + K_d \dot{e}) \tag{4-28}$$

The inversion of J_q is possible since this Jacobian is always nonsingular. Equation (4-28) is the final result that permits coordinated control of both the spacecraft and its manipulator, based on inertial measurements of the spacecraft and end-effector locations and orientations. If no such measurements are available, the error e can be estimated by integrating in real time the equations of motion, but then errors due to model uncertainties will be introduced. This method of motion control is demonstrated with an example.

4.7 EXAMPLES

As an example of the general framework outlined in the previous section, a controller will be designed capable of controlling a spacecraft's position and attitude and simultaneously the motion of its manipulator's end-effector. To this end, the example system introduced in section 2.5.2 and shown in Figure 4.13 will be used. Its kinematic, mass and inertia properties are given in Table I. The spacecraft is assumed to be equipped with thrusters that can provide forces and torques proportional[7] to the commanded control input. The equations of motion for this system are given by Equation (2-88), see also section E.2. In this case the independent coordinates vector, z_0, and the vector of coordinates to be controlled, z_1, are:

$$z_0 = [{}^0x_{cm}, {}^0y_{cm}, \theta, q_1, q_2]^T, \quad z_1 = [x_S, y_S, \theta, x_E, y_E]^T \tag{4-29}$$

where ${}^0x_{cm}$ and ${}^0y_{cm}$ are the system CM coordinates with respect to an inertia frame, θ is the spacecraft's attitude, q_1, q_2 are the manipulator joint angles, x_S, y_S are the spacecraft's CM coordinates and finally x_E, y_E are the end-effector's coordinates.

---

[7]In practice, this can be achieved by adjusting the pulse duration of the thrusters. For example, for some particular thruster with minimum pulse duration of 30 ms and minimum impulse bit of 0.5 lbf-sec, the minimum force is 0.003 N, see [38].

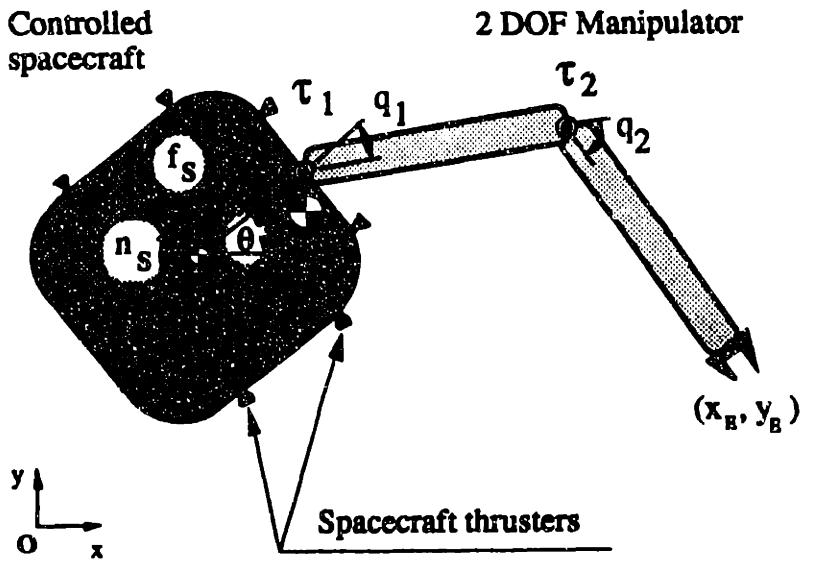

Figure 4.13. A two-DOF manipulator on a three-DOF free-flying spacecraft.

The Jacobians $\mathbf{J}_q$ and $\mathbf{J}_z$ required by the controller of Equation (4-28) are derived using sub-Jacobians derived in Appendix E. The result is given here:

$$\mathbf{J}_q = \begin{bmatrix} 1 & 0 & -\varepsilon s_1-\zeta s_{12} & -\varepsilon s_1-\zeta s_{12} & -\zeta s_{12} \\ 0 & 1 & \delta+\varepsilon c_1+\zeta c_{12} & \varepsilon c_1+\zeta c_{12} & \zeta c_{12} \\ 0 & 0 & 1 & 0 & 0 \\ 0 & 0 & 0 & 1 & 0 \\ 0 & 0 & 0 & 0 & 1 \end{bmatrix} \tag{4-30}$$

$$\mathbf{J}_z = \begin{bmatrix} \cos\theta & -\sin\theta & 0 & 0 & 0 \\ \sin\theta & \cos\theta & 0 & 0 & 0 \\ 0 & 0 & 1 & 0 & 0 \\ 0 & 0 & \cos\theta & -\sin\theta & 0 \\ 0 & 0 & \sin\theta & \cos\theta & 0 \end{bmatrix} \begin{bmatrix} 1 & 0 & -\varepsilon s_1-\zeta s_{12} & -\varepsilon s_1-\zeta s_{12} & -\zeta s_{12} \\ 0 & 1 & \delta+\varepsilon c_1+\zeta c_{12} & \varepsilon c_1+\zeta c_{12} & \zeta c_{12} \\ 0 & 0 & 1 & 0 & 0 \\ 1 & 0 & -\beta s_1-\gamma s_{12} & -\beta s_1-\gamma s_{12} & -\gamma s_{12} \\ 0 & 1 & \alpha+\beta c_1+\gamma c_{12} & \beta c_1+\gamma c_{12} & \gamma c_{12} \end{bmatrix} \tag{4-31}$$

where $s_1 = \sin(q_1)$, $c_{12} = \cos(q_1+q_2)$, etc. Both Jacobians are 5×5 matrices and functions of the barycentric vectors $\alpha,\beta,\gamma,\delta,\varepsilon,\zeta$, defined in the Appendix. Simple inspection reveals that $\mathbf{J}_q$ is always nonsingular, and that $\mathbf{J}_z$ is nonsingular unless $s_2 = 0$, which corresponds to a kinematically singular manipulator.

The controller described by Equation (4-28) is used to calculate the required reaction jet forces and torques, ${}^0f_S$ and ${}^0n_S$, and the manipulator joint torques, τ. It allows the specification of a desired trajectory for both the spacecraft and the manipulator. Hence, the motion of the whole system can be coordinated. If the given trajectory is not feasible, the desired motion will not be achieved, but the controller will try instead to come as close as possible to the specified trajectory.

In the simulations that follow, the inertially fixed frame is set at the position of the system CM at the initial time, when $(\theta,q_1,q_2) = (21^\circ,-58^\circ,60.3^\circ)$ and the end-effector is at (2.0, 0.0). Hence, these results are comparable to the ones in section 4.5. In this coordinate frame, the end-effector is commanded to move to point (1.5, 1.5). The spacecraft is commanded to move to $(\theta,x_S,y_S) = (15^\circ,0.5,0.5)$. The gains used are K_p = diag(30,30,30,30,30) and K_d = diag(60,60,60,60,60). It is assumed here that no disturbances are exerted on the system. Figure 4.14 shows the motion of the system in inertial space. The end-effector converges along a straight line to the desired point, while the spacecraft assumes the desired location and attitude.

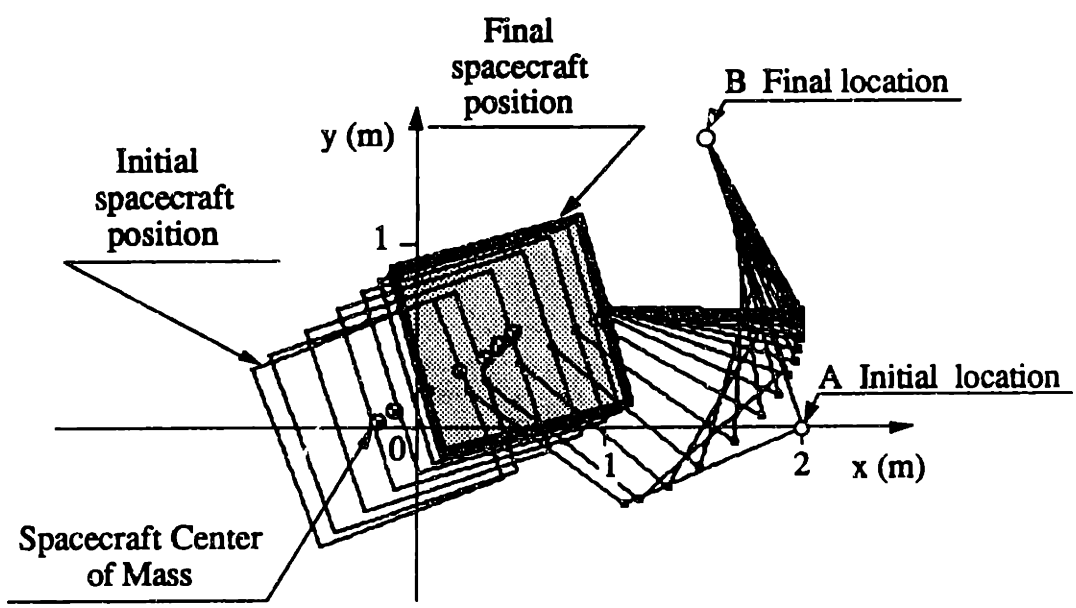

Figure 4.14. Coordinated spacecraft/manipulator motion of the example system.

Note that if the spacecraft were fixed at its initial location, the end-effector would have reached point B in an almost singular configuration. If the spacecraft were free-floating and its reaction jets were turned off, then point B could not have been reached from point A following the straight line path, due to the existence of dynamic singularities. In contrast to these schemes, coordinated control permits the end-effector to reach point B in a favorable configuration, away from singularities.

Figure 4.15 shows the error in the spacecraft's position and attitude during the end-effector motion. These errors are eliminated in about 12 sec. Figure 4.16 shows the reaction jet forces required to move the spacecraft during the first five seconds of the maneuver. Since the error converges asymptotically to zero and no disturbances act on the system, the reaction jet forces approach asymptotically to zero as soon as the motion stops.

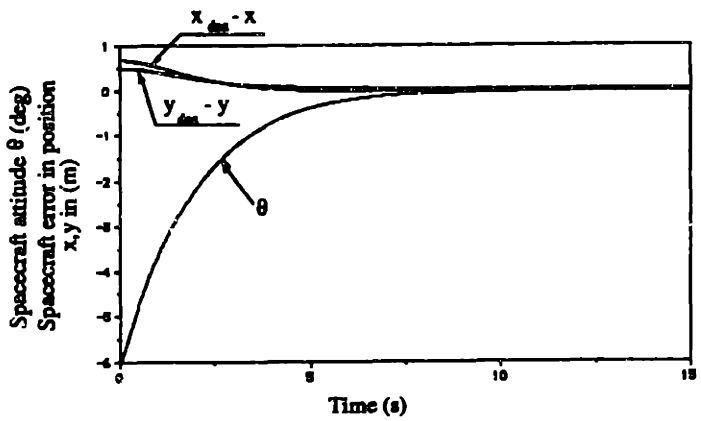

Figure 4.15. Motion of the spacecraft during the maneuver shown in Figure 4.14.

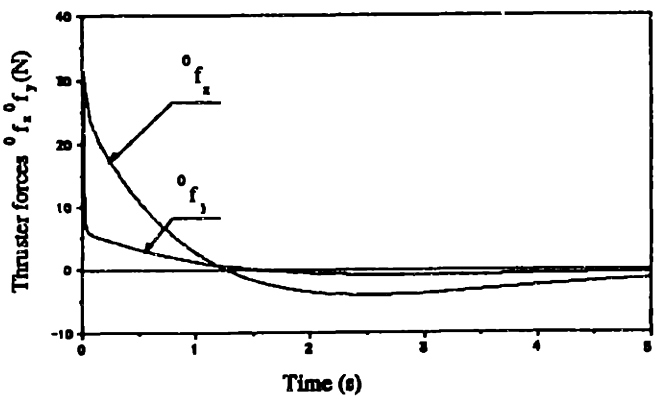

Figure 4.16. Thruster forces required during the maneuver shown in Figure 4.14.

By changing the spacecraft set-point, the spacecraft is commanded not to move. Figure 4.17 shows the error in the spacecraft's position and attitude during the same end-effector motion as above. As shown in Figure 4.17, small deviations from the initial position of the spacecraft are eliminated when the manipulator stops.

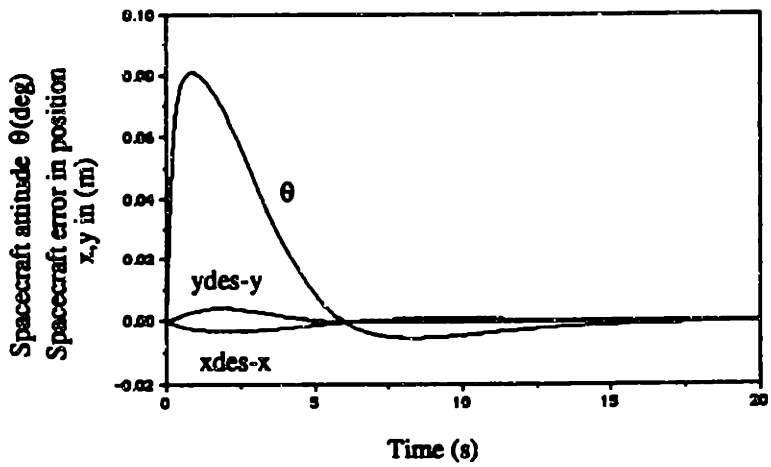

Figure 4.17. Small motions of a spacecraft during a manipulator maneuver.

Next the same manipulator maneuver is simulated but this time a constant disturbance force of (-1.5 N, -0.5 N) is exerted on the end-effector tip. The spacecraft is commanded to remain fixed. Such assumed constant forces are not expected in space; nevertheless here it is desired to see what is the effect of such a severe assumption. The end-effector trajectory is shown in Figure 4.18.

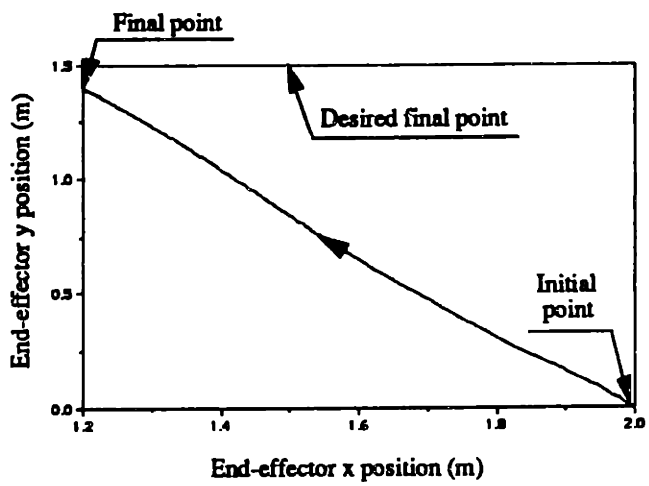

Figure 4.18. End-effector misses the desired location due to a disturbance.

Note that the desired location (1.5, 1.5) is missed because a PD results in steady state errors in the presence of constant disturbances. Figure 4.19 shows the required thruster forces. It can be seen that thrusters continue operating after the end of the motion in order to cancel the disturbance. Note that the two components of the thruster forces, ${}^0f_x$ and ${}^0f_y$ are not equal to the components of the disturbance, because these are fixed at the spacecraft frame, while the disturbance was assumed of fixed direction in inertial space. This constant thruster operation is undesired because the life of the system is greatly reduced. However, this required to compensate for disturbances or to apply useful forces in space.

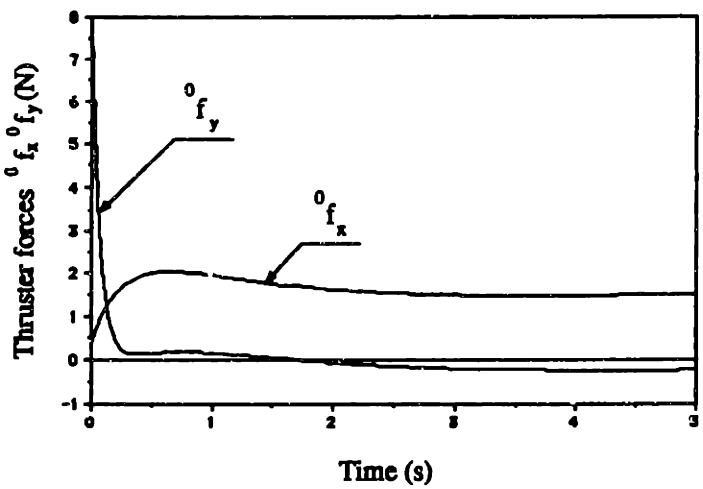

Figure 4.19. Thruster forces required to keep a spacecraft fixed, in the presence of disturbances.

The same as above steps can be followed to design a controller to control some other variables. To do this, first define an appropriate vector $\mathbf{z}_1$ and a transformation Jacobian $\mathbf{J}_z$ given by Equation (4-21). The new error $\mathbf{e}$ is then defined by Equation (4-24) and the control forces are given by Equation (4-25). In this section, a transposed Jacobian-based controller was used for simplicity. However, other controllers can be equally well used, if $\mathbf{z}_1$ and $\mathbf{J}_z$ are properly defined. For example planning algorithms, like the ones based on resolved-rate control, can be used to generate desired spacecraft positions, attitudes and

joint angles which can be fed to thrusters and joint servos. Other control laws like resolved acceleration, impedance and adaptive control laws can be used equally well.

4.8 SUMMARY

A fundamental study has been performed of the characteristics of control algorithms which may be applied to the motion control of space manipulators. The results obtained show that nearly any control algorithm which can be applied to conventional terrestrial fixed-base manipulators, with a few additional conditions, can be directly applied to space manipulators. The steps required to do this include the identification of the right inertia, Jacobian and transformation matrices. These elements also can be used to find the feasible motions for the system, and avoid commands that are physically impossible. It is hoped that these results will encourage the development of more effective control algorithms for space manipulator systems.

5 Failure Recovery Control for Space Manipulators

5.1 INTRODUCTION

In space systems, it is very important to be able to tolerate failures of such systems and their components, since such failures can jeopardize an entire mission. These systems are often designed with redundant subsystems and components to give them higher reliability. They may be also designed to operate after a failure, but with reduced capabilities. For example, imagine the consequences of a failed Space Shuttle manipulator actuator so that it cannot drive the manipulator back into its stowed position. In such a case it would be highly desirable to be able to use the working manipulator joints to control partially the system and "recover" some of its functions. In this chapter, the question of the control of a space manipulator system after a failure of one of its joints functions is addressed.

A possible scenario for failure recovery control is as follows: The i^{th} joint of a manipulator system fails in some way, such as its actuator, controller or control circuitry, but its brakes and encoders still function. Then, assume that working joints can be used to control the i^{th} joint, and drive this joint to some point, where it is locked using the brakes. It could then be stowed using the system's other actuators. The joint could also be driven to some "optimal" joint position determined according to some criterion, for example to maximize a broken system's workspace. The system could then be used with a reduced number of DOF, and hence the system "recover" to some extent from the failure. The basic thrust of this chapter is to show that such failure recovery control is possible and to identify conditions that are required for its use.

5.2 SYSTEMS WITH FEWER CONTROL INPUTS THAN OUTPUTS

The situation introduced above can be recognized to be a subset of a more general problem, which is the control of systems having fewer actuators than DOF. Such instances may occur for example in the control of walking machines, where the "joint" formed by a leg touching the ground may be uncontrolled, or where some DOF may be passively controlled by springs and/or dampers. Similar situations can be found in the control of flexible links, where one actuator is supposed to stabilize an infinite mode system, etc. Next, some interesting cases where the number of control inputs is smaller than the number of controlled variables are discussed.

5.2.1 Linear systems

The question to be addressed here is: "How many controls are needed to set a controlled variable **y** equal to any $\mathbf{y}_{des}$, at steady state?". The answer to this question can be found by adopting ideas from regulator theory, see for example [37]. First, a MIMO linear system in its standard state space form is considered:

$$\dot{\mathbf{x}} = \mathbf{A}\mathbf{x} + \mathbf{B}\mathbf{u} \tag{5-1a}$$

$$\mathbf{y} = \mathbf{C}\mathbf{x} \tag{5-1b}$$

where **x** is an n×1, **u** an m×1, and **y** an r×1 vector and **A** an n×n, **B** an n×m, and **C** an r×n matrix. It is well known that if the pair (**A**, **B**) is state controllable, then the state **x** can be transferred to any point in the state space $\mathbf{R}^n$. However, controllability does not imply that the state can stay at any point indefinitely; in order for this to happen, a point must be an *equilibrium* for the system. Hence, **u** not only must stabilize and shape the closed loop dynamics, but also change the equilibrium point of the system. A control input that can achieve the two first tasks and possibly change the system equilibrium, is the following:

$$\mathbf{u} = -\mathbf{K}\mathbf{x} + \mathbf{u}^* \tag{5-2}$$

where $\mathbf{u}^*$ is a constant vector. Substituting Equation (5-2) in (5-1) and setting $\dot{\mathbf{x}} = 0$, the following expressions can be written for the steady state value of $\mathbf{x}$, $\mathbf{x}_{ss}$, and for $\mathbf{y}_{des}$:

$$\mathbf{x}_{ss} = (\mathbf{A}-\mathbf{BK})^{-1}\mathbf{B}\mathbf{u}^* \tag{5-3a}$$

$$\mathbf{y}_{des} = \mathbf{C}(\mathbf{A}-\mathbf{BK})^{-1}\mathbf{B}\mathbf{u}^* \tag{5-3b}$$

The inverse in Equation (5-3) always exists, since controllability implies that there exists a gain matrix $\mathbf{K}$ that can move all the eigenvalues of $(\mathbf{A}-\mathbf{BK})$ in the left half plane. Note that the dimensions of the matrix $\mathbf{C}(\mathbf{A}-\mathbf{BK})^{-1}\mathbf{B}$ are $r \times m$. Equation (5-3b) can be used to find how many controls are needed to set $\mathbf{y} = \mathbf{y}_{des}$. Since it is desired to find the minimum number of controls that can achieve this task, the case of more controls than controlled variables ($r<m$) is not of interest. If $r>m$, Equation (5-3b) cannot be solved for $\mathbf{u}^*$ for *any* given $\mathbf{y}_{des}$. A solution exists only in specific cases. Finally, if $r=m$ and $\mathbf{C}(\mathbf{A}-\mathbf{BK})^{-1}\mathbf{B}$ is nonsingular, a solution for $\mathbf{u}^*$ exists for an arbitrary $\mathbf{y}_{des}$. The conclusion is that to secure that *any* set-point can be achieved, in general one needs as many controls as controlled variables.

These remarks also are applicable to nonlinear systems that can be input-output linearized. For example, manipulator nonlinear dynamics can be input-output linearized by including a nonlinear feedforward term in the control law, because then, the remaining dynamics reduce in a double integrator, see also section 4.3.1.

5.2.2 Inverted pendulums

The problem of controlling two serially connected inverted pendulums mounted on a cart can provide some important insights. Here, the focus is in analyzing what such a system is capable of doing; a reader interested in switching laws for this example is referred to [56]. Figure 5.1 shows a three-DOF pendulum-cart system, where the only available control input is the force f applied on the cart.

Equations of motion for this system can be written using any standard method. Assuming that the mass of the cart m_0 is large with respect to pendulum masses, m_1, and m_2, and linearizing the system around some equilibrium point $(q_0, q_1, q_2) = (q_0, 0, 0)$ the following linear equations result:

$$\frac{d}{dt}\begin{bmatrix} x_1 \\ x_2 \\ x_3 \\ x_4 \\ x_5 \\ x_6 \end{bmatrix} = \begin{bmatrix} 0 & 1 & 0 & 0 & 0 & 0 \\ 0 & 0 & 0 & 0 & 0 & 0 \\ 0 & 0 & 0 & 1 & 0 & 0 \\ 0 & 0 & a_1 & 0 & a_2 & 0 \\ 0 & 0 & 0 & 0 & 0 & 1 \\ 0 & 0 & a_3 & 0 & a_4 & 0 \end{bmatrix}\begin{bmatrix} x_1 \\ x_2 \\ x_3 \\ x_4 \\ x_5 \\ x_6 \end{bmatrix} + \begin{bmatrix} 0 \\ b_1 \\ 0 \\ b_2 \\ 0 \\ b_3 \end{bmatrix} u \qquad (5\text{-}4)$$

where all a_i (i=1,...,4) are nonzero, unless gravity is zero, all b_i (i=1,2,3) are nonzero, $u=f/m_0$ and $(x_1, x_2, x_3, x_4, x_5, x_6) = (q_0, \dot{q}_0, q_1, \dot{q}_1, q_2, \dot{q}_2)$.

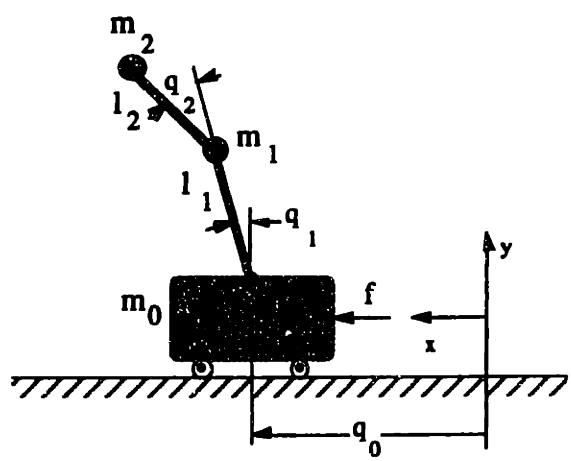

Figure 5.1. A double inverted pendulum on a moving cart.

The open-loop system has two stable poles, two unstable poles and two poles at the origin. Applying the controllability rank condition to this system, it is easy to find that unless gravity is zero, the system is controllable. Also, a set of gains K can be found to stabilize the system. As discussed in the previous section, this is not enough to guarantee that the controlled variable y = x can be driven to *any* desired point. Condition (5-3) must also be

satisfied. Note that in this case, n=6 but m=1, that is only one control is available. As noted above, in general it is not possible to achieve any y_{des}. However, it is easy to see that condition (5-3) can still be satisfied when the desired set-point is $y_{des} = (q_{0,des},0,0,0,0,0)$, because then it follows that $\mathbf{u}^* = 0$. Therefore, since in this case both the system is controllable and condition (5-3) holds, one can move the cart anywhere and at the same time keep the double pendulum vertical.

5.2.3 Manipulators

The same ideas also apply to manipulators. It is well known that a manipulator can be transformed to a double integrator system with some appropriate nonlinear feedforward action, see also section 4.3.1. Applying a state feedback controller to that double integrator system, the following system results:

$$\frac{d}{dt}\begin{bmatrix}\mathbf{q}\\ \dot{\mathbf{q}}\end{bmatrix} = \begin{bmatrix}\mathbf{0} & \mathbf{1}\\ \mathbf{K}_p & \mathbf{K}_d\end{bmatrix}\begin{bmatrix}\mathbf{q}\\ \dot{\mathbf{q}}\end{bmatrix} + \begin{bmatrix}\mathbf{0}\\ \mathbf{1}\end{bmatrix}\mathbf{u}^* \qquad (5\text{-}5)$$

where $\mathbf{q}, \mathbf{u} \in \mathbf{R}^N$, and $\mathbf{K}_p$, $\mathbf{K}_d$, $\mathbf{1}$ are N×N matrices for an N-DOF system. It is easy to show that this system is controllable and that condition (5-3) can be solved for $\mathbf{u}^*$ for any state $(\mathbf{q},\dot{\mathbf{q}}) = (\mathbf{q},\mathbf{0})$. This confirms the well known fact that to control an N-DOF manipulator, just N and not 2N actuators are needed.

5.3 CONTROLLABILITY OF A SPACE MANIPULATOR WITH A FAILED JOINT

In the previous section, conditions that allow a linear or linearized system's output to be driven to some constant set-point were determined. It was shown that although in general one needs as many controls as outputs, in many important cases fewer controls can still be used. In this section, state controllability for a space manipulator after a joint failure is investigated.

As shown in the previous chapters, equations of motion for space manipulators are given by the following general representation:

$$\mathbf{H}(\mathbf{q})\,\ddot{\mathbf{q}} + \mathbf{C}(\mathbf{q},\dot{\mathbf{q}})\,\dot{\mathbf{q}} = \tau \tag{5-6}$$

If the spacecraft is kept at a fixed position and orientation, then $\mathbf{H}$ and $\mathbf{C}$ are the matrices that correspond to a fixed-based manipulator. If the system is free-floating, then $\mathbf{H} = \mathbf{H}^*$ and $\mathbf{C} = \mathbf{C}^*$, while if it is free-flying, then $\mathbf{H} = \mathbf{H}^+$ and $\mathbf{C} = \mathbf{C}^+$, while the control input τ is substituted by $[\mathbf{Q}_r^T, \mathbf{Q}_\theta^T, \mathbf{Q}_q^T]^T$, see Equations (2-61) and (2-62). It can be seen that Equation (5-6) describes not only space manipulators, but also SCARA manipulators, since gravity does not affect their dynamics.

Next, it is assumed that the i^{th} joint function has failed, and that joint friction is very small so that it can be neglected; then $\tau_i = 0$. The objective is to control this joint with the remaining active joints. This control objective can be stated formally as: find conditions under which it may be possible to drive angle q_i to a desired value in a stable manner, when $\tau_i = 0$. It can be recognized that if not all joint controllers operate, it is not possible to use feedback linearization to convert Equation (5-6) to a double integrator system, that would permit the application of established linear control methods for this problem.

The first step is to note that the system has infinite equilibria of the form $(\mathbf{q},\dot{\mathbf{q}}) = (\mathbf{q},\mathbf{0})$; driving q_i to $q_{i,des}$ corresponds to driving the state to one particular equilibrium. In the neighborhood of an equilibrium point, a system's model can be linearized into the form:

$$\mathbf{H}(\mathbf{q}_{des})\,\delta\ddot{\mathbf{q}} = \delta\tau = \delta[\tau_1,\ldots,\tau_{i-1},0,\tau_{i+1},\ldots,\tau_N]^T \tag{5-7}$$

Equation (5-7) can be written in the standard form as:

$$\frac{d}{dt}\begin{bmatrix}\delta\mathbf{q}\\ \delta\dot{\mathbf{q}}\end{bmatrix} = \begin{bmatrix}\mathbf{0} & \mathbf{1}\\ \mathbf{0} & \mathbf{0}\end{bmatrix}\begin{bmatrix}\delta\mathbf{q}\\ \delta\dot{\mathbf{q}}\end{bmatrix} + \begin{bmatrix}\mathbf{0}_i\\ \mathbf{H}^{-1}\mathbf{1}_i\end{bmatrix}\mathbf{u} \tag{5-8}$$

where $\mathbf{u} = \delta[\tau_1,\ldots,\tau_{i-1},\tau_{i+1},\ldots,\tau_N]^T \in \mathbf{R}^{N-1}$ and $\mathbf{1}_i$ and $\mathbf{0}_i$ are N×(N-1) matrices obtained from the unit and zero N×N matrices after their i^{th} column, the one that corresponds to the failed joint, is removed. It is easy to see that the controllability matrix for this linearized system, C, is:

$$\mathbf{C} = \begin{bmatrix} \mathbf{H}^{-1}\mathbf{1}_i & \mathbf{0}_i \\ \mathbf{0}_i & \mathbf{H}^{-1}\mathbf{1}_i \end{bmatrix} \tag{5-9}$$

Clearly, since C has 2(N-1) columns, its rank is at most 2(N-1) and not 2N for the system to be controllable, and therefore the system is *uncontrollable* with a 2(N-1) dimensional controllable subspace. It might be noted that it is well known that the double inverted pendulum system is controllable, although its two joints are not actively controlled. However, there is one important difference and that is gravity. Indeed, the effect of gravity is to introduce a matrix of rank 2 at the lower left corner of the "A" matrix in Equation (5-8), and that makes the system controllable.

The fact that a failed space robotic manipulator has an uncontrollable linearized model does not prove that the nonlinear system is uncontrollable. More general methods that deal directly with nonlinear controllability must be used, see for example [10,22]. In general, controllability conditions for nonlinear systems must be applied to specific systems, since they rely on forming successive Lie brackets and testing a rank condition of a "distribution" formed by these brackets [22,46]. Although it may be possible to utilize properties of mechanical systems to deduce controllability results for general mechanical systems, this was not attempted. It can be shown that for a two-DOF manipulator with a failed joint on a inertially fixed spacecraft, shown in Figure 1, the nonlinear controllability conditions require nonzero joint velocities $\dot{\mathbf{q}}$ to assure state controllability at some state $(\mathbf{q},\dot{\mathbf{q}})$. Since the system is not controllable everywhere in its state space, it is concluded that it is not controllable.

Recall that the main interest here is to control q_i and not necessarily to control the entire configuration $\mathbf{q}$. Therefore, in the next section the attention is focused in controlling q_i at the expense of some other joint q_j. If this task can be achieved, then joint angle q_i can be locked at its desired position, and normal operation of the remaining DOF may resume, or the system maybe stowed effectively.

5.4 FAILURE RECOVERY CONTROL

In the previous section it was shown that if N-1 actuators are in operation, the controllable subspace is $\mathbf{R}^{2(N-1)}$, in other words, N-1 DOF can be controlled. A question that arises next is whether q_i is among the angles that can be controlled.

To answer this question, first define the vectors $\mathbf{e}_i = [0,\ldots, 0, 1, 0,\ldots,0]^T \in \mathbf{R}^{2N}$ where the 1 is at the i^{th} position, which span the system's state space. It can be seen that $\mathbf{e}_i$, ($i \leq N$), is the unit vector in the direction of coordinate q_i, and that vector $\mathbf{e}_{N+i}$, ($i \leq N$), is in the direction of $\dot{q}_i$. It is well known that in order to be able to reach any q_i and $\dot{q}_i$, $\mathbf{e}_i$ and $\mathbf{e}_{N+i}$ must belong in the controllable subspace, [37]. Note that due to the form of the controllability matrix given by Equation (5-9), if $\mathbf{e}_i$, ($i \leq N$), belongs in the controllable subspace, $\mathbf{e}_{N+i}$, ($i \leq N$), does also.

Assume first that all the h_{ij} entries of the inertia matrix $\mathbf{H}$ are zero, except h_{ii}. This results in an inertia matrix $\mathbf{H}$ having the form:

$$\mathbf{H} = \begin{bmatrix} \mathbf{x} & \mathbf{0} & \mathbf{x} \\ \mathbf{0} & h_{ii} & \mathbf{0} \\ \mathbf{x} & \mathbf{0} & \mathbf{x} \end{bmatrix} \tag{5-10}$$

where $\mathbf{x}$ is a nonzero matrix and $\mathbf{0}$ a zero matrix of appropriate dimensions. Note that due to properties of inverse inertia matrices, $\mathbf{H}^{-1}$ has the same zero elements as $\mathbf{H}$. Then, it is easy to see that all the elements of the i^{th} row of the product $\mathbf{H}^{-1}\mathbf{1}_i$ are zero, and therefore,

the vector e_i, which has a nonzero element at the i^{th} position, does not belong in the controllable subspace spanned by the columns of matrix C, given by Equation (5-9). Due to the structure of C, the same observations hold for e_{N+i}. Hence, it can be concluded that if all $h_{ij}=0$ $(i\neq j)$, the failed joint cannot be controlled. However, if some h_{ij} is nonzero, the i^{th} and $(N+i)^{th}$ rows are in general nonzero and hence, e_i and e_{N+1} can be chosen to be basis vectors of the controllable subspace. Then the system state can be driven to a desired any q_i and $\dot{q}_i$. In other words, this means that to control the angle of a failed joint, there must be *dynamic coupling* between the link with the failed joint and a link with a working joint. Physically, this condition requires that the control input corresponding to some coordinate be able to affect some other coordinate. In many cases, this condition is satisfied. For example, all rotational DOF of a planar system are coupled. On the other hand, the second and third joints of the manipulator shown in Figure 5.2 are not coupled to the first one, and in this case $h_{1j} = 0$ (j=2,3).

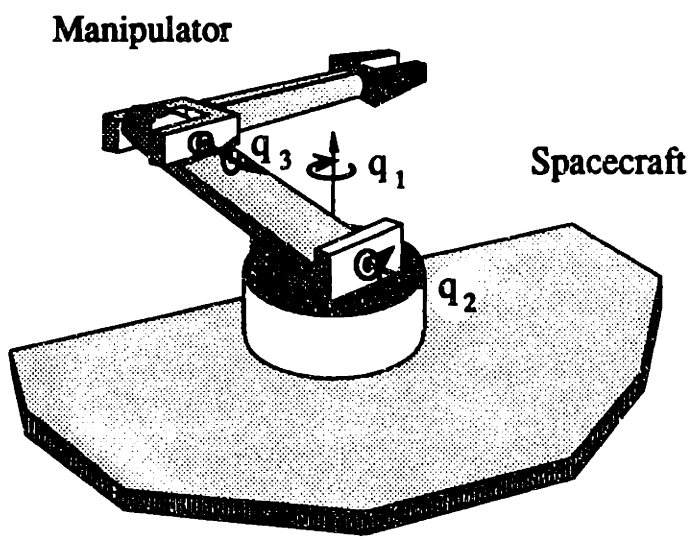

Figure 5.2. A space manipulator whose first joint is not coupled dynamically to the other two.

If the first motor of such a manipulator is not working, no motion of the other motors will affect the angle that corresponds to the non-working one. Similarly, by mere inspection of

the inertia matrix of a free-flying space robotic system, given by Equation (2-58), it can be seen that the translational DOF that correspond to the system CM are not coupled to the rotational DOF which correspond to the spacecraft attitude and to the manipulator revolute joints. This confirms the fact that if a spacecraft's thrusters do not operate, there is no way to control the translation of the system CM by using manipulator actuators or spacecraft reaction wheels.

Now, assuming that some nonzero h_{ij} has been found, the task is to design a controller which will use input j to control the i^{th} DOF corresponding to the failed joint. To this end, write the i^{th} equation of motion, see Equation (5-6), as follows:

$$\sum_{j=1}^{N} h_{ij}\ddot{q}_j + \sum_{j=1}^{N}\sum_{k=1}^{N} h_{ijk}\dot{q}_j\dot{q}_k = 0 \tag{5-11}$$

Since it was assumed that $h_{ij} \neq 0$, Equation (5-10) can be solved for $\ddot{q}_j$ and substituted in the remaining Equations (5-6) to yield the following N-1 equations of motion:

$$\mathbf{H}^{\#}(\mathbf{q})\ddot{\mathbf{z}} + \mathbf{C}^{\#}(\mathbf{q}, \dot{\mathbf{q}}) = \tau^{\#} \tag{5-12}$$

where $\mathbf{H}^{\#}$ is a (N-1)×(N-1) matrix, $\tau^{\#} \in \mathbf{R}^{N-1}$ contains all nonzero control torques, $\mathbf{C}^{\#}$ contains nonlinear terms and finally $\mathbf{z} \in \mathbf{R}^{N-1}$ contains all coordinates to be controlled:

$$\mathbf{z} = [q_1, \ldots, q_{j-1}, q_{j+1}, \ldots, q_N]^T \tag{5-13}$$

It is easy to show that z can be driven to any $\mathbf{z}_{des}$, whenever $\mathbf{H}^{\#}$ exists and is nonsingular[1]. For example, consider the following nonlinear feedback-linearizing control:

$$\tau^{\#} = \mathbf{C}^{\#}(\mathbf{q}, \dot{\mathbf{q}}) + \mathbf{H}^{\#}(\mathbf{q})\{\mathbf{K}_p(\mathbf{z}_{des}-\mathbf{z}) - \mathbf{K}_d\dot{\mathbf{z}}\} \tag{5-14}$$

---

[1]Since h_{ij} is at the denominator of the entries of $\mathbf{H}^{\#}$, this matrix is not defined when becomes zero and therefore, there is some region in which actuator j can be used. If this region is not sufficient, then it may be possible to use some other joint.

where $\mathbf{K}_p$ and $\mathbf{K}_d$ are (N-1)×(N-1) positive definite diagonal matrices and where it was assumed implicitly that joint encoders still work. Applying control law (5-14) to the reduced system equations (5-12), a stable linear decoupled system is obtained. Clearly, for this system, $\mathbf{z} \rightarrow \mathbf{z}_{des}$, $\dot{\mathbf{z}} \rightarrow 0$, asymptotically. Recall that q_i belongs in z; therefore, the task of controlling the failed joint i is achieved. However, these conditions do not guarantee stability for the overall system; the behavior of Equation (5-11) must be analyzed. When $\mathbf{z} \rightarrow \mathbf{z}_{des}$, $\dot{\mathbf{z}} \rightarrow 0$, Equation (5-11) reduces to:

$$h_{ij}\ddot{q}_j + h_{ijj}\dot{q}_j^2 \equiv 0 \tag{5-15}$$

where h_{ij}, h_{ijj}, are functions of q_j only. Equation (5-15) is in general *unstable*, unless $h_{ijj}\dot{q}_j/h_{ij}$ is always positive. However, this condition cannot be guaranteed and when it is violated, q_j will drift and not converge to some constant. Hence, although the control law given by Equation (5-14) drives q_i to a desired set point, it may destabilize another DOF. However, if a condition to guarantee that $\dot{q}_j \rightarrow 0$ could be found, then the system would remain stable. This issue is addressed next.

Note that Equation (5-11) can be written also as:

$$\frac{d}{dt}\left\{\frac{\partial T}{\partial \dot{q}_i}\right\} - \frac{\partial T}{\partial q_i} = 0 \tag{5-16}$$

where T is the system's kinetic energy, given by:

$$T = \frac{1}{2}\dot{\mathbf{q}}^T \mathbf{H}(\mathbf{q})\,\dot{\mathbf{q}} \tag{5-17}$$

Equation (5-16) can be integrated and assuming that the system is initially at rest, and taking the limit as $\mathbf{z} \rightarrow \mathbf{z}_{des}$, $\dot{\mathbf{z}} \rightarrow 0$, the following expression for the asymptotic behavior of $\dot{q}_j$ results:

$$\lim_{t \rightarrow \infty}(\dot{q}_j) = h_{ij}^{-1}\int_0^{\infty} \frac{\partial T}{\partial q_i}\,dt \tag{5-18}$$

Expression (5-18) shows that $\dot{q}_j$ will reach zero, if the integrand is identically zero. This is equivalent to requiring that q_i be *ignorable*, that is that the inertia matrix **H** is invariant with respect to this coordinate. Note that when q_i is ignorable, Equation (5-16) becomes an *integral of motion*, and then the system order is N-1. However, $\mathbf{H}^{\#}$ is not a positive definite matrix and this restricts in general the range of possible maneuvers.

It remains to examine when a coordinate can be ignorable. In some cases, this is a feature of the system itself. For example, the inertia matrix of a two DOF free-flying manipulator system with a fixed spacecraft, given by Equations (4-13) is not a function of the first joint angle. This means that in some range, one can control the first joint by the second motor - obviously it can always be controlled by the first motor. In other cases, the invariance of the inertia matrix can be obtained by design, as was done by [6] with the aim of designing a controller with configuration-independent behavior.

To conclude this section, we note that in order to design a controller for failure recovery, two basic conditions must be satisfied: (a) There must exist dynamic coupling between the broken joint and some other joint during a maneuver, and (b) the angle corresponding to the failed joint must be ignorable. Recall that two minor conditions were also assumed: (a) that joint friction is negligible and (b) that the system is initially at rest. In the next section, failure recovery control is demonstrated using two examples.

5.5 EXAMPLES

Example 1. Consider first a two DOF manipulator mounted on a spacecraft fixed in inertial space by using jet actuators. The equations of motion for this system are written below:

$$h_{11}\ddot{q}_1 + h_{12}\ddot{q}_2 - 2h\dot{q}_2^2 - 2h\dot{q}_1\dot{q}_2 = \tau_1 \qquad (5\text{-}19a)$$

$$h_{12}\ddot{q}_1 + h_{22}\ddot{q}_2 + h\dot{q}_1^2 = \tau_2 \qquad (5\text{-}19b)$$

where h_{ij} are given by Equation (4-13) and $h = m_2 l_2 (l_1 + r_1)\sin(q_2)$. Note that any planar space system can be reduced to this case by fixing all its coordinates except two, which then are q_1 and q_2. Next, assume that the first joint has failed, that is $\tau_1 = 0$. Obviously this system is dynamically coupled because h_{12} is nonzero, except at two distinct angles q_2 at the most. Hence, failure control may be possible in a region where q_2 stays away from these values. Note that in this case all h_{ij} are functions of q_2 only, and q_1 is ignorable. Therefore, Equation (5-19a) can be integrated to yield:

$$h_{11}\dot{q}_1 + h_{12}\dot{q}_2 = 0 \tag{5-20}$$

where it was assumed that the system was initially at rest. Equation (5-20) can be solved for $\dot{q}_2$ which is then substituted in Equation (5-19b) to yield the only equation of motion for this system:

$$-(h_{11}h_{22}-h_{12}^2)/h_{12}\,\ddot{q}_1 + h\dot{q}_1^2 = \tau_2 \tag{5-21}$$

where $-(h_{11}h_{22}-h_{12}^2)/h_{12}$ is the 1×1 $\mathbf{H}^{\#}$ matrix for this system. Note that since $(h_{11}h_{22}-h_{12}^2)$ is the determinant of the full inertia matrix $\mathbf{H}$, it is always positive, and therefore the sign of $\mathbf{H}^{\#}$ is opposite to the sign of h_{12}; $\mathbf{H}^{\#}$ is not positive definite. However, if h_{12} is nonzero, the control law (5-14) can be applied and the result is:

$$\tau_2 = h\dot{q}_1^2 - (h_{11}h_{22}-h_{12}^2)/h_{12}\{K_p(q_{1,des}-q_1)-K_d\dot{q}_1\} \tag{5-22}$$

This control law guarantees $q_1 \rightarrow q_{1,des}$ and $\dot{q}_1 \rightarrow 0$, asymptotically. Also, due to the integral of motion (5-20), $\dot{q}_2 \rightarrow 0$, and the system is asymptotically stable.

Example 2. Next consider the free-floating space manipulator example system of section 3.8. Its inertia matrix is given by Equation (3-41) and is a function of both joint angles q_1

and q_2. Assume that the second joint has failed, that is $\tau_2 = 0$, see Figure 5.3. A simple joint control law is used here:

$$\tau_1 = K_p(q_{2,des}-q_2)-K_d\dot{q}_2 \tag{5-23}$$

with K_p = 50 Nm/rad, and K_d = 45 Nmsec/rad, and q_2 in radians. In order to maximize the system's reach, the desired position for the second joint angle is set to be $q_{2,des} = 0^\circ$. The initial conditions are $(\theta, q_1, q_2) = (39.6^\circ, -134.2^\circ, 134.4^\circ)$. System parameters are given by Table I.

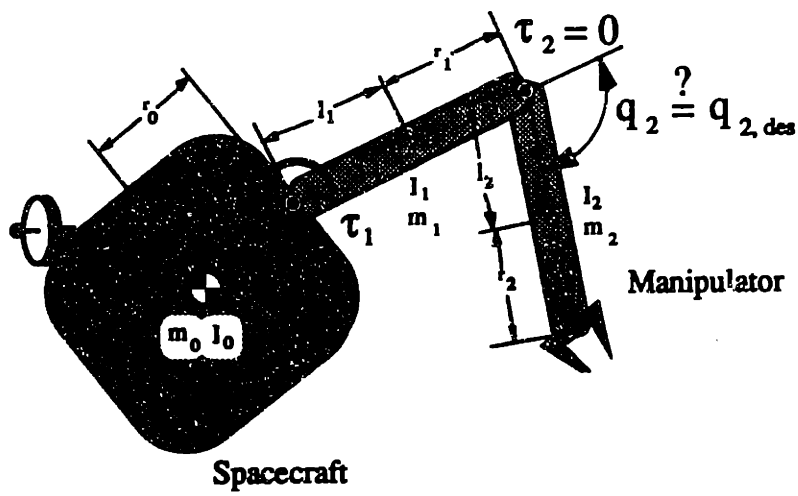

Figure 5.3. A space manipulator with a failed joint.

Figure 5.4 shows the time history of the joint angles and the spacecraft attitude. Since q_2 is not ignorable, the system drifts as predicted, although q_2 reaches its set-point of 0°. Figure 5.5 shows the actual motion of the system in the inertial space. The system is initially at rest and the end-effector is at point A. When control action starts, the end-effector follows the path shown in Figure 5 and continues to drift; instability is obvious.

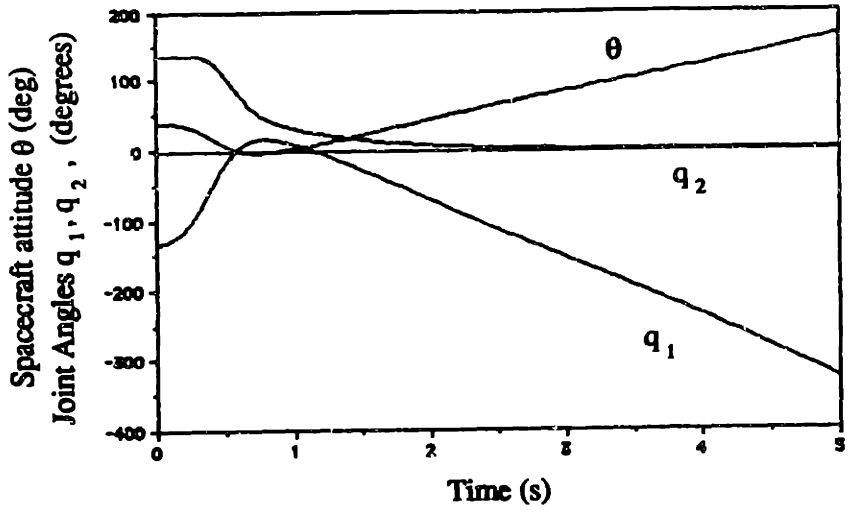

Figure 5.4. Spacecraft attitude and joint angles history during a failure recovery maneuver. Motion is unstable.

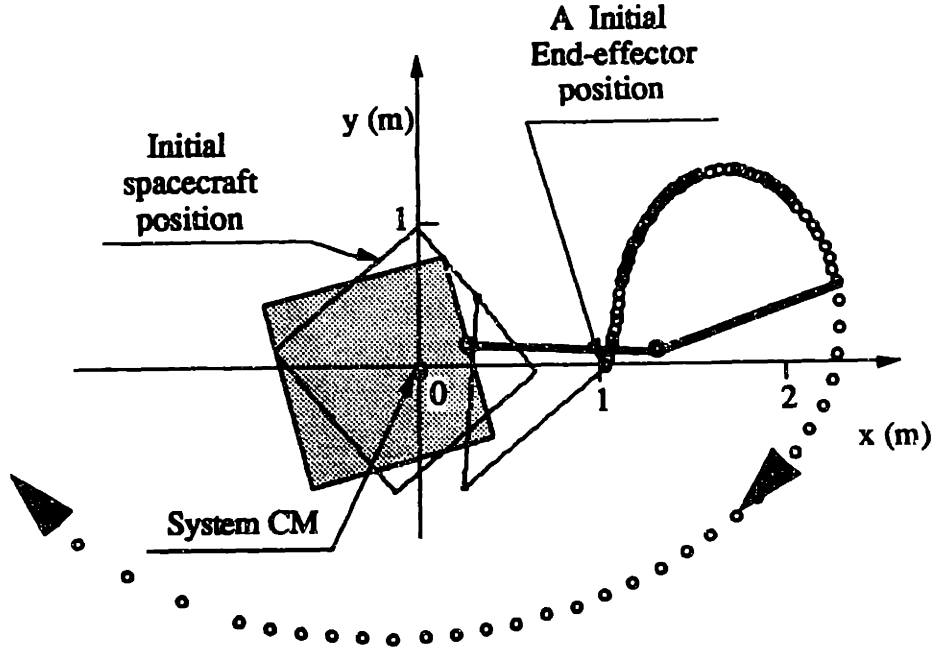

Figure 5.5. A failure recovery maneuver in inertial space. Motion is unstable.

Close examination of the entries of the inertia matrix given by Equations (E-22) and (E-24) reveals the fact that if the center of mass of the second link lies on the second joint axis, in other words if l_2 is zero, then all d_{2i} (i=0,1,2) are zero and q_2 is ignorable. Note that this

can be achieved by changing the mass distribution of the second link, for example by using counterweights. Such a system's parameters are given by Table IV.

Table IV. System parameters for the two-DOF manipulator example.

Body	l_i (m)	r_i (m)	m_i (Kg)	I_i (Kg m^2)
0	.5	.5	40	6.667
1	.5	.5	4	0.333
2	.0	.1	3	0.250

To show this, the same case as above is simulated, but this time $l_2 = 0$. As shown in Figure 5.6, this time q_2 converges to the desired set-point and the motion is stable, as predicted. Figure 5.7 depicts the same maneuver in inertial space. The end-effector follows the path from point A to point B and stops at B. Once the system reaches the steady state configuration, joint 2 can be locked and operation of joint 1 may resume.

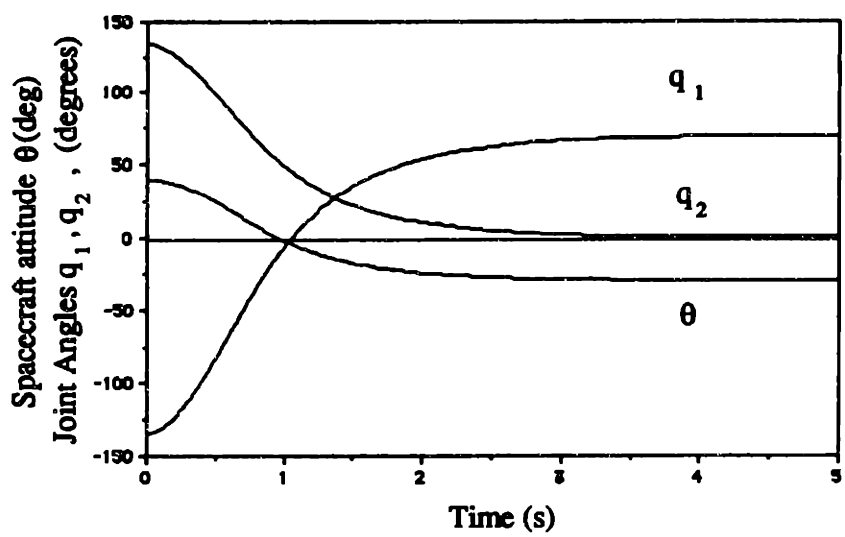

Figure 5.5. Spacecraft attitude and joint angles history during a failure recovery maneuver. Motion is stable.

Note that since the CM of the second link is on the joint axis, no torques due to the offset of bearing forces at the joint can be applied to the second link, (this offset is zero). Hence, this link can only translate and this is why its inertial orientation remains constant. The controller produces a torque that rotates the first link till q_2 becomes equal to the set-point, which in the case of Figure 5.6, is zero.

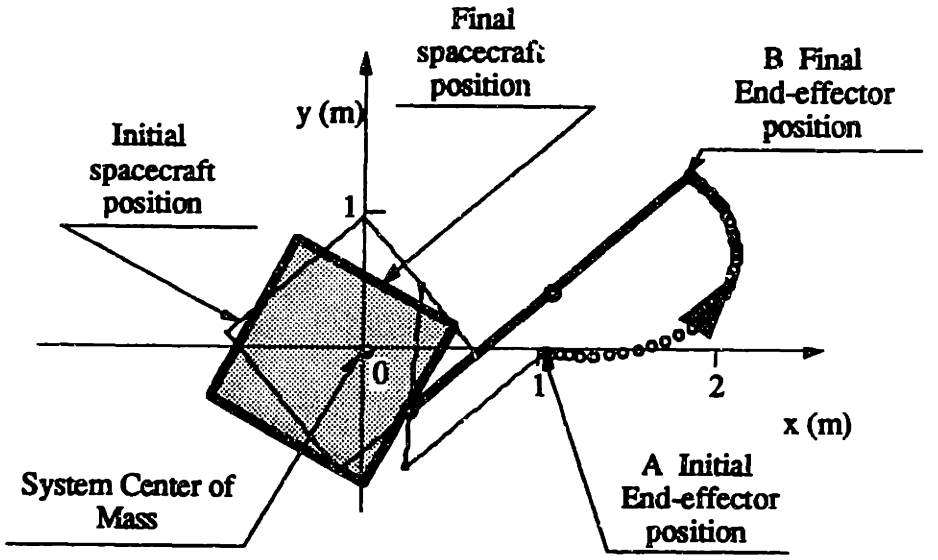

Figure 5.7. A failure recovery maneuver in inertial space. Motion is stable.

It should be noted that designing a system to be invariant with respect to some coordinate has limitations similar to the ones observed in studies of dynamic decoupling of fixed-based manipulators, [6]. For example, for the planar system used here, both joint angles can be made ignorable. However, this is also the upper limit for planar systems. On the other hand, the observations made in this chapter may help in improving the reliability of non-redundant space systems. If redundancy is available, then the same principles can be used still and the system may be able to be fully operational, even after a failure is experienced.

5.6 SUMMARY

In this chapter, the possibility of using the working joints of a space system to control a failed joint was explored. This is a problem that belongs to a more general class of problems, namely the control of systems with fewer actuators than DOF. Results showed that in order to be able to design a failure recovery controller, dynamic coupling and invariance of the inertia matrix with respect to the angle of the failed joint must exist. Although this type of control may not always feasible, the analysis presented here can lead to new developments in this important direction.

6 Conclusions and Future Research

6.1 CONCLUSIONS

The main motivation of this thesis was to investigate what is the structure, requirements and limitations of controllers to be used in the control of spacecraft-borne manipulators. The basic assumption that effective control is possible only if based on knowledge of the structure of a system's "plant," lead to a modeling methodology that yielded an explicit and compact kinematic and dynamic description for free-flying systems, taking into account forces due to spacecraft thrusters, to end-effector forces and to disturbances.

It was shown that when the system's thrusters are turned off and no other forces act on the system, i.e. when the system is free-floating, then the kinematic and dynamic structure of such a system is essentially the same to that of a fixed-based system. Exceptions are the dependence of the system's Jacobian on the mass and inertia properties of the entire system, and the existence of Dynamic Singularities. These Dynamic Singularities are fixed in a manipulator's joint space and are function of the mass and inertia properties of the system. Their occurrence in a system's inertial workspace depends upon the path taken by the manipulator in reaching some inertial workspace point. *All* control algorithms that use an inverse Jacobian will fail computationally at such points, while *all* those that use a transposed Jacobian will result in large unrecoverable errors. Path Independent Workspaces which contain all points that cannot induce Dynamic Singularities and can be reached by any path, were identified. The remaining workspace was called a Path Dependent Workspace because its points can be reached by carefully planned paths, only.

It was shown that the implication of the above results on the control of a free-floating system is that it may not be output controllable in the Path Dependent Workspace. It was shown further that nearly *any* motion control algorithm which can be implemented on a terrestrial robotic manipulator also can be applied successfully to a free-floating space manipulator if certain mild conditions are met. Also, the sensory requirements for free-floating systems were shown to be exactly the same to those required by fixed-based controllers. However, if a system's kinematic and dynamic properties are not known with sufficient accuracy, end-point feedback and measurement of a spacecraft's attitude may be required.

The control of free-flying manipulators, capable of translating in inertial space and applying forces and torques, was considered also. Coordinated Control that allows the simultaneous control of both a spacecraft and of its manipulator was designed. This controller was designed systematically, based on an appropriate description of the "plant" kinematics and dynamics. Depending on the task requirements, existing control algorithms for fixed-based systems can be modified and applied in the control of free-flying systems.

Finally, the important problem of Failure Recovery Control of a spacecraft-borne manipulator was addressed. It was shown that a joint angle whose actuator has failed still can be controlled, at the expense of some other joint, provided that dynamic coupling between the two exists and that the inertia matrix of the system is invariant with respect to the angle that corresponds to the failed actuator.

6.2 DIRECTIONS FOR FUTURE RESEARCH

In Chapter 3, it was mentioned that dynamic singularities can be avoided by using manipulator redundancy. Such redundancy also can be used to minimize fuel expenditure in free-flying systems, or to improve a system's reliability, an important and under-

explored issue. These issues become more important in the view of future multiple-arm systems.

There is a number of interesting problems related to path-planning that remain unresolved. For example, it was mentioned in Chapter 4 that if a system is free-floating, then an end-effector path can be selected in such a way that the attitude of a system's spacecraft will be controlled also. Despite some efforts so far, such paths remain elusive. Further, practical end-effector paths that could allow a free-floating system to use its Path Dependent Workspace without the associated problems, would be desired.

On earth but even more so in space, system calibration is very important in order to improve a system's accuracy. It would be desirable to design a self-calibrating system that would be capable of identifying itself as well as its payloads. To this end, adaptive controllers for space systems could be considered also.

System calibration is required because it is very hard to use closed-loop feedback and hence, to reduce system uncertainty. This difficulty is due to the lack of effective end-point sensing techniques. Techniques that would reduce this problem would be very useful in space.

In Chapter 5, failure recovery control was achieved, provided that some restrictive conditions hold. It would be useful to develop planning or control algorithms that would not be restricted in their usage.

This thesis focused on fundamentals of space manipulators but assumed idealized models for such systems. From a more practical point of view, other important issues must be treated also. These may include among others, the control of multiple manipulator systems, joint or link flexibilities, interactions of manipulators and payloads at grasping, sensing and sensor data fusion, communication delays, telerobotic and human factor issues, as well as safety and reliability issues.

References

[1] Abraham, R., and Marsden, J. E., Foundations of Mechanics, Benjamin-Cummins, Reading, MA, 1978.

[2] Akin, D. L., Minsky, M. L., Thiel, E. D., and Kurtzman, C. R., "Space Applications of Automation, Robotics and Machine Intelligence Systems (ARAMIS) - Phase II," NASA Contractor Report 3734, NASA, 1983.

[3] Alexander, H., and Cannon, R., "Experiments on the Control of a Satellite Manipulator," *Proc. of the American Control Conference*, Seattle, WA, June 1987.

[4] Arimoto, S., and Miyazaki, F., "Stability and Robustness of PID Feedback Control for Robot Manipulators of Sensory Capability," in M. Brady and R. R. Paul (eds.), *Robotics Research: An International Symposium*, MIT Press, Cambridge, MA, 1984, pp. 783-799.

[5] Asada, H., and Slotine, J. J. E., *Robot Analysis and Control*, John Wiley and Sons, New York, NY, 1986.

[6] Asada, H., and Youcef-Toumi, K., *Direct-Drive Robots: Theory and Practice*, MIT Press, Cambridge, MA, 1987.

[7] Atkeson, C. G., An, C. H., and Hollerbach, J., "Estimation of Inertial Parameters of Manipulator Loads and Links," *Int. Journal of Robotics Research*, Vol. 5, No. 3, Fall 1986, pp. 101-119.

[8] Automation and Robotics Panel of the Consortium for Space/Terrestrial Automation and Robotics and the California Space Institute of the University of California, "An Examination of Automation and Robotics in the Context of Space Operations," Chiou, W.C. (ed.), *SPIE Proceedings Series*, Vol. 1006, Nov. 1988, pp. 12-19.

[9] Baillieul, J., "Equilibrium Mechanics in Rotating Systems," *Proc. of IEEE Conference on Decision and Control*, Los Angeles, CA, December 1987.

[10] Brockett, R. W., "Nonlinear Systems and Differential Geometry," *Proceedings of the IEEE*, Vol. 64, No. 1, January 1976, pp. 61-72.

[11] Brunez, M. A., Clarke, M. M., and Quinn A., "Requirements Development for a Free-Flying Robot - the ROBIN," in *Proc. of the IEEE International Conference on Robotics and Automation*, San Fransisco, CA, April 1986.

[12] Campbell, P. D., "Teleoperation and Autonomy in Space Station Robotic Systems," in "Space Station Automation IV," Chiou, W.C. (ed.), *SPIE Proceedings Series*, Vol. 1006, November 1988, pp. 56-62.

[13] Craig, J. J., et al., "Adaptive Control of Mechanical Manipulators," *International Journal of Robotics Research*, Vol. 6, No. 2, Summer 1987.

[14] Craig, J., *Introduction to Robotics, Mechanics and Control*, Addison Wesley, Reading, MA, 1986.

[15] Critchlow, A. J., *Introduction to Robotics*, Macmillan Publishing Company, New York, NY, 1985.

[16] Dubowsky, S., and Torres, M., "Path Planning for Space Manipulators to Minimize the Use of Attitude Control Fuel," *Proc. of the International Symposium on Artificial Intelligence, Robotics and Automation in Space (I-SAIRAS)*, Kobe, Japan, November 1990.

[17] Dubowsky, S., and Vafa, Z., "A Virtual Manipulator for Space Robotic Systems," *Proc. of the Workshop on Space Telerobotics*, Pasadena, CA, January 1987.

[18] Dubowsky, S., Vance, E., and Torres, M., "The Control of Space Manipulators Subject to Spacecraft Attitude Control Saturation Limits," *Proc. of the NASA Conference on Space Telerobotics*, JPL, Pasadena, CA, Jan. 31-Feb. 2, 1989.

[29] Erickson, J. D., "Manned Spacecraft Automation and Robotics," in *Proceedings of the IEEE*, Vol. 75, No 3, March 1987, pp. 417-426.

[20] Frisch, H. P., "A Vector-Dyadic Development of the Equations of Motion for N Coupled Rigid Bodies and Point Masses," NASA TN D-7767, Washington, DC, 1974.

[21] Goldstein, H., *Classical Mechanics*, Addison-Wesley, Reading, MA, 1980.

[22] Hermann, R., and Krener, A., J., "Nonlinear Controliability and Observability," *IEEE Transactions on Automatic Control*, Vol. AC-22, No. 5, October 1977, pp. 728-740.

[23] Hinkal, S. W., Andary J. F., Watzin J. G., and Provost, D. E., "The Flight Telerobotic Servicer (FTS): A Focus for Automation and Robotics on the Space Station," *Acta Astronautica*, Vol. 17, No 8, 1988, pp. 759-768.

[24] Ho, J. Y. L., "Direct Path Method for Flexible Multibody Spacecraft Dynamics," *Journal of Spacecraft and Rockets*, Vol 14, 1977, pp. 102-110.

[25] Hogan, N., "Impedance Control: An Approach to Manipulation: Part I-Theory, Part II-Implementation,"*J. of Dynamic Systems, Measurement and Control*, Vol 107, 1985, pp. 1-24.

[26] Hollerbach, J. M., "A Recursive Lagrangian Formulation of Manipulator Dynamics and a Comparative Study of Dynamics Formulation Complexity," *IEEE Transactions on Systems, Man and Cybernetics*, SMC-10, 1980, pp. 730-736.

[27] Hooker, W. W., "A Set of r Dynamical Attitude Equations for an Arbitrary n-Body Satellite Having r Rotational Degrees of Freedom," *AIAA Journal*, Vol. 8, No. 7, July 1970, pp. 1205-1207.

[28] Hooker, W. W., "Equations of Motion for Interconnected Rigid and Elastic Bodies: A Derivation Independent of Angular Momentum," *Celestial Mechanics*, Vol. 11, 1975, pp. 337-359.

[29] Hooker, W. W., and Margulies, G., "The Dynamical Attitude Equations for an n-Body Satellite," *Journal of Astronautical Sciences*, Vol XII, No 4, Winter 1965, pp. 123-128.

[30] Hughes, P. C., *Spacecraft Attitude Dynamics*, John Wiley, New York, NY, 1986.

[31] Jerkovsky, W., "The Structure of Multibody Dynamics Equations," *Journal of Guidance and Control*, Vol 1, No. 3, 1978, pp.173-182.

[32] Kane, T. R., and Levinson, D. A., "The Use of Kane's Dynamical Equations in Robotics," *Int. J. of Robotics and Automation*, Vol. 2, No. 3, 1983, pp. 3-21.

[33] Khatib, O., "A Unified Approach for Motion and Force Control of Robot Manipulators: The Operational Space Formulation," *IEEE Journal of Robotics and Automation*, Vol. RA-3, No. 1, February 1987, pp. 43-53.

[34] Koditschek, D., "Application of a New Lyapunov Function to Global Adaptive Attitude Tracking," *Proc. of the 27th Conf. on Decision and Control*, Austin, TX, December 1988.

[35] Korn, G., and Korn, T., *Mathematical Handbook for Scientists and Engineers*, Second Edition, McGraw-Hill, New York, NY, 1968.

[36] Kreutz, K., and Wen, J., T., "Attitude Control of an Object Commonly Held by Multiple Arms: A Lyapunov Approach," *Proc. of the American Control Conference*, Atlanta, GA, June 1988.

[37] Kwakernaak, H., and Sivan, R., *Linear Optimal Control Systems*, Wiley Interscience, New York, NY, 1972.

[38] Larson, V. R., and Evans, S., A., "Propulsion for the Space Station," in *Commercial Opportunities in Space*, F. Shahrokli, et al. (eds.), Progress in Astronautics and Aeronautics, Vol. 110, AIAA, 1988.

[39] Likins, P. W., "Analytical Dynamics and Nonrigid Spacecraft Simulation," JPL Technical Report 32-1593, July 1974.

[40] Longman, R., "The Kinetics and Workspace of a Robot Mounted on a Satellite That Is Free to Rotate and Translate," *Proc. of the AIAA Guidance, Navigation and Control Conference*, Minneapolis, MN, August 1988.

[41] Longman, R., Lindberg, R., and Zedd, M., "Satellite-Mounted Robot Manipulators-New Kinematics and Reaction Moment Compensation," *International Journal of Robotics Research*, Vol. 6, No. 3, Fall 1987, pp. 87-103.

[42] Luh, J. Y. S., Walker, M., and Paul, R. P., "On-Line Computational Scheme for Mechanical Manipulators," *J. of Dynamic Systems, Measurement and Control*, Vol 102, 1980, pp. 69-76.

[43] Luh, J. Y. S., Walker, M., and Paul, R. P., "Resolved-Acceleration Control of Mechanical Manipulators," *IEEE Transactions on Automatic Control*, AC-25, 3, 1980, pp.468-474.

[44] Masutani, Y., Miyazaki, F., and Arimoto, S., "Sensory Feedback Control for Space Manipulators," *Proc. of the IEEE International Conference on Robotics and Automation*, Scottsdale, AZ, May 1989.

[45] Nakamura, Y., and Mukherjee, R., "Nonholonomic Path Planning of Space Robots," *Proc. of the IEEE International Conf. on Robotics and Automation*, Scottsdale, AZ, May 1989.

[46] Nijmeijer, H., and van der Schaft, A. J., *Nonlinear Dynamical Control Systems*, Springer Verlag, New York, NY, 1990.

[47] Ogata, K., *Modern Control Engineering*, Prentice Hall Inc., Englewood Cliffs, NJ, 1970.

[48] Papadopoulos, E., and Dubowsky, S., "On the Control of Space Manipulators," in *Proc. of the Eighth CISM-IFToMM Symposium on Theory and Practice of Robots and Manipulators*, Cracow, Poland, July 1990.

[49] Papadopoulos, E., and Dubowsky, S., "On the Dynamic Singularities in the Control of Free-Floating Space Manipulators," *Proc. of the ASME Winter Annual Meeting*, San Fransisco, CA, December 1989. Also submitted for publication in the *ASME Journal of Dynamic Systems, Measurement and Control.*

[50] Papadopoulos, E., and Dubowsky, S., "On the Nature of Control Algorithms for Space Manipulators," *Proc. of the IEEE International Conference on Robotics and Automation*, Cincinnati, OH, May 1990. Also submitted for publication in the *IEEE Transactions on Robotics and Automation.*

[51] Pars, L. A., *Treatise on Analytical Dynamics*, John Wiley and Sons, New York, NY, 1965.

[52] Reuter, G. J., et al. "An Intelligent, Free-Flying Robot," in "Space Station Automation IV," Chiou, W.C. (ed.), *SPIE Proceedings Series*, Vol. 1006, November 1988, pp. 20-27.

[53] Roberson, R. E., and Wittenburg, J., "A Dynamical Formalism for an Arbitrary Number of Rigid Bodies, with Reference to the Problem of Satellite Attitude Control," in *Proc. of the IFAC Congress, London*, 1966, Butterworth, London, 1968.

[54] Rosenberg, R. M., *Analytical Dynamics of Discrete Systems*, Plenum Press, New York, NY, 1977.

[55] Sargent, D., "Shuttle On-Orbit Flight Control Interaction with Remote Manipulator System Payloads," Guidance and Control Seminar Series, MIT, Cambridge, MA, November 27, 1989.

[56] Schaefer, J., F., and Cannon, R., H., "On the Control of Unstable Mechanical Systems," *Proc. of the Third Congress of the IFAC*, London, June 1966.

[57] Slotine, J.-J. E., and Li, W., "On the Adaptive Control of Robot Manipulators," *International Journal of Robotics Research*, Vol. 6, No. 3, Fall 1987.

[58] Spofford, J., and Akin, D., "Redundancy Control of a Free-Flying Telerobot," *Proc. of the AIAA Guidance, Navigation and Control Conference*, Minneapolis, MN, August 1988.

[59] Sreenath, N., "Nonlinear Control of Mutibody Systems in Shape Space," *Proc. of the IEEE International Conference on Robotics and Automation*, Cincinnati, OH, May 1990.

[60] Umetani, Y., and Yoshida, K., "Experimental Study on Two Dimensional Free-Flying Robot Satellite Model," *Proc. of the NASA Conference on Space Telerobotics*, Pasadena, CA, January 1989.

[61] Umetani, Y., and Yoshida, K., "How to reduce the Fluctuation of Space Vehicle During Manipulator Movement," *Proc. of the Sixteenth International Symposium on Space Technology and Science*, Sapporo, Japan, 1988.

[62] Vafa, Z., and Dubowsky, S., "On the Dynamics of Manipulators in Space Using the Virtual Manipulator Approach," *Proc. of the IEEE International Conference on Robotics and Automation*, Raleigh, NC, March 1987.

[63] Vafa, Z., and Dubowsky, S., "On the Dynamics of Space Manipulators Using the Virtual Manipulator, with Applications to Path Planning," *J. of Astronautical Sciences*, (In Press).

[64] Vafa, Z., and Dubowsky, S., "The Kinematics and Dynamics of Space Manipulators: The Virtual Manipulator Approach," *International Journal of Robotics Research*, Vol. 9, No. 4, August 1990, pp. 3-21.

[65] Vafa, Z., "The Kinematics, Dynamics and Control of Space Manipulators: The Virtual Manipulator Concept," Ph.D. Thesis, Department of Mechanical Engineering, MIT, Cambridge, MA, 1987.

[66] Varsi, G., and Herman D., "Space Station as a Vital Focus for Advancing the Technologies of Automation and Robotics," *Acta Astronautica*, Vol. 17, No 3, 1988, pp. 347-354.

[67] Watson, J. K., "Engineering Considerations for On-Orbit Welding Operations," *Journal of the Astronautical Sciences*, Vol. 34, No. 2, April-June 1986.

[68] West, H., Papadopoulos, E., Dubowsky, S., and Cheah H., "A Method for Estimating the Mass Properties of a Manipulator by Measuring the Reaction Moments at its Base," in *Proc. of the IEEE International Conf. on Robotics and Automation*, Scottsdale, AZ, May 1989.

[69] Whitney, E., D., "Resolved Motion Rate Control of Manipulators and Human Prostheses," *IEEE Trans. Man-Machine Systems*, Vol. 1 MMS-10, 1969, pp.47-53.

[70] Whittaker, E. T., *A Treatise on the Analytical Dynamics of Particles and Rigid Bodies*, Fourth Edition, Dover Publications, New York, NY, 1944.

[71] Wiesel,W. E., *Spaceflight Dynamics*, McGraw-Hill, New York, NY, 1989.

[72] Wittenburg, J., *Dynamics of Rigid Bodies*, B.G. Teubner, Stuttgart, 1977.

Appendix A: Vectors and Dyadics

A dyad is an ordered pair of vectors, written one next to the other as $\underline{a}\ \underline{b}$. A dyadic is a linear polynomial of dyads [21]:

$$\underline{D} = \underline{a}\ \underline{b} + \underline{c}\ \underline{d} + \ldots \tag{A-1}$$

The dot product of a dyadic and a vector is a vector:

$$\underline{D} \cdot \underline{e} = \underline{a}\ (\underline{b} \cdot \underline{e}) + \underline{c}\ (\underline{d} \cdot \underline{e}) + \ldots \tag{A-2a}$$

$$\underline{e} \cdot \underline{D} = \underline{b}\ (\underline{a} \cdot \underline{e}) + \underline{d}\ (\underline{c} \cdot \underline{e}) + \ldots \tag{A-2b}$$

The unit dyadic, $\underline{1}$ is defined by:

$$\underline{1} \cdot \underline{a} = \underline{a} \cdot \underline{1} = \underline{a} \tag{A-3}$$

Using dyadics, the double vector of three vectors can be written as:

$$\underline{a} \times (\underline{b} \times \underline{c}) = \underline{b}\ (\underline{a} \cdot \underline{c}) - \underline{c}\ (\underline{a} \cdot \underline{b}) = \underline{D} \cdot \underline{b} \tag{A-4}$$

where the dyadic $\underline{D}$ is given by:

$$\underline{D} = (\underline{c} \cdot \underline{a})\underline{1} - \underline{c}\ \underline{a} \tag{A-5}$$

In other words, $\underline{D}$ acts as an operator on a vector, resulting in another vector. Next consider a triple cross product of three vectors, and use Equation (A-5):

$$\underline{a} \times (\underline{b} \times (\underline{a} \times \underline{c})) = \underline{c} \times \underline{a}\ (\underline{a} \cdot \underline{b}) \tag{A-6a}$$

$$= \underline{a} \times ((\underline{c} \cdot \underline{b})\underline{1} - \underline{c}\ \underline{b}) \cdot \underline{a} =$$

$$= \underline{a} \times \underline{D} \cdot \underline{a} \tag{A-6b}$$

where in this case, $\underline{\mathbf{D}} = (\underline{\mathbf{c}} \cdot \underline{\mathbf{b}})\underline{\mathbf{1}} - \underline{\mathbf{c}}\,\underline{\mathbf{b}}$. Another useful triple cross product identity is:

$$\underline{\mathbf{c}} \times (\underline{\mathbf{a}} \times (\underline{\mathbf{a}} \times \underline{\mathbf{b}})) = \underline{\mathbf{c}} \times (\underline{\mathbf{a}}\,(\underline{\mathbf{a}} \cdot \underline{\mathbf{b}}) - \underline{\mathbf{b}}\,(\underline{\mathbf{a}} \cdot \underline{\mathbf{a}})) =$$

$$= \underline{\mathbf{c}} \times \underline{\mathbf{a}}\,(\underline{\mathbf{a}} \cdot \underline{\mathbf{b}}) - \underline{\mathbf{c}} \times \underline{\mathbf{b}}\,\|\underline{\mathbf{a}}\|^2$$

$$= \underline{\mathbf{a}} \times \underline{\mathbf{D}} \cdot \underline{\mathbf{a}} - \underline{\mathbf{c}} \times \underline{\mathbf{b}}\,\|\underline{\mathbf{a}}\|^2 \qquad \text{(A-7)}$$

where identities (A-6a) and (A-6b) were used, $\|\cdot\|$ denotes the norm of a vector and again, $\underline{\mathbf{D}} = (\underline{\mathbf{c}} \cdot \underline{\mathbf{b}})\underline{\mathbf{1}} - \underline{\mathbf{c}}\,\underline{\mathbf{b}}$. Finally, another useful identity is provided below without proof:

$$(\underline{\mathbf{a}} \times \underline{\mathbf{b}}) \cdot (\underline{\mathbf{c}} \times \underline{\mathbf{d}}) = (\underline{\mathbf{a}} \cdot \underline{\mathbf{c}})(\underline{\mathbf{b}} \cdot \underline{\mathbf{d}}) - (\underline{\mathbf{a}} \cdot \underline{\mathbf{d}})(\underline{\mathbf{b}} \cdot \underline{\mathbf{c}}) \qquad \text{(A-8a)}$$

$$= \underline{\mathbf{a}} \cdot ((\underline{\mathbf{d}} \cdot \underline{\mathbf{b}})\underline{\mathbf{1}} - \underline{\mathbf{d}}\,\underline{\mathbf{b}}) \cdot \underline{\mathbf{c}} \qquad \text{(A-8b)}$$

Appendix B: Matrix Operations

When one writes matrix equations, physical vectors are expressed as column vectors whose components are the projections of the physical vector on the selected frame of reference. Similarly, dyadics correspond to matrices and that is another reason for their usefulness (besides the fact that result in more compact notation). The identities that follow are very useful in establishing the connection between physical vectors and dyadics with vectors and matrices and are needed when one writes matrix equations. Unless otherwise noted, all vectors are expressed in the same reference frame. The components of a vector a in some reference frame are a_x, a_y, and a_z.

B.1 The dot product $\underline{c} = \underline{a} \cdot \underline{b}$ is written as:

$$\mathbf{c} = \mathbf{a}^T \mathbf{b} = \mathbf{b}^T \mathbf{a} \tag{B-1}$$

B.2 The cross product $\underline{c} = \underline{a} \times \underline{b}$ is written as:

$$\mathbf{c} = \mathbf{a}^\times \mathbf{b} = -\mathbf{b}^\times \mathbf{a} \tag{B-2}$$

where the symbol $(\bullet)^\times$ denotes the construction of a skew-symmetric matrix from the components of $(\bullet)$, according to the following:

$$\mathbf{a}^\times = \begin{bmatrix} 0 & -a_z & a_y \\ a_z & 0 & -a_x \\ -a_y & a_x & 0 \end{bmatrix} \tag{B-3}$$

Some useful properties are the following:

$$(\mathbf{a}^\times)^T = -\mathbf{a}^\times \tag{B-4}$$

$$\mathbf{a}^\times \mathbf{a} = \mathbf{0} \tag{B-5}$$

B.3 The scalar quantity, $T = \underline{a} \cdot \underline{D} \cdot \underline{b}$ is written as:

$$T = \mathbf{a}^T \mathbf{D} \mathbf{b} \tag{B-6}$$

B.4 The double cross product $\underline{p} = \underline{a} \times (\underline{b} \times \underline{c})$, is written as:

$$\begin{aligned} \mathbf{p} &= \mathbf{a}^\times \mathbf{b}^\times \mathbf{c} \\ &= (-\mathbf{a}^\times \mathbf{c}^\times)\,\mathbf{b} = (\mathbf{a}^\times \mathbf{c}^{\times T})\,\mathbf{b} \\ &= \mathbf{D}\,\mathbf{b} \end{aligned} \tag{B-7}$$

B.5 Equation (B-7) provides the means to find the matrix that corresponds to a dyadic. Compare Equations (A-4) and (A-5) to Equation (B-7). Obviously, **D** is given by:

$$\mathbf{D} = -\mathbf{a}^\times \mathbf{c}^\times = \mathbf{c}^T\mathbf{a}\mathbf{1} - \mathbf{c}\mathbf{a}^T \tag{B-8a}$$

$$\mathbf{D} = \begin{bmatrix} a_z c_z + a_y c_y & -a_y c_x & -a_z c_x \\ -a_x c_y & a_x c_x + a_z c_z & -a_z c_y \\ -a_x c_z & -a_y c_z & a_y c_y + a_x c_x \end{bmatrix} \tag{B-8b}$$

Note that if **a** = **c**, the above corresponds to a translation by **a** used in Steiner's theorem; otherwise, it can be thought of as a "mixed translation" matrix. One must be careful to express both vectors **a** and **c** in the same frame of reference. This introduces the next set of properties.

B.6 Transformations of vectors and inertia matrices. Two frames of reference are considered in this section. A left superscript (^{0}) denotes the 0 frame, and a missing superscript denotes the "inertial" frame. $\mathbf{T}_0$ transforms a vector given in the 0^{th} frame to the inertial frame. The following properties are given without proof:

$$\mathbf{a} = \mathbf{T}_0\, {}^0\mathbf{a} \tag{B-9}$$

$$\mathbf{a}^\times = (\mathbf{T}_0\, {}^0\mathbf{a})^\times = \mathbf{T}_0\, {}^0\mathbf{a}^\times\, \mathbf{T}_0^T \tag{B-10}$$

$$D = T_0 \, {}^0D \, T_0^T \tag{B-11}$$

As noted earlier, both vectors that are used in forming an inertia matrices D must be expressed in the same frame. Otherwise, one of the two vectors must be first expressed in the other's frame and then a matrix can be formed according to the following identity:

$$D = - a^{\times} c^{\times} = - T_0 ({}^0a^{\times}) \, {}^0A_1 \, ({}^1c^{\times}) \, T_1^T \tag{B-12a}$$

where ${}^0A_1$ transforms a vector given in frame 1 to the 0^{th} frame, and $T_1 = T_0 \, {}^0A_1$. Sometimes it is useful to express a mixed inertia matrix in the frame of one of the vectors. This can be achieved by the following identity:

$${}^0D = - {}^0a^{\times} \, ({}^0A_1 \, {}^1c^{\times} \, {}^0A_1^T) \tag{B-13}$$

B.7 Time derivatives of the transformation matrix T_0. This is given by:

$$\dot{T}_0 = \omega^{\times} T_0 = T_0 \, {}^0\omega^{\times} \tag{B-14}$$

B.8 Partial derivatives of quadratic terms:

$$\frac{\partial}{\partial x} (x^T A y) = A y \tag{B-15}$$

$$\frac{\partial}{\partial y} (x^T A y) = A^T x \tag{B-16}$$

In particular if A is symmetric, then:

$$\frac{\partial}{\partial x} (x^T A x) = 2 A x \tag{B-17}$$

Appendix C: An Expression for $\underline{\rho}_k$

The system of N+1 vectorial equations in N+1 unknown vectors $\underline{\rho}_k$ as given by Equations (C-1) and (C-2) is solved here:

$$\underline{\rho}_k - \underline{\rho}_{k-1} = \underline{r}_{k-1} - \underline{l}_k \qquad k = 1,...,N \qquad \text{(C-1)}$$

$$\sum_{k=0}^{N} m_k \underline{\rho}_k = 0 \qquad \text{(C-2)}$$

From Equation (C-1):

$$\underline{\rho}_k = \underline{\rho}_{k-1} + \underline{r}_{k-1} - \underline{l}_k \qquad k = 1,...,N \qquad \text{(C-3)}$$

Writing Equation (C-3) for k=1 to k=k and adding up the k equations, yields $\underline{\rho}_k$ as a function of $\underline{\rho}_0$:

$$\underline{\rho}_k = \underline{\rho}_0 + \sum_{j=1}^{k} (\underline{r}_{j-1} - \underline{l}_j) \qquad i = 1,...,N \qquad \text{(C-3)}$$

Equation (C-3) is substituted in Equation (C-2) which yields:

$$M\underline{\rho}_0 + \sum_{i=0}^{N} m_i \sum_{j=1}^{i} (\underline{r}_{j-1} - \underline{l}_j) = 0 \qquad \text{(C-4)}$$

Solving Equation (C-4) for $\underline{\rho}_0$ and using a sum property results in:

$$\underline{\rho}_0 = -\sum_{i=0}^{N} \frac{m_i}{M} \sum_{j=1}^{i} (\underline{r}_{j-1} - \underline{l}_j)$$

$$= -\sum_{i=1}^{N} (\underline{r}_{i-1} - \underline{l}_i) \sum_{j=i}^{N} \frac{m_j}{M}$$

$$= -\sum_{i=1}^{N} (\underline{r}_{i-1} - \underline{l}_i)(1-\mu_i) \qquad \text{(C-5)}$$

Parameter μ_i is defined by Equation (2-6). The sum in Equation (C-5) is broken at i=k and then it is substituted in Equation (C-3) to yield:

$$\underline{\rho}_k = \sum_{i=1}^{k} (\underline{r}_{i-1} - \underline{l}_i)\,\mu_i - \sum_{i=k+1}^{N} (\underline{r}_{i-1} - \underline{l}_i)(1-\mu_i) \qquad k = 0,\ldots,N \qquad \text{(C-6)}$$

If k=0, the first sum in Equation (C-6) is zero and the result is identical to Equation (C-5). Equation (C-6) is repeated in Chapter 2 as Equation (2-4). Equation (C-6) is not in its most useful form because the sums contain vectors fixed in body i-1 and i. It is preferable to cluster all vectors fixed in the same body in one term. This results is the following:

$$\underline{\rho}_0 = -\underline{r}_0(1-\mu_1) - \sum_{i=1}^{N-1} \{\underline{r}_i(1-\mu_{i+1}) - \underline{l}_i(1-\mu_i)\} + \underline{l}_N(1-\mu_N) \qquad \text{(C-6a)}$$

$$\underline{\rho}_k = \underline{r}_0\mu_1 + \sum_{i=1}^{k-1} \{\underline{r}_i\mu_{i+1} - \underline{l}_i\mu_i\} - \{\underline{r}_k(1-\mu_{k+1}) + \underline{l}_k\mu_k\} - \sum_{i=k+1}^{N-1} \{\underline{r}_i(1-\mu_{i+1}) - \underline{l}_i(1-\mu_i)\} + \underline{l}_N(1-\mu_N) \qquad k = 1,\ldots,N-1 \qquad \text{(C-6b)}$$

$$\underline{\rho}_N = \underline{r}_0\mu_1 + \sum_{i=1}^{N-1} \{\underline{r}_i\mu_{i+1} - \underline{l}_i\mu_i\} - \underline{l}_N\mu_N \qquad \text{(C-6c)}$$

Using the definition of the vector $\underline{c}_i$, given by Equation (2-6), it is easy to see that:

$$\underline{c}_i = \underline{l}_i\mu_i + \underline{r}_i(1-\mu_{i+1}) \qquad i = 0,\ldots,N$$

$$= \underline{l}_i - \underline{l}_i (1-\mu_i) + \underline{r}_i (1-\mu_{i+1}) \qquad i = 0,...,N$$

$$= \underline{r}_i + \underline{l}_i \mu_i - \underline{r}_i \mu_{i+1} \qquad i = 0,...,N \qquad \text{(C-7)}$$

Equations (C-6) can be simplified using Equations (C-7) and result in the very compact form given as Equation (2-11).

Appendix D: Derivations Involving $\underline{h}$

D.1 A USEFUL PROPERTY

Consider the sum S of mass-weighted brackets:

$$S = \sum_{k=0}^{N} m_k \left[\underline{v}_{jk}, \underline{v}_{ik}\right] \tag{D-1}$$

where the symbol [•,•] represents an ordered pair of the vectors $\underline{v}_{ik}$, $\underline{v}_{jk}$. For example, such an ordered pair is the cross product $\underline{v}_{jk}\times\underline{v}_{ik}$, or the dyadic $\{(\underline{v}_{jk} \cdot \underline{v}_{ik})\,\underline{1} - \underline{v}_{jk}\underline{v}_{ik}\}$. Since the vectors $\underline{v}_{jk}$ are equal to a specific vector according to Equation (2-10), it makes sense to examine if this sum can be simplified. Such simplification can indeed result by breaking S in five pieces, as the index k takes the values (0...i-1), i, (i+1...j-1), j, (j+1...N), where it is assumed that i<j. For simplicity, set:

$$\hat{\mu}_1 = M\,\mu_i$$

$$\hat{\mu}_2 = M\,(\mu_{i+1} - \mu_i) = m_i$$

$$\hat{\mu}_3 = M\,(\mu_j - \mu_{i+1})$$

$$\hat{\mu}_4 = M\,(\mu_{j+1} - \mu_j) = m_j$$

$$\hat{\mu}_5 = M\,(1 - \mu_{j+1}) \tag{D-2}$$

$$\hat{\mu}_1 + \hat{\mu}_2 + \hat{\mu}_3 + \hat{\mu}_4 + \hat{\mu}_5 = M \tag{D-3}$$

Equation (D-3) results by adding up expressions (D-2). Using the $\hat{\mu}_i$'s, Equation (2-7) can be rewritten in the following two equivalent forms:

$$\hat{\mu}_1\,\underline{1}_i^* + \hat{\mu}_2\,\underline{c}_i^* + (\hat{\mu}_3 + \hat{\mu}_4 + \hat{\mu}_5)\,\underline{r}_i^* = 0 \tag{D-4}$$

$$\hat{\mu}_1\left[\underline{1}_j^*, \underline{1}_i^*\right] + \hat{\mu}_2\left[\underline{1}_j^*, \underline{c}_i^*\right] + (\hat{\mu}_3 + \hat{\mu}_4 + \hat{\mu}_5)\left[\underline{1}_j^*, \underline{r}_i^*\right] = 0 \tag{D-5}$$

where Equation (D-5) is obtained from Equation (D-4) by forming brackets with $\underline{l}_j^*$ from the left. Similarly, Equation (2-7) written for body j can be transformed to:

$$(\hat{\mu}_1 + \hat{\mu}_2 + \hat{\mu}_3)\,[\underline{l}_j^*, \underline{r}_i^*] + \hat{\mu}_4\,[\underline{c}_j^*, \underline{r}_i^*] + \hat{\mu}_5\,[\underline{r}_j^*, \underline{r}_i^*] = 0 \qquad \text{(D-6)}$$

Finally, the sum S is written as (i<j):

$$S = \hat{\mu}_1\,[\underline{l}_j^*, \underline{l}_i^*] + \hat{\mu}_2\,[\underline{l}_j^*, \underline{c}_i^*] + \hat{\mu}_3\,[\underline{l}_j^*, \underline{r}_i^*] + \hat{\mu}_4\,[\underline{c}_j^*, \underline{r}_i^*] + \hat{\mu}_5\,[\underline{r}_j^*, \underline{r}_i^*] \qquad \text{(D-7)}$$

Subtracting Equations (D-5) and (D-6) from Equation (D-7) we find that:

$$S = -M\,[\underline{l}_j^*, \underline{r}_i^*] \qquad i<j \qquad \text{(D-8a)}$$

This is a very rewarding result, because it saves someone from many sin() and cos() manipulations in deriving equations. Similarly, if i>j, S is given by:

$$S = -M\,[\underline{r}_j^*, \underline{l}_i^*] \qquad i>j \qquad \text{(D-8b)}$$

The last case that remains is when i=j. It is easy to see that in such a case:

$$S = \mu_i\,M[\underline{l}_i^*, \underline{l}_i^*] + m_i[\underline{c}_i^*, \underline{c}_i^*] + (1-\mu_{i+1})M[\underline{r}_i^*, \underline{r}_i^*] \qquad i=j \qquad \text{(D-8c)}$$

If the [•] represents a cross product, then S is obviously zero for i=j.

D.2 SIMPLIFICATION OF THE EXPRESSION FOR $\underline{h}$.

Using property (A-5), the double cross products in Equation (2-42) can be written in the following compact form:

$$\underline{h}_{cm} = \sum_{j=0}^{N} \sum_{i=0}^{N} \sum_{k=0}^{N} \underline{D}_{ijk} \bullet \underline{\omega}_j \qquad \text{(D-9)}$$

where:

$$\underline{D}_{ijk} = \underline{I}_i\,\delta_{ij}\delta_{jk} + m_k\,\{(\underline{v}_{jk} \bullet \underline{v}_{ik})\,\underline{1} - \underline{v}_{jk}\underline{v}_{ik}\} \qquad i, j, k = 0,\ldots,N \qquad \text{(D-10)}$$

The dyadics $\underline{\mathbf{D}}_{ijk}$ are functions of the distribution of inertia through the system and are formed from the barycentric vectors $\underline{\mathbf{v}}_{ik}$. The terms δ_{ij}, δ_{jk} are Kronecker deltas. The summation over k in Equation (D-8) can be eliminated using the useful property proved in section D.1. Indeed, setting the brackets in Equation (D-1) equal to the dyadic $\{(\underline{\mathbf{v}}_{jk} \cdot \underline{\mathbf{v}}_{ik})\ \underline{\mathbf{1}} - \underline{\mathbf{v}}_{jk}\underline{\mathbf{v}}_{ik}\}$ and applying Equation (D-8), $\underline{\mathbf{h}}_{cm}$ is written as:

$$\underline{\mathbf{h}}_{cm} = \sum_{j=0}^{N} \sum_{i=0}^{N} \underline{\mathbf{D}}_{ij} \cdot \underline{\omega}_j \tag{D-11}$$

where the dyadic $\underline{\mathbf{D}}_{ij}$ is given by:

$$\underline{\mathbf{D}}_{ij} = -M\{(\underline{\mathbf{l}}_j^* \cdot \underline{\mathbf{r}}_i^*)\ \underline{\mathbf{1}} - \underline{\mathbf{l}}_j^*\ \underline{\mathbf{r}}_i^*\} \qquad i<j \tag{D-12a}$$

$$\underline{\mathbf{D}}_{ii} = \underline{\mathbf{I}}_i + (m_0+\ldots+m_{i-1})\{\|\underline{\mathbf{l}}_i^*\|^2\underline{\mathbf{1}} - \underline{\mathbf{l}}_i^*\ \underline{\mathbf{l}}_i^*\} + \\ + m_i\{\|\underline{\mathbf{c}}_i^*\|^2\underline{\mathbf{1}} - \underline{\mathbf{c}}_i^*\ \underline{\mathbf{c}}_i^*\} + \\ + (m_i+\ldots+m_N)\{\|\underline{\mathbf{r}}_i^*\|^2\underline{\mathbf{1}} - \underline{\mathbf{r}}_i^*\ \underline{\mathbf{r}}_i^*\} \qquad i=j \tag{D-12b}$$

$$\underline{\mathbf{D}}_{ij} = -M\{(\underline{\mathbf{r}}_j^* \cdot \underline{\mathbf{l}}_i^*)\ \underline{\mathbf{1}} - \underline{\mathbf{r}}_j^*\ \underline{\mathbf{l}}_i^*\} \qquad i>j \tag{D-12c}$$

where $\underline{\mathbf{1}}$ is the unit dyadic. $\underline{\mathbf{D}}_{ii}$ appears in the derivation of the Newton-Euler equations of multibody systems and was called the inertia dyadic of the i^{th} augmented body by [29]. Indeed, $\underline{\mathbf{I}}_i + m_i\{\|\underline{\mathbf{c}}_i^*\|^2\underline{\mathbf{1}} - \underline{\mathbf{c}}_i^*\ \underline{\mathbf{c}}_i^*\}$ is the inertia of body i calculated with respect to its barycenter (parallel-axes theorem), etc. No $\underline{\mathbf{D}}_{ij}$ ($i\neq j$) were defined in [29].

D.3 TIME DERIVATIVE OF $\underline{\mathbf{h}}$.

First, the time derivative of $\underline{\mathbf{r}}_{cm} \times \underline{\mathbf{p}}$ is written using Fquations (2-38) and (2-37) as:

$$\frac{d}{dt}(\underline{\mathbf{r}}_{cm} \times \underline{\mathbf{p}}) = \underline{\mathbf{r}}_{cm} \times \underline{\mathbf{f}}_{ext} \tag{D-13}$$

The system angular momentum about the CM, given by Equation (2-42) is repeated here:

$$\underline{h}_{cm} = \sum_{k=0}^{N} \underline{I}_k \cdot \underline{\omega}_k + \sum_{j=0}^{N} \sum_{i=0}^{N} \sum_{k=0}^{N} m_k \underline{v}_{ik} \times \underline{\omega}_j \times \underline{v}_{jk} \qquad \text{(D-14)}$$

Recalling that $\underline{v}_{jk}$ is a body-fixed vector of body i, the time derivative of $\underline{h}_{cm}$ is written as:

$$\begin{aligned} \dot{\underline{h}}_{cm} = & \sum_{k=0}^{N} \underline{I}_k \cdot \dot{\underline{\omega}}_k + \sum_{k=0}^{N} \underline{\omega}_k \times \underline{I}_k \cdot \underline{\omega}_k + \\ & + \sum_{j=0}^{N} \sum_{i=0}^{N} \sum_{k=0}^{N} m_k \underline{v}_{ik} \times \dot{\underline{\omega}}_j \times \underline{v}_{jk} \\ & + \sum_{j=0}^{N} \sum_{i=0}^{N} \sum_{k=0}^{N} m_k \underline{v}_{ik} \times \underline{\omega}_j \times \underline{\omega}_j \times \underline{v}_{jk} \end{aligned} \qquad \text{(D-15)}$$

Using property (A-4), the first and second sums can be combined using the definition of the $\underline{D}_{ij}$ inertia matrices, see the previous section. Similarly, using property (A-7), the second and fourth sums can be combined. The result follows:

$$\begin{aligned} \dot{\underline{h}}_{cm} = & \sum_{j=0}^{N} \sum_{i=0}^{N} \underline{D}_{ij} \cdot \dot{\underline{\omega}}_j + \\ & + \sum_{j=0}^{N} \sum_{i=0}^{N} \underline{\omega}_j \times \underline{D}_{ji} \cdot \underline{\omega}_j + \\ & + \sum_{j=0}^{N} \sum_{i=0}^{N} \|\dot{\underline{\omega}}_j\|^2 \sum_{i=0}^{k} m_k \underline{v}_{jk} \times \underline{v}_{ik} \end{aligned} \qquad \text{(D-16)}$$

The last sum can be simplified using the summation property, see section D.1., where the [•,•] is now interpreted as a cross product. The result is given as Equation (2-45).

D.4 NON-INTEGRABILITY OF THE ANGULAR MOMENTUM EQUATION

This section investigates with the possibility of integrating the conservation of angular momentum equation to yield a spacecraft's orientation as a function of the manipulator's

joint angles and possibly of time, see Equation (3-5). In general, this is a difficult problem and the interested reader is referred to [54]. Here, the non-integrability of the conservation of angular momentum is demonstrated via two examples.

To do this, the following theorem will be used, see [35]. Consider the Pfaffian equation:

$$A\,dx + B\,dy + C\,dz = 0 \tag{D-17}$$

This equation can be integrated and result in an equation of the form f(x,y,z) = 0, iff the following condition is true:

$$A\left\{\frac{\partial B}{\partial z} - \frac{\partial C}{\partial y}\right\} + B\left\{\frac{\partial C}{\partial x} - \frac{\partial A}{\partial z}\right\} + C\left\{\frac{\partial A}{\partial y} - \frac{\partial B}{\partial x}\right\} = 0 \tag{D-18}$$

Example 1. Now consider the one DOF example used in section 2.5.1. The conservation of angular momentum for this system, see Equation (2-49), yields the following:

$$D(q)\dot{\theta} + D_q(q)\dot{q} = h_0 \tag{D-19}$$

where D(q) and $D_q(q)$ are explicitly given in Appendix E, Eq.(E-5). The above can be written as:

$$D(q)d\theta + D_q(q)dq - h_0 dt = 0 \tag{D-20}$$

where time t is considered to be one of the variables. In order for Equation (D-20) to be integrable, condition (D-18) must hold, with A=D(q), B=D_q(q), C=h_0 and (x,y,z) = (θ,q,t). After going through the algebra, condition (D-18) results in the requirement that $\mu r_0 l_1 \sin(q) h_0$ be identically equal to zero. Assuming that r_0 and l_1 are not zero, see Figure 2.5, there is only one possibility for this to hold: h_0 must be zero, or in other words, the (constant) system angular momentum must be zero. In such a case, the variables in

Equation (D-20) can be separated and using indefinite integral properties, see [35, p.957], the following result can be obtained:

$$\theta = \theta_0 + (q-q_0)/2 + E\left\{\tan^{-1}(F\tan(q/2)) - \tan^{-1}(F\tan(q_0/2))\right\} \qquad \text{(D-21)}$$

where:

$$A = I_0 + I_1 + \mu(r_0^2 + l_1^2) \qquad B = I_1 + \mu l_1^2 \qquad \text{(D-22a)}$$

$$C = \mu r_0 l_1 \cos(q) \qquad \mu = \frac{m_0 m_1}{M} \qquad \text{(D-22b)}$$

$$E = \frac{2B - A}{(A^2 - 4C^2)^{1/2}} \qquad F = \frac{A - 2C}{(A^2 - 4C^2)^{1/2}} \qquad \text{(D-22c)}$$

As a numerical example, assume that the system mass and geometry properties are the ones given in Table II, and let $q_0 = \theta_0 = 0°$. Then, the resulting final θ that corresponds to a final $q=45°$ is equal to -8.8657°; that is the spacecraft rotates clockwise and results in a final attitude that is a function of the final *joint angle* q. Using Eq. (D-21), θ can be completely eliminated from the kinematics and dynamics of the system. This is the only non-trivial case where the angular momentum equation can be integrated.

Table V. Parameters for a one DOF manipulator system.

Body	l_i (m)	r_i (m)	m_i (Kg)	I_i (Kg m^2)
0	.5	.5	40	6.667
1	.5	.5	4	0.333

Example 2. Consider next the two DOF example of section 2.5.2. Assuming a system initially at rest and using Equation (2-49), the angular momentum is written as:

$$D(q_1,q_2)\dot{\theta} + \{D_1(q_1,q_2)+D_2(q_1,q_2)\}\,\dot{q}_1 + D_2(q_1,q_2)\,\dot{q}_2 = 0 \qquad \text{(D-23)}$$

where D, D_1, and D_2 are defined by Eqs. (E-24). The above is again a Pfafian of the form (D-17). Hence, in order to be able to obtain a function of the form $f(\theta,q_1,q_2)=0$, the integrability condition (D-18) must hold. This holds iff the following conditions are simultaneously satisfied:

$$d_{00}\tilde{d}_{12} = \tilde{d}_{20}\tilde{d}_{10} \tag{D-24a}$$

$$d_{11}\tilde{d}_{20} = \tilde{d}_{12}\tilde{d}_{10} \tag{D-24b}$$

$$d_{22}\tilde{d}_{10} = \tilde{d}_{20}\tilde{d}_{12} \tag{D-24c}$$

where $\tilde{d}_{ij}$ is equal to d_{ij}, given by Equation (E-22), but without the cos(•) terms. These can only be satisfied if $m_2 = 0$ and $I_2 = 0$. But then, the three-body system reduces to a two-body one, a case proven to be integrable. The conclusion is that there is no nontrivial three-body system for which the angular momentum can be integrated once more.

Appendix E: Example derivations

E.1 A ONE DOF MANIPULATOR EXAMPLE

In this section, the equations of motion for a one link manipulator will be derived, in order to demonstrate the theoretical analysis presented in Chapter 2. The system has four DOF. Three DOF are due to the spacecraft and a one DOF to the manipulator. Obviously, for this example, N=1.

1. Preliminary quantities. The first step is to calculate the barycentric vectors, according to Equations (2-7) and (2-8). The center of mass of an individual link is assumed to be on the line connecting the two joints, so only the x-components of all vectors in the i^{th} frame are non-zero. The left superscripts denoting the i^{th} frame are dropped for simplicity, see also Figure 2.4.

$$
\begin{aligned}
r_0^* &= \frac{1}{M} r_0 m_0 \\
c_0^* &= -\frac{1}{M} r_0 m_1 \\
l_0^* &= -\frac{1}{M} r_0 m_1 - l_0 \\
r_1^* &= \frac{1}{M} l_1 m_0 + r_1 \\
c_1^* &= \frac{1}{M} l_1 m_0 \\
l_1^* &= -\frac{1}{M} l_1 m_1 \qquad \text{(E-1)}
\end{aligned}
$$

$$
M = m_0 + m_1 \qquad \text{(E-2)}
$$

where M is the total system mass. For simplicity set:

$$
\alpha \equiv {}^0v_{0N,E} = r_0^* \qquad \text{(E-3a)}
$$

$$
\beta \equiv {}^1v_{1N,E} = c_1^* + r_1 \qquad \text{(E-3b)}
$$

T_0 is given by Equation (2-21) with $\mathbf{a} = [0, 0, 1]^T$ and ${}^1T_0$ by Equation (2-20b):

$$T_0(\theta) = \text{Rot}(\theta) = \begin{bmatrix} \cos(\theta) & -\sin(\theta) \\ \sin(\theta) & \cos(\theta) \end{bmatrix} \tag{E-4a}$$

$${}^1T_0(q) = \text{Rot}(q) \tag{E-4b}$$

There is just one F_i matrix, which in this case reduces to a scalar, $F_1 = 1$. The inertia terms are found using Equation (2-64) and (E-1). Only the inertia components corresponding to rotations around an axis perpendicular to the plane of motion are of interest:

$$d_{00} = I_0 + \mu r_0^2 \tag{E-5a}$$

$$d_{01} = \mu r_0 l_1 \cos(q) = d_{10} \tag{E-5b}$$

$$d_{11} = I_1 + \mu l_1^2 = D_{qq} \tag{E-5c}$$

$$\mu = \frac{m_0 m_1}{M} \tag{E-5d}$$

where μ is the system reduced mass. From Equation (2-68):

$$\hat{d}_{01} = \mu r_0 l_1 \sin(q) = -\hat{d}_{10} \tag{E-6}$$

The definitions (2-75) result in the following:

$$D = d_{00} + 2\, d_{01} + d_{11} \tag{E-7a}$$

$$D_q = d_{01} + d_{11} \tag{E-7b}$$

$$D_{qq} = d_{11} \tag{E-7c}$$

2. Kinematics. The end-effector position and the end-effector orientation are written as, see also Equation (2-22):

$$x_E = x_{cm} + \alpha \cos(\theta) + \beta \cos(\theta+q) \tag{E-8a}$$

$$y_E = y_{cm} + \alpha \sin(\theta) + \beta \sin(\theta+q) \tag{E-8b}$$

$$\theta_E = \theta+q_1 \tag{E-8c}$$

In this case, the end-effector orientation is trivially written. In the general case, it can be described by the orientation matrix T_i.

3. Differential kinematics. The submatrices that make up the Jacobian J^+ are found as functions of the above barycentric vectors using Equations (2-33):

$$^0J_{11} = \begin{bmatrix} -\beta s \\ \alpha+\beta c \end{bmatrix} \qquad ^0J_{12} = \begin{bmatrix} -\beta s \\ \beta c \end{bmatrix} \qquad ^0J_{22} = F_1 = 1 \tag{E-9}$$

The end-effector Jacobian is assembled according to Equations (2-35):

$$^0J^+(q) = \begin{bmatrix} 1 & 0 & -\beta s & -\beta s \\ 0 & 1 & \alpha+\beta c & \beta c \\ 0 & 0 & 1 & 1 \end{bmatrix} \tag{E-10a}$$

$$J^+(\theta, q) = \begin{bmatrix} \cos(\theta) & -\sin(\theta) & 0 \\ \sin(\theta) & \cos(\theta) & 0 \\ 0 & 0 & 1 \end{bmatrix} {}^0J^+(q) \tag{E-10b}$$

where the matrix multiplying $^0J^+(q)$ in the above, is the term $\text{diag}(T_0, T_0)$ for planar systems, see Equation (2-35a). Note that the rank of $J^+(\theta, q)$ is always three, which means that if the spacecraft DOF are used, any point on the plane can be reached with any end-effector orientation. The differential kinematics for the motion of the manipulator end-effector are written as follows:

$$\dot{x} = \begin{bmatrix} \dot{x}_E \\ \dot{y}_E \\ \dot{\theta}_E \end{bmatrix} = J^{+} \begin{bmatrix} \dot{x}_{cm} \\ \dot{y}_{cm} \\ \dot{\theta} \\ \dot{q} \end{bmatrix} \tag{E-11}$$

4. Dynamics. Only a force f_E and a torque n_E acting at the manipulator tip will be considered here. Any other forces or torques can be taken into account in a similar way. The force f_E is assumed to be of constant direction in inertial space and its components are $f_{x,E}$, $f_{y,E}$. Obviously, in the planar case n_E is equal to ${}^0n_E$. The generalized forces are found using Equations (2-61):

$$\begin{bmatrix} Q_x \\ Q_y \end{bmatrix} = T_0^T \begin{bmatrix} f_{x.E} \\ f_{y.E} \end{bmatrix} \tag{E-12a}$$

$$Q_\theta = n_E + (T_0 {}^0J_{11})^T \begin{bmatrix} f_{x.E} \\ f_{y.E} \end{bmatrix} \tag{E-12b}$$

$$Q_q = \tau + n_E + (T_0 {}^0J_{12})^T \begin{bmatrix} f_{x.E} \\ f_{y.E} \end{bmatrix} \tag{E-12c}$$

The equations of motion describing rotations are written using Eqs. (2-75) through (2-78):

$$M\,{}^0\ddot{x}_{cm} = Q_x \tag{E-13a}$$

$$M\,{}^0\ddot{y}_{cm} = Q_y \tag{E-13b}$$

$$D\ddot{\theta} + D_q\ddot{q} - (2\,\dot{\theta}\,\dot{q} + \dot{q}^2)\,\hat{d}_{01} = Q_\theta \tag{E-13c}$$

$$D_q\ddot{\theta} + D_{qq}\ddot{q} + \dot{\theta}^2\,\hat{d}_{01} = Q_q \tag{E-13d}$$

In matrix form, the equations of motion (see also Equations (2-78)), are written as:

$$H^+(q)\begin{bmatrix} \ddot{x}_{cm} \\ \ddot{y}_{cm} \\ \ddot{\theta} \\ \ddot{q} \end{bmatrix} + \begin{bmatrix} 0 \\ 0 \\ c_1^+ \\ c_2^+ \end{bmatrix} = \begin{bmatrix} 0 \\ 0 \\ 0 \\ \tau \end{bmatrix} + J^+(\theta,q)^T \begin{bmatrix} f_E \\ n_E \end{bmatrix} \tag{E-14}$$

where the inertia matrix, $H^+(q)$, and the nonlinear terms, C_1^+ and C_2^+, are given by:

$$H^+(q) = \begin{bmatrix} M & 0 & 0 & 0 \\ 0 & M & 0 & 0 \\ 0 & 0 & D(q) & D_q(q) \\ 0 & 0 & D_q(q) & D_{qq} \end{bmatrix} \tag{E-15}$$

$$C_1^+ = c_1^+ = -(2\,\dot{\theta}\,\dot{q} + \dot{q}^2)\,\hat{d}_{10} \tag{E-16a}$$

$$C_2^+ = c_2^+ = \dot{\theta}^2\,\hat{d}_{10} \tag{E-16b}$$

The above equations provide a complete description of a one DOF manipulator system.

E.2 A TWO DOF MANIPULATOR EXAMPLE

In this section, the basic equations describing a two DOF system on a 3 DOF spacecraft are derived.

1. Preliminary quantities. As in the previous example, r_i and l_i are assumed to be parallel to the x axis of the i^{th} frame. Hence, only the x-component of the barycentric vector ${}^iv_{ik}$ is non-zero and is found by using Equations (2-7) and (2-8), written in the i^{th} frame:

$$\begin{aligned} r_0^* &= \frac{1}{M} r_0 m_0 \\ c_0^* &= -\frac{1}{M} r_0 (m_1+m_2) \\ l_0^* &= -\frac{1}{M} r_0 (m_1+m_2) - l_0 \\ r_1^* &= \frac{1}{M}\left\{ r_1 (m_0+m_1) + l_1 m_0 \right\} \\ c_1^* &= \frac{1}{M} (l_1 m_0 - r_1 m_2) \end{aligned}$$

$$l_1^* = -\frac{1}{M}\left\{l_1(m_1+m_2)+r_1m_2\right\}$$
$$r_2^* = \frac{1}{M}l_2(m_0+m_1) + r_2$$
$$c_2^* = \frac{1}{M}l_2(m_0+m_1)$$
$$l_2^* = -\frac{1}{M}l_2m_2 \qquad \text{(E-17)}$$
$$M = m_0 + m_1 + m_2 \qquad \text{(E-18)}$$

where M is the total mass of the system. For simplicity, set:

$$\alpha \equiv {}^0v_{0N,E} = r_0^* \qquad \text{(E-19a)}$$
$$\beta \equiv {}^1v_{1N,E} = r_1^* \qquad \text{(E-19b)}$$
$$\gamma \equiv {}^2v_{2N,E} = c_2^* + r_2 \qquad \text{(E-19c)}$$
$$\delta \equiv {}^0v_{00,S} = c_0^* \qquad \text{(E-20a)}$$
$$\varepsilon \equiv {}^1v_{10,S} = l_1^* \qquad \text{(E-20b)}$$
$$\zeta \equiv {}^2v_{20,S} = l_2^* \qquad \text{(E-20c)}$$

T_0 is given by Equation (E-4a) and the ${}^0T_i$ are given by:

$${}^0T_1 = \mathrm{Rot}(q_1) \qquad \text{(E-21a)}$$
$${}^0T_2 = \mathrm{Rot}(q_1)\,\mathrm{Rot}(q_2) \qquad \text{(E-21b)}$$

The inertia terms d_{ij} and $\hat{d}_{ij}$ are found using Equations (2-64) and (2-68); their explicit form is given below. One should recall that these terms are functions of the barycentric vectors, so the required additions and multiplications are less than what they appear to be:

$$d_{00} = I_0 + \frac{m_0(m_1+m_2)}{M}r_0^2$$

$$d_{10} = \frac{m_0r_0}{M}\left\{l_1(m_1+m_2) + r_1m_2\right\}\cos(q_1) = d_{01}$$

$$d_{20} = \frac{m_0 m_2}{M} r_0 l_2 \cos(q_1+q_2) = d_{02}$$

$$d_{11} = I_1 + \frac{m_0 m_1}{M} l_1^2 + \frac{m_1 m_2}{M} r_1^2 + \frac{m_0 m_2}{M} (l_1+r_1)^2$$

$$d_{21} = \left\{ \frac{m_1 m_2}{M} r_1 l_2 + \frac{m_0 m_2}{M} l_2 (l_1+r_1) \right\} \cos(q_2) = d_{12}$$

$$d_{22} = I_2 + \frac{m_2(m_0+m_1)}{M} l_2^2 \qquad \text{(E-22)}$$

$$\hat{d}_{01} = \frac{m_0 r_0}{M} \left\{ l_1(m_1+m_2) + r_1 m_2 \right\} \sin(q_1) = -\hat{d}_{10}$$

$$\hat{d}_{02} = \frac{m_0 m_2}{M} r_0 l_2 \sin(q_1+q_2) = -\hat{d}_{20}$$

$$\hat{d}_{12} = \left\{ \frac{m_1 m_2}{M} r_1 l_2 + \frac{m_0 m_2}{M} l_2 (l_1+r_1) \right\} \sin(q_2) = -\hat{d}_{21} \qquad \text{(E-23)}$$

Dropping the left superscript (^{0}), the inertia sums defined by Equation (2-48) or (2-78) are:

$$D_j \equiv D_j = d_{0j} + d_{1j} + d_{2j} \qquad j = 0, 1, 2 \qquad \text{(E-24a)}$$

$$D \equiv D = D_0 + D_1 + D_2 \qquad \text{(E-24b)}$$

$$D_q \equiv [D_1+D_2 \quad D_2] \qquad \text{(E-24c)}$$

$$D_{qq} \equiv \begin{bmatrix} d_{11}+2d_{12}+d_{22} & d_{12}+d_{22} \\ d_{12}+d_{22} & d_{22} \end{bmatrix} \qquad \text{(E-24d)}$$

2. Kinematics. The end-effector position is found using Equation (2-22); in this case the end-effector orientation is trivial to write:

$$x_E = x_{cm} + \alpha \cos(\theta) + \beta \cos(\theta+q_1) + \gamma \cos(\theta+q_1+q_2) \qquad \text{(E-25a)}$$

$$y_E = y_{cm} + \alpha \sin(\theta) + \beta \sin(\theta+q_1) + \gamma \sin(\theta+q_1+q_2) \qquad \text{(E-25b)}$$

$$\theta_E = \theta+q_1+q_2 \qquad \text{(E-25c)}$$

3. Differential kinematics. The Jacobian submatrices in Equation (2-33) are given by:

$$ {}^0\mathbf{J}_{11} = \begin{bmatrix} -\beta s_1 - \gamma s_{12} \\ \alpha + \beta c_1 + \gamma c_{12} \end{bmatrix} \quad {}^0\mathbf{J}_{12} = \begin{bmatrix} -\beta s_1 - \gamma s_{12} & -\gamma s_{12} \\ \beta c_1 + \gamma c_{12} & \gamma c_{12} \end{bmatrix} \quad {}^0\mathbf{J}_{22} = [1 \quad 1] \quad \text{(E-26)} $$

where $s_1 \equiv \sin(q_1)$, $c_{12} \equiv \cos(q_1+q_2)$ etc. The Jacobian $\mathbf{J}^+$ relating the end-effector motion to the controlled velocities is written using Equations (2-35):

$$ {}^0\mathbf{J}^+(q) = \begin{bmatrix} 1 & 0 & -\beta s_1 - \gamma s_{12} & -\beta s_1 - \gamma s_{12} & -\gamma s_{12} \\ 0 & 1 & \alpha + \beta c_1 + \gamma c_{12} & \beta c_1 + \gamma c_{12} & \gamma c_{12} \\ 0 & 0 & 1 & 1 & 1 \end{bmatrix} \quad \text{(E-27a)} $$

$$ \mathbf{J}^+(\theta, q) = \begin{bmatrix} \cos(\theta) & -\sin(\theta) & 0 \\ \sin(\theta) & \cos(\theta) & 0 \\ 0 & 0 & 1 \end{bmatrix} {}^0\mathbf{J}^+(q) \quad \text{(E-27b)} $$

In this case, it is desired to examine the effect of forces and torques acting on the spacecraft, due to jet actuators or momentum wheels. In addition to the end-effector Jacobian, one must use a Jacobian written for the spacecraft CM. To this end, the Jacobian given by Equations (2-28) and (2-30) with k=0 and m=CM is required. For simplicity, ${}^0\mathbf{J}_{12,S}$ is used instead of ${}^0\mathbf{J}_{120,cm}$, etc.

$$ {}^0\mathbf{J}_{11,S} = \begin{bmatrix} -\varepsilon s_1 - \zeta s_{12} \\ \delta + \varepsilon c_1 + \zeta c_{12} \end{bmatrix} \quad {}^0\mathbf{J}_{12,S} = \begin{bmatrix} -\varepsilon s_1 - \zeta s_{12} & -\zeta s_{12} \\ \varepsilon c_1 + \zeta c_{12} & \zeta c_{12} \end{bmatrix} \quad {}^0\mathbf{J}_{22,S} = [0 \quad 0] \quad \text{(E-28)} $$

The Jacobian ${}^0\mathbf{J}_S^+$ relating the end-effector motion to the controlled velocities is written using Equations (2-30):

$$ {}^0J_S^+(q) = \begin{bmatrix} 1 & 0 & -\varepsilon s_1 - \zeta s_{12} & -\varepsilon s_1 - \zeta s_{12} & -\zeta s_{12} \\ 0 & 1 & \delta + \varepsilon c_1 + \zeta c_{12} & \varepsilon c_1 + \zeta c_{12} & \gamma c_{12} \\ 0 & 0 & 1 & 0 & 0 \end{bmatrix} \tag{E-29} $$

4. Dynamics. In this case it is assumed that a force f_E and a torque n_E (both fixed in inertial space) are applied at the manipulator end-effector. Also, a force ${}^0f_S$ and a torque ${}^0n_S$ are applied to the center of mass of the spacecraft and are defined in the spacecraft frame; these are due to the spacecraft jet actuators. The generalized forces are written below using Equations (2-61):

$$ Q_x = {}^0f_{x,S} + \cos(\theta) f_{x,E} + \sin(\theta) f_{y,E} \tag{E-30a} $$

$$ Q_y = {}^0f_{y,S} - \sin(\theta) f_{x,E} + \cos(\theta) f_{y,E} \tag{E30-b} $$

$$ Q_\theta = {}^0n_S + n_E + {}^0J_{11,S}{}^T \begin{bmatrix} {}^0f_{x,S} \\ {}^0f_{y,S} \end{bmatrix} + (T_0\,{}^0J_{11})^T \begin{bmatrix} f_{x,E} \\ f_{y,E} \end{bmatrix} \tag{E-30c} $$

$$ Q_q = \begin{bmatrix} Q_{q1} \\ Q_{q2} \end{bmatrix} = \begin{bmatrix} \tau_1 + n_E \\ \tau_2 + n_E \end{bmatrix} + {}^0J_{12,S}{}^T \begin{bmatrix} {}^0f_{x,S} \\ {}^0f_{y,S} \end{bmatrix} + (T_0\,{}^0J_{12})^T \begin{bmatrix} f_{x,E} \\ f_{y,E} \end{bmatrix} \tag{E-30d} $$

The inertia matrix for this system is written using the Equation (2-76) where all terms were defined above. The nonlinear terms are written using Eqs. (2-74), (2-77) and (E-23), as:

$$ c_1^+(q_1, q_2, \dot\theta, \dot q_1, \dot q_2) = -\{\dot q_1{}^2 + 2\dot\theta \dot q_1\}(\hat d_{01} + \hat d_{02}) - \{\dot q_2{}^2 + 2\dot\theta \dot q_2 + 2\dot q_1 \dot q_2\}(\hat d_{02} + \hat d_{12}) \tag{E-31a} $$

$$ c_{2,1}^+(q_1, q_2, \dot\theta, \dot q_1, \dot q_2) = \dot\theta^2(\hat d_{01} + \hat d_{02}) - \{\dot q_2{}^2 + 2\dot\theta \dot q_2 + 2\dot q_1 \dot q_2\}\hat d_{12} \tag{E-31b} $$

$$ c_{2,2}^+(q_1, q_2, \dot\theta, \dot q_1, \dot q_2) = \dot\theta^2(\hat d_{02} + \hat d_{12}) + \{\dot q_1{}^2 + 2\dot\theta \dot q_1\}\hat d_{12} \tag{E-31c} $$

and:

$$ C_2^+ = [c_{2,1}^+, c_{2,2}^+]^T \tag{E-31d} $$

$$C^+ = [\,0,\,0,\,c_1^+,\,c_{2,1}^+,\,c_{2,2}^+]^T \tag{E-33e}$$

The equations of motion are written using Equation (2-78):

$$M\,{}^0\ddot{x}_{cm} = Q_x \tag{E-32a}$$

$$M\,{}^0\ddot{y}_{cm} = Q_y \tag{E-32b}$$

$$D\ddot{\theta} + D_q\ddot{q} + c_1^+ = Q_\theta \tag{E-32c}$$

$$D_q^T\ddot{\theta} + D_{qq}\ddot{q} + C_2^+ = Q_q \tag{E-32d}$$

Finally, equations (E-32) are written in matrix form as:

$$H^+(q)\begin{bmatrix}\ddot{x}_{cm}\\ \ddot{y}_{cm}\\ \ddot{\theta}\\ \ddot{q}\end{bmatrix} + C^+(q,\dot{\theta},\dot{q}) = \begin{bmatrix}0\\0\\0\\\tau\end{bmatrix} + J^+(\theta,q)^T\begin{bmatrix}f_E\\ n_E\end{bmatrix} + {}^0J_S^+(q)^T\begin{bmatrix}{}^0f_S\\ {}^0n_S\end{bmatrix} \tag{E-32}$$

Appendix F: Properties of H^* and C^*

Due to the defining equation for H^*, see Equation (3-26) and the dimensions of the D-terms, given after the definitions (2-50), H^* is a is an N×N matrix. Also, from the same definitions, it is obvious that H^* is a function of the configuration q only. It is also easy to prove that H^* is symmetric. Indeed, because of Equations (2-50) and (2-52), ${}^0D_{qq}$ is symmetric. The term ${}^0D_q^T\,{}^0D^{-1}\,{}^0D_q$ is also symmetric because the inertia matrix ${}^0D$, is symmetric positive definite.

It remains to prove that H^* is positive definite. To this end, note that the full system inertia matrix H^+ is positive definite. Due to properties of positive definite matrices, the same is true for the sub-partition H^r that corresponds to the rotational part of H^+:

$$H^r(q) = \begin{bmatrix} {}^0D(q) & {}^0D_q(q) \\ {}^0D_q(q)^T & {}^0D_{qq}(q) \end{bmatrix} \tag{F-1}$$

The inverse of H^r exists and can be written using standard linear algebra techniques as:

$$H^{r\,-1} = \begin{bmatrix} {}^0D^{-1} + {}^0D^{-1}\,{}^0D_q\,H^{*-1}\,{}^0D_q^T\,{}^0D^{-1} & {}^0D^{-1}\,{}^0D_q\,H^{*-1} \\ H^{*-1}\,{}^0D_q^T\,{}^0D^{-1} & H^{*-1} \end{bmatrix} \tag{F-2}$$

Note that since $H^{r\,-1}$ exists, H^{*-1} also exists. Since H^{*-1} appears at the bottom right corner of a positive definite matrix, it must be a positive definite matrix itself.

Another interesting property, useful to adaptive controllers for manipulators is that $\dot{q}^T(\dot{H}^* - 2C^*)\dot{q}$ is zero. This can be shown by noting that the increase in the kinetic energy of the system is due to the energy provided by manipulator actuators. Therefore, the time derivative of the kinetic energy (power) must be equal to the power of the actuators:

$$\dot{T} = \dot{q}^T \tau \tag{F-3a}$$

$$= \dot{q}^T H^*(q)\, \ddot{q} + \frac{1}{2} \dot{q}^T \dot{H}^* \dot{q}$$

$$= \dot{q}^T \{ \tau - C^*(q, \dot{q})\, \dot{q} + \frac{1}{2} \dot{H}^* \dot{q}) \tag{F-3b}$$

where, the equations of motion, given by Equation (3-28) was used. From Equations (F-3a) and (F-3b), the required property follows:

$$\dot{q}^T \{ \frac{1}{2} \dot{H}^* - C^*(q, \dot{q}) \}\, \dot{q} = 0 \tag{F-4}$$

It can be shown that by a suitable selection of C^*, $\dot{H}^* - 2C^*$ becomes skew-symmetric.